M.Sc. Agricultural Engineering

ABSTRACT

Sydney David Fisk

A STUDY OF THE PERFORMANCE AND COST OF OPERATION OF WHEEL-TYPE DRAINAGE TRENCHING MACHINES

A study of the effect of digging depth on the speed of wheel-type subdrainage trenching machines revealed an inverse linear relationship for the range of depths observed in several different soils. Both soil texture and machine characteristics affected the depth-speed relationship to a degree which prevented the use of a generalized formula for all machines in all soil types.

Data are presented for 20 delay factors which occurred during normal trenching operations. An analysis of these delays showed that an average of 58.6 percent of the available digging time was lost. Delays which could most easily be reduced included making junctions and setting grade targets.

The costs associated with the operation of trenching machines were shown in a proposed cost schedule. Results of a questionnaire revealed a large variation in costs between contractors.

Methods of increasing digging speed and reducing time losses and costs of operation were described.

DRAINAGE TRENCHING MACHINE PERFORMANCE AND COSTS

(suggested short title)

INTERFACIAL PHENOMENA IN CATIONIC MAGNETITE FLOTATION

INTERFACIAL PHENOMENA
IN CATIONIC MAGNETITE FLOTATION

James A. Finch

A thesis submitted to the Faculty of
Graduate Studies and Research in partial
fulfillment of the requirements for the
Degree of Master of Science

Department of Metallurgical Engineering
McGill University
Montreal, Canada

July 1971

M.Sc. ABSTRACT Metallurgical Engineering

J. A. Finch

INTERFACIAL PHENOMENA IN CATIONIC MAGNETITE FLOTATION.

Surface tension of dodecylamine acetate solutions at pH 4, 7 and 9.5 were determined by the maximum bubble pressure, capillary rise and drop weight techniques. Agreement was good at pH 4 and 7, but de-wetting at pH 9.5 rendered the latter two techniques inoperable. At pH 9.5, the bubble pressure technique indicated a significant dependence on surface age.

Contact angles were determined on magnetite by the suction potential technique at pH 9.5 and compared to captive bubble determinations (θ_E). Both advancing, θ_A, and retreating, θ_R, contact angles were determined. θ_R was zero at all concentrations, while θ_A corresponded to θ_E. Variations in θ_A were explained by variations in the value of $(\gamma_{lv} - \gamma_c)$, where γ_c is the critical surface tension of wetting.

Work of adhesion, W_A, was a maximum at 6×10^{-5}M, corresponding to the minimum concentration for magnetite flotation. Flotation increased with concentration, W_A decreased. This was explained by the noted surface aging phenomenon.

TABLE OF CONTENTS

LIST OF FIGURES

LIST OF TABLES

CHAPTER ONE

Introduction

In the fundamental understanding of the flotation process, the energies of the various interfaces involved are of prime importance. The work of adhesion equation offers a relationship between these surface energies and floatability. The equation is readily derived and is frequently quoted in relation to flotation[1-5]. However, it has met with little use and even less success[6,7] which is possibly due to the techniques employed in measuring the essential parameters. To study this possibility, a number of the available methods were compared.

Work of Adhesion and Flotation

Fig. 1(a) shows a stable bubble-particle arrangement while Fig. 1(b) represents the bubble and particle apart.

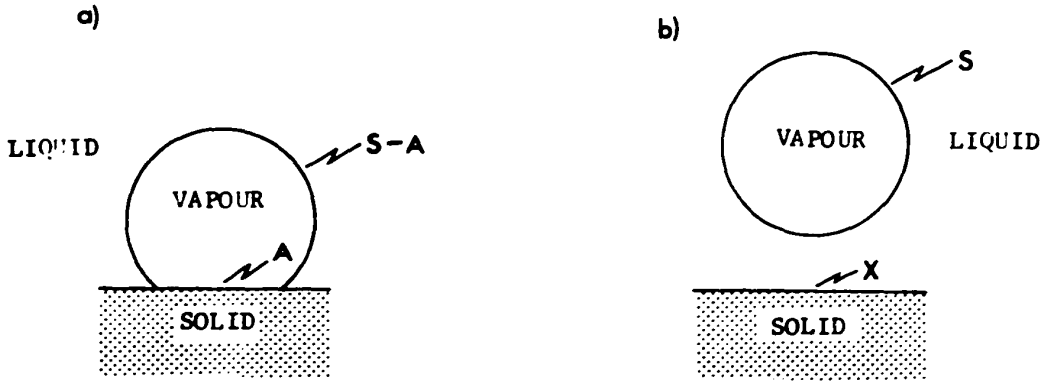

Figure 1. Free Energy Change upon Bubble - Particle Contact.

Considering condition (b), the total surface energy of the system, W_b, is given by[7]:

$$W_b = X\gamma_{ls} + S\gamma_{lv} \quad \ldots 1$$

where X = surface area of the solid

S = surface area of gas bubble.

Assuming that the gas bubble is negligibly distorted, the total surface energy of condition (a) is:

$$W_a = (X - A)\gamma_{ls} + (S - A)\gamma_{lv} + A\gamma_{sv} \quad \ldots 2$$

where A = area of the solid covered by gas bubble.

Thus the energy required for disruption, W, of the bubble and particle is given by:

$$W = W_b - W_a$$

$$= X\gamma_{ls} + S\gamma_{lv} - (X - A)\gamma_{ls} + (S - A)\gamma_{lv} + A\gamma_{sv} \quad \ldots 3$$

$$= A(\gamma_{ls} + \gamma_{lv} - \gamma_{sv})$$

Let $W_A = \frac{W}{A}$ = Work of Adhesion

Hence $$W_A = \gamma_{ls} + \gamma_{lv} - \gamma_{sv} \quad \ldots 4$$

Eq. 4 is of little use since γ_{ls} and γ_{sv} cannot be

directly measured. However, if the vapour - liquid - solid point of contact is considered to be in equilibrium, a force balance gives:

$$\gamma_{sv} - \gamma_{sl} = \gamma_{lv} \cos \theta \qquad \ldots 5$$

This relationship is known as the Young equation after T. Young who derived it[8].

Substituting Eq. 5 into Eq. 4 gives:

$$W_A = \gamma_{lv} (1 - \cos\theta) \qquad \ldots 6$$

In this form, the work of adhesion equation is usable, since γ_{sv} and γ_{sl} are eliminated. To calculate W_A, measurements of the liquid surface tension and contact angle are required. It is the methods available for these determinations which are to be compared.

From the derivation of W_A, it is clear that W_A is a measure of the energy of bubble particle attachment. Variations in W_A, therefore, should predict variations in mineral floatability.

The flotation system investigated is dodecylamine acetate - magnetite with special consideration to the alkaline regions.

CHAPTER TWO

SURFACE TENSION

Theory

Since the only surface tension factor contained in the work of adhesion formula (Eq. 6) is that of the solution, the discussion can be restricted to the liquid - vapour interface, which is shown in Fig. 2.

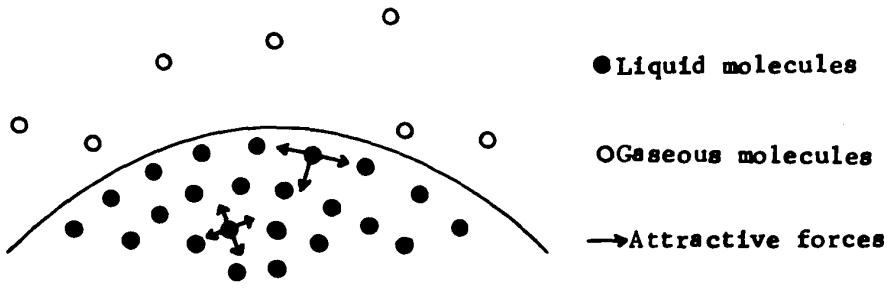

Figure 2. Molecular Attractive Forces at a Liquid - Vapour Interface.

All molecules are influenced by surrounding molecules which exert attractive forces. This force can be structural as with the H-bonding in water, non-specific as the Van der Waals or London attractive forces, or both[9]. From Fig. 2, the molecules in the liquid bulk are equally affected in all directions while those in the surface region suffer a

resultant force normal to the liquid surface and directed into the liquid bulk. Hence the surface suffers a depletion of molecules or conversely an extension of intermolecular distance. The latter concept implies that the surface is both in tension and storing energy[9,10]. Thus, the surface condition is variously described as that of 'surface tension' or 'surface energy'. Numerically the terms are equivalent so long as the surface energy refers to the excess surface free energy and not the total surface energy[11,12].

A thermodynamic treatment of surface free energy can be made by assuming the surface is itself an extra phase, i.e. a transition zone between adjoining phases[9,13]. If the surface area is increased by an infinitessimal amount, dA, the total free energy change in the system, dF, is given by:

$$dF = \gamma_{lv} dA \qquad \ldots 7$$

Alternatively, $$\gamma_{lv} = \left(\frac{dF}{dA}\right)_{T,P,n} = F_s$$

T, P, and n refer to temperature, pressure and chemical composition respectively and F_s is the excess surface free energy. Surface energy is, therefore, the work required to increase the surface area by unit area. The units are ergs.cm^{-2} or dynes.cm^{-1} for surface tension.

Currently, several theories are proposed to further the understanding of the surface tension phenomenon[9,10,14-19]. The theory of Fowkes[9,10] has gained wide acceptance[20,21].

Fowkes discusses the forces contributing to the surface energy. Earlier it was noted that water molecules exert two attractive forces over their neighbours, an H-bonding mechanism and a London force of attraction. Fowkes termed the London force a dispersion force because it is available for interaction with molecules of an alien phase. In water, if γ_w^d is the dispersion force and γ_w^H the force contributed by the H-bonding, then γ_w, the surface tension of water, can be considered as:

$$\gamma_w = \gamma_w^H + \gamma_w^d \qquad \ldots 8$$

A similar argument applies to mercury where γ_{Hg}^d is reinforced by a metallic bonding force contribution, γ_{Hg}^m. Thus γ_{Hg} is:

$$\gamma_{Hg} = \gamma_{Hg}^m + \gamma_{Hg}^d \qquad \ldots 8a$$

Hydrocarbons do not have a structural force contribution so the surface tension is entirely derived from the dispersion forces. Therefore, surface tensions of hydrocarbons are lower than, say, water.

Using this concept of the forces contributing to the surface tension, Fowkes was able to predict a value for the interfacial tension of mercury and water which is confirmed experimentally[10]. Thus the veracity of the theory is substantiated. However, Fowkes' theory is difficult to use in flotation systems where surfactant solutions are employed with an indeterminate γ^d. It does offer a possible direction for future studies[22].

(a) Solution Chemistry

Solution chemistry is an involved field, especially when dealing with the surfactant solutions upon which the flotation process is based.

Typical of the reagents used as collectors are members of the heteropolar or amphipathic group, e.g. dodecylamine. The common feature is that each molecule comprises a hydrophyllic polar head and a hydrophobic, hydrocarbon chain, as depicted in Fig. 3.

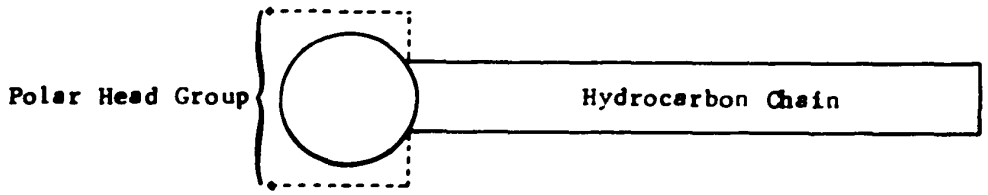

Figure 3. Heteropolar or Amphipathic Group.

Because of these differing characteristics, the liquid - vapour interface represents a low energy region for such species since both the hydrophobic and hydrophyllic groups can be energetically satisfied, as shown in Fig. 4.

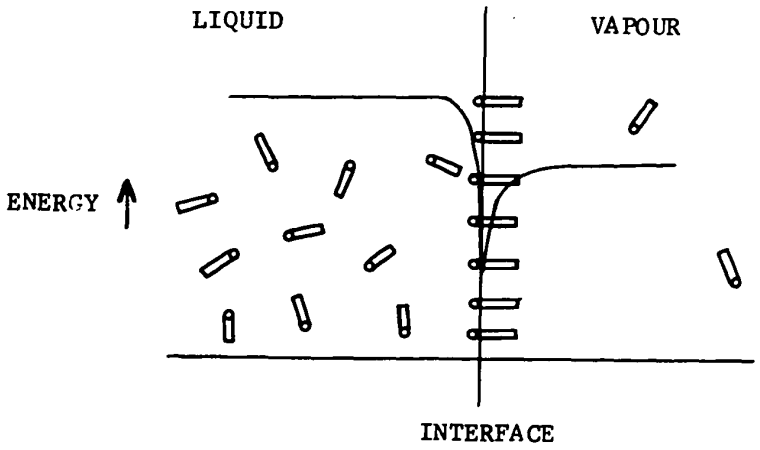

Figure 4. Energy Level as a Function of Distance from the Interface for Heteropolar Molecules.

These molecules are termed surface active agents, or surfactants, and, because they have a lower surface energy than pure water, their presence at the water surface reduces the surface tension. The tendency to preferentially adsorb at the liquid - vapour interface and, consequently, lower the surface tension, is termed positive adsorption.

Gibbs[23] first attempted to relate the bulk concentration of surfactant solute to the lowering in

surface tension in 1876. He noted that as the concentration was increased the surface tension altered very little until a certain concentration, A (see Fig. 5), was reached.

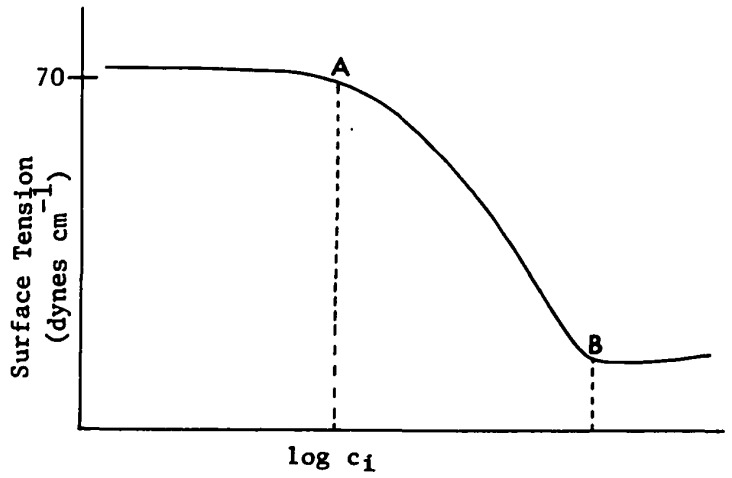

Figure 5. Surface Tension vs. log. Surfactant Concentration.

The value depends on the relative strengths of the hydrophobic and hydrophyllic species. Above this concentration sufficient surfactant is present to noticeably reduce the surface tension as the high surface energy water molecules are replaced by the relatively low surface energy surfactant species. At equilibrium, the drop in surface tension, $d\gamma_{lv}$

particle attachment using Eq. 11. Both concluded that bubble-particle stability means that the adsorption density must be greatest at the solid - vapour interface, the least considered interface in flotation. Smolders[28], from contact angle observations made on low surface energy solids against surfactant solutions, came to the same conclusion. Padday's observations[29], however, indicate that high adsorption density of surfactant at the solid - vapour interface is not always apparent.

From Eq. 11, the steady increase in Γ_{lv} which causes the decrease in surface tension will be reflected in an ever increasing slope, $d\gamma_{lv}/d \log c$. At concentration B, however, the lowering in surface tension abruptly ceases. If the surface was not saturated with surfactant molecules, further surfactant would lower the surface tension. Since this does not occur at concentrations greater than 'B' the surface has been entirely transformed to a surface of surfactant, i.e. the solution surface is covered with a monolayer of surfactant. Therefore the surface tension measured at concentration'B' is the surface tension of the surfactant used.

Such discontinuities in bulk solution properties led McBain[30] to introduce the concept of molecule clustering to form colloidal aggregates or micelles in the bulk solution. Concentration B is referred to as the

critical micelle concentration or c.m.c. The hydrocarbon chains form an 'oily phase' and the polar head groups are projected into the surrounding aqueous phase. Figs. 6(a) and (b) show the two common proposals[31,32], (a) the spherical model of Adam[33] and (b) the cylindrical structure of Harkins[34]. The exact shape and the number of molecules involved are unknown[35].

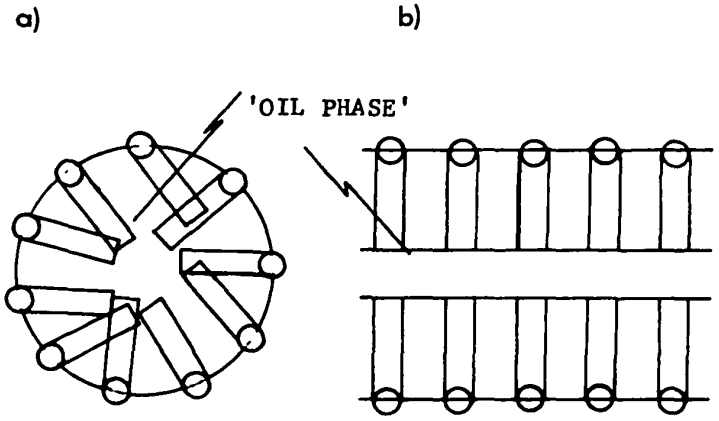

Figure 6. (a) Spherical Micelle (after Adam[33]).

(b) Cylindrical Micelle (after Harkins[34]).

surface energy of water eliminated, a rise in the surface tension value is to be expected[31]. The presence of the minimum is, therefore, generally attributed to contaminants, their removal being considered complete when the minimum is removed[28,29]. However, the presence of inorganic salt impurities does not have the same effect[42,43]. The value of the c.m.c. is lowered but the shape tends to remain the same.

Lowering of the c.m.c. is also known to occur with organic impurities[44], which presumably reduce the electrostatic repulsion between polar head groups and promotes micelle formation. A similar mechanism is proposed to account for c.m.c. depression in the presence of inorganic salts[45]. Such observations are not usually included in estimates of material purity[28,29]. Further, work by Mysels[46] has demonstrated that with carefully prepared materials the surface tension continues to decrease after the c.m.c., although at a reduced rate.

(i) Equilibrium and Dynamic Surface Tensions

A frequent observation of the surface tension of surfactant solutions is that two distinct, reproducible values for the surface tension are obtained. These are called the equilibrium value and the dynamic value. The

phenomenon is due to differences in the history of the surface on which the measurements are made.

Dynamic surface tension refers to a surface tension not corresponding to the equilibrium state of the liquid surface under consideration. The transient deviations from the equilibrium result from differences in the adsorption density of surfactant. Lange[47] notes two processes which could give rise to a dynamic surface tension condition:

(1) Surface aging at constant area of interface;

(2) Variations in interfacial areas available for adsorption of surfactant.

In both cases, the movement of the solute molecules to the surface must take place over a finite period of time.

The phenomenon of surface aging has recently prompted increased attention as a means of explaining observations made under dynamic conditions[48,49]. Flotation is a dynamic process since upon introduction of fresh bubbles, the liquid - vapour interface involved in successful mineral flotation is probably not at equilibrium. This effect has not been considered in flotation studies. Generally, it is avoided in order to permit the use of the Gibbs adsorption equation, which describes an equilibrium state[27]. Recently this rigid interpretation of the equilibrium state has been modified[47] and the Gibbs

adsorption equation is considered applicable to non-equilibrium states under certain conditions.

Surface aging occurs because the solute species requires a finite time to move from the bulk of solution to the surface. Two mechanisms can control the rate of this movement[50]:

(1) Movement of solute molecules from the bulk to the sub-surface (the layer immediately below the surface);

(2) Movement of the solute molecules from the sub-surface into the surface layer.

The former is referred to as the "rate of diffusion", the latter as the "rate of real adsorption".

(i. i) Rate of Diffusion

Several attempts have been made to quantify this phenomenon after Milner[51] first suggested that it was a cause of the observed time effect in certain solutions. Among the most notable were by Bond and Puls[52] and Langmuir and Schaefer[53]. Ward and Tordai[54] improved on the previous work and developed a general theory of molecular diffusion through the solution bulk to the surface.

Upon creation of a fresh surface in a solution of uniform concentration, C_o, the concentration in the sub-surface, C^1, initially equivalent to C_o, will be effectively

reduced to zero. This is caused by adsorption into the 'bare' interface of virtually all the solute in the sub-surface. The effect will be to produce a concentration gradient $C_o - C^1$, where $C^1 = 0$, so there will be a resultant general flow of molecules to the surface. From Fick's laws, Ward and Tordai showed that:

$$\Gamma_{lv} = 2 C_o \left(\frac{Dt}{\pi}\right)^{\frac{1}{2}} \qquad \ldots 12$$

where D is the diffusion coefficient and t the time after surface formation. Eq. 12 will only hold if there is no build-up of molecules in the sub-surface, i.e. $C^1 = 0$. Initially $C^1 = 0$ will hold as the surface will have available many vacancies. With time, however, molecules will not so readily be accommodated in the surface and so $C^1 > 0$. Under such circumstances a back-diffusion will be set up. Ward and Tordai analysed this situation and developed a back diffusion term, M:

$$M = 2\left(\frac{D}{\pi}\right)^{\frac{1}{2}} \int_o^{t^{\frac{1}{2}}} \phi(z)\, d\left[(t - z)^{\frac{1}{2}}\right] \qquad \ldots 13$$

where $\phi(z)$ is the concentration of surfactant in the sub-surface at any time z. By varying z from 0 to t, theoretically the back diffusion occuring over time t can be estimated. This gives the full diffusion equation:

$$\Gamma_{lv} = 2\left(\frac{D}{\pi}\right)^{\frac{1}{2}} \left\{ C_o t^{\frac{1}{2}} - \int_o^{t^{\frac{1}{2}}} \phi(z)\, d\left[(t - z)^{\frac{1}{2}}\right] \right\} \qquad \ldots 14$$

Thus if either D or Γ_{lv} is known the other can be found. The major difficulty in using Eq. 14 is that $\phi(z)$ as a function of time is not known. However, if it is assumed that only diffusion is controlling the movement of molecules, then at any instant the concentration in the sub-surface, $\phi(z)$, is in equilibrium with the concentration in the surface. This concept led Lange[47] to suggest that the Gibbs adsorption equation may be valid for non-equilibrium surface tensions. At the equilibrium surface tension value, the concentration in the sub-surface will be the same as the bulk concentration, C_o. Thus a plot of equilibrium surface tension, γ_{lv}, against C_o gives values of γ_{lv} uniquely associated with a sub-surface concentration equal to C_o. From the surface tension versus time graph for a given bulk concentration, the values of γ_{lv} for a given time can be associated with values of $\phi(z)$. Thus $\phi(z)$ against time, z, can be found and hence $\phi(z)$ against $(t - z)^{\frac{1}{2}}$ plotted. By planimetry from this curve, the integral, I, where:

$$I = \int_o^{t^{\frac{1}{2}}} \phi(z)\, d\left[(t - z)^{\frac{1}{2}}\right] \qquad \ldots 15$$

can be determined. Since t and C_o are known and Γ_{lv} can be measured by means of the Gibbs adsorption equation, D,

aging controlled by diffusion.

(i, ii) Rate of Real Adsorption

No single theory has been developed to explain this phenomenon, it being generally referred to as an energy barrier[50,54,56]. Alexander[58] suggests that re-orientation of solute molecules at the surface may be responsible. Randomly oriented molecules at the surface slowly re-orientate to allow further adsorption into the surface. An alternative theory proposed by Alexander is that the solute species are hydrated and that the hydration layer evaporates once at the surface, allowing more surfactant to enter the surface. Sutherland[56] discussed the possibility that the energy barrier was electrical in nature, that surfactant ions at the surface tend to repel incoming surfactant ions, thus developing a significant aging time. There is some suggestion that contaminants may be responsible[41], again due to the presence of ions, but Hutchinson[41] could find no conclusive evidence.

In comparison to the diffusion theory the aging phenomenon due to a restriction on the movement of solute molecules from the sub-surface to the surface is less well defined.

(b) Dodecylamine Solutions

Dodecylamine is a primary amine since only one hydrogen of the basic ammonia molecule, NH_3, has been replaced. The formula is $C_{12}H_{25}NH_2$. As amine, the solubility is very low, the most recent data[59] giving a maximum solubility of 2×10^{-5}M. When converted to a salt, the solubility is greatly increased. In this study, the acetate salt was used.

$$C_{12}H_{25}NH_2 + CH_3C(O)OH \rightarrow C_{12}H_{25}NH_3^+ \ ^-O(O)CCH_3$$

Upon dissolving in water, ionisation readily occurs:

$$C_{12}H_{25}NH_3^+ \ ^-O(O)CCH_3 \rightleftharpoons C_{12}H_{25}NH_3^+ + CH_3C(O)O^-$$

The dodecylamine ion, $C_{12}H_{25}NH_3^+$ is a typical amphipathic species.

The solubility of dodecylamine ions is controlled by the relative strengths of the hydrophyllic head group, NH_3^+ and the hydrophobic, $C_{12}H_{25}$, chain. This is reflected in the surface tension - concentration relationship; the concentrations A and B (c.m.c.) ultimately depend on this effect[27,61]. For amines such as decylamine, $C_{10}H_{21}NH_2$, the ion solubility is greater since the hydrocarbon chain is shorter. The surface tension requires greater concentrations of amine (about ten times) to effect the same surface tension decrease[27,44]. The reverse is true

for octadecylamine ions, $C_{18}H_{37}NH_3^+$. Thus, the longer the hydrocarbon chain, the more readily the ion is attracted to the interface.(Traube's rule[61]). The effect of the hydrocarbon chain is similar to the observations made by Grahame[36] on the ease with which longer chained surfactant species adsorbed at a mercury - liquid interface. Grahame used the term 'squeezing out effect', since the water molecules 'squeeze out' the hydrocarbon chain plus ionic head into the interface[36].

Another factor which affects the solubility of the dodecylamine ion and the surface tension characteristics is the solution pH. In the presence of hydroxyl ions, OH^-, the following reaction occurs:

$$C_{12}H_{25}NH_3^+ + OH^- \overset{K_B}{\rightleftharpoons} C_{12}H_{25}NH_2 + H_2O$$

where $K_B = 2.4 \times 10^{-11}$ (62)

The solubility will, therefore, decrease with increasing pH, due to the conversion of amine ions to the relatively insoluble undissociated amine molecule. This variation with pH can be calculated[63,64]. Thus, the c.m.c. is lowered with increasing pH, as shown by Manser[65], who indicated a straight line relationship up to pH 11.

De Bruyn[66] noted that in alkaline regions carbon dioxide can react with free amine molecules. The result is

the precipitation of either amine carbonates or carbamates:

$$2\ C_{12}H_{25}NH_2 + H_2O + CO_2 \rightleftharpoons (C_{12}H_{25}NH_3)_2^{2+}\ CO_3^{2-}$$

dodecylammonium carbonate

$$2\ C_{12}H_{25}NH_2 + CO_2 \rightleftharpoons C_{12}H_{25}NH_3^{+}\ {}^{-}O(O)CNH\ C_{12}H_{25}$$

dodecylammonium carbamate.

To avoid precipitation, CO_2-free water is used[66]. This is achieved by flushing double-distilled water with pure nitrogen.

Very little work has been done on the surface tension of dodecylamine solutions. Ralston[67] investigated the surface tension variation with concentration for neutral solutions, giving a c.m.c. value of 1.2×10^{-2}M. Morrow[6] repeated some of this work, and obtained the same relationship. The c.m.c. of dodecylamine solutions has been determined by Lawrence et al.[68] from the pH drift noted in neutral solution upon the addition of increasing concentrations of solute[66]. This pH drift can be calculated from the ionisation constant of the amine[62,66]. Lawrence et al. measured this drift by means of a glass electrode pH meter and observed a discontinuity at 0.275 g/100 g of solution. The discontinuity is attributed to the onset of micelle formation. The concentration is approximately 1.15×10^{-2}M, thus confirming the c.m.c.

value obtained by Ralston.

Surface aging is considered by Ralston to be of negligible time duration[67]. The work of Morrow[6], Somasundaran[26], and Sandvik[69] who did not consider surface aging, with no scatter of results as a consequence, substantiates negligible aging times. For example, the observation of millisecond aging times is quite common[47,48,50,54,70,71].

(c) Methods

(i) Review

Many methods are available for surface tension determination[72]. However, little comparative work has been carried out to test the reliability of the techniques for given conditions, especially surfactant solutions. The need for a reliable method is emphasised by Owens[48], who notes that different techniques can give consistently different values for the same solution. The main comparative work has been performed by: Kragh (du Noüy ring and maximum bubble pressure)[42]; Sandvik and Digrè (maximum bubble pressure, drop weight and du Noüy ring)[69]; Sonntag and Strenge (drop weight and Wilhelmy plate)[73]; Zettlemoyer et al. (Wilhelmy plate, drop volume and du Noüy ring)[74]; Padday and Russell ('modified' Wilhelmy plate, du Noüy ring, sessile drop and capillary rise)[75]; and

methods and include the drop weight/volume, maximum bubble pressure, du Noüy ring and Wilhelmy plate. The latter are known as equilibrium or static methods, and include the capillary rise, sessile drop and modified Wilhelmy plate[75,79].

The capillary rise is considered to be a standard by some workers[77,80] but shortcomings in work on surfactant solutions have been recorded[76]. The main problem noted is possible interaction between the glass walls and the solution leading to the development of a contact angle and hence decreased calculated surface tensions. Such a phenomenon is utilised in certain contact angle measurements[27,81]. Nevertheless the method is still in use in flotation studies[82,83] and was, therefore, included in the work. Its distinct advantage is the ease of equipment construction and operation.

Of the other equilibrium methods, experiments with the sessile drop have produced mixed results, Tartar et al. obtaining good reproducibility[76] whilst Padday[75] and Zettlemoyer et al.[74] found precision lacking. Theoretically, it should be the most accurate method but practical difficulties in defining a position on a curved surface limit its applicability. It is claimed that neither adsorption across the solid - liquid interface nor evaporation from the solution - air interface affect the

results. However, work by Cupples[84] and Hommelen[85] indicate that these errors can be substantial.

The modified Wilhelmy plate method[75,79] is considered by Padday[75] to be the best equilibrium method available. However, it has only recently been developed and has received limited testing. An increasing criticism of all equilibrium methods is that they do not correspond to the conditions prevailing in the systems under investigation[48,49]. To understand such systems, dynamic surface tension determinations offer a closer analogy.

An important feature of the the liquid - vapour interface as found in the flotation system is that the interface results from the creation of fresh air bubbles in the liquid bulk. This is simulated in the principle of operation of the 'maximum bubble pressure' technique of Simon[86] for surface tension determination. Since it is important to choose a technique which yields information about the desired system[48,49], the maximum bubble pressure method is a good choice for studying flotation[69]. It is worth noting that the technique has been used more extensively in recent years[42,48,49,57,69,71,87-92]. Advantages claimed for the method are its freedom from contact angle[93] and its self-cleaning capacity due to continual flushing with fresh air[94,95].

In order to assess any variations in surface tension data accruing from the different methods, in the present case, capillary rise versus maximum bubble pressure, a third comparative method was considered necessary.

The third choice was the drop weight technique of Harkins and Brown[96,97]. It has a number of advantages over the other dynamic methods, the du Noüy ring and the Wilhelmy plate. All three are considered of relatively simple construction and operation, but the drop weight apparatus lends itself more readily to complete enclosure of the test solution, helping to avoid the ever-present, deleterious surface contamination[81]. Also, so long as the tip from which the drop detaches is completely wetted, the drop weight technique is free from contact angle considerations. Such does not apply to either the du Noüy ring or Wilhelmy plate, especially with collector solutions designed to create de-wetting[55]. Heating to dull-red heat[57] or amalgamation with mercury[56] have been utilised to try to overcome this disadvantage, but elimination of this source of error must remain in doubt. Recent work by Zettlemoyer et al.[74] and Sandvik et al.[69], using the du Noüy ring, revealed very poor reproducibility. Sandvik[69] and Somasundaran[27] both consider adsorption at the surface of the ring to be appreciable.

The drop weight method, on the other hand, has been

extensively employed and has met with considerable success. Zettlemoyer et al.[74], Sonntag et al.[73], Rehfeld[98], Shergold et al.[99], Parreira[100] and Sandvik[69] all used the technique in aqueous solutions with high reproducibility. Sandvik[69] also noted good agreement between the maximum bubble pressure and drop weight techniques on dodecylamine solutions up to 1.2×10^{-4}M. Its inclusion, therefore, as the third system seems well founded. Variations on the original technique of Harkins are offered by Parreira[100], and Gaddum[101,102]. The former used a syringe as the dropping tip, whilst the latter devised a technique more properly described as the drop volume technique, since the drops are collected in a measuring tube and the volume increase per drop calculated. Such a method enables 'poor'[97] drops to be eliminated during the test.

(ii) Capillary Rise

Upon immersing an open, vertical capillary tube into a liquid (see Fig. 7), the liquid will naturally rise to a maximum height h, from which the surface tension can be calculated.

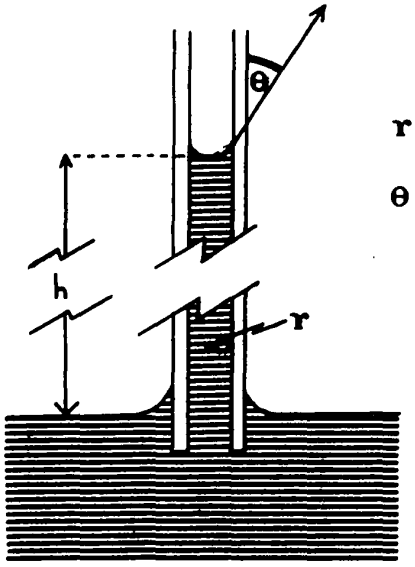

Figure 7. Liquid Equilibrium in an Open, Vertical Capillary.

A force balance gives:

$$2\pi r \gamma_{lv} \cos\theta = \pi r^2 \rho h g \qquad \ldots 16$$

thus $$\gamma_{lv} = \frac{r\rho hg}{2\cos\theta} \qquad \ldots 17$$

where ρ = density of liquid.

It is generally assumed that $\theta = 0$, i.e. that complete

$$\gamma_{lv} = K\Delta h \qquad \ldots 20$$

Eq. 20 was used in the present investigation.

(iii) Maximum Bubble Pressure

The method was first suggested by Simon[86] and was brought into prominence later by Sugden[94,104].

A capillary tube of known bore is suspended in the test liquid and the pressure of the gas is gradually increased until a bubble of gas (e.g. air) is forced out. The excess pressure, ΔP, residing inside the bubble is inversely proportional to the bubble radius, r_B:

$$\Delta P \propto \frac{1}{r_B} \qquad \ldots 21$$

Consequently, the excess pressure is greatest when r_B is least. From Fig. 8 it can be seen that the maximum excess pressure corresponds to a hemispherical interface at the capillary tip (i.e. $r_B = r$, the bore radius). Thus:

$$\Delta P_{max} \propto \frac{1}{r} \qquad \ldots 22$$

As soon as ΔP_{max} is exceeded the bubble becomes unstable and breaks away from the tip. Relating the observed ΔP_{max} (read from a suitable manometer) to the surface tension forces which create this phenomenon gives:

$$\Delta P_{max} = \frac{2\gamma_{lv}}{r} \quad \ldots 23$$

But $$\Delta P_{max} = \rho_m g h \quad \ldots 24$$

where ρ_m = density of manometer fluid

h = maximum reading on manometer.

Thus substituting and rearranging:

$$\gamma_{lv} = \frac{1}{2} \rho_m g h r \quad \ldots 25$$

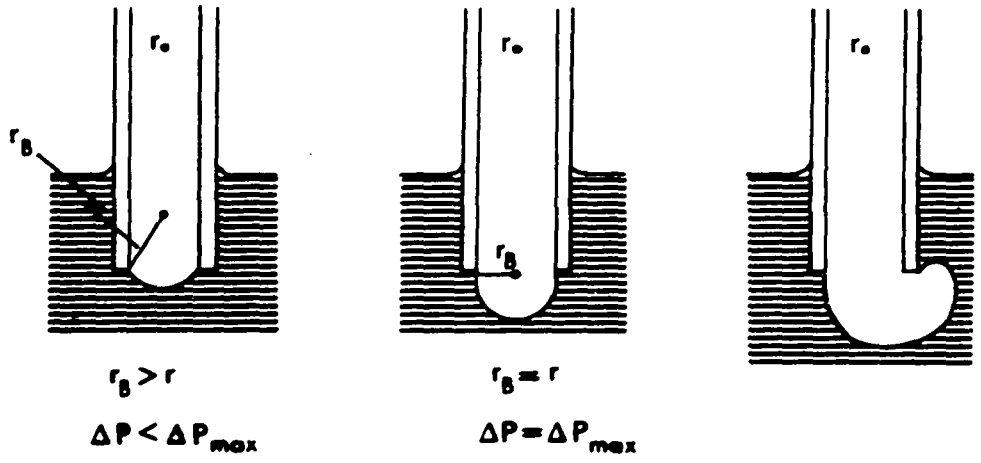

Figure 8. Bubble Growth at Capillary Tip.

There are, however, both theoretical and practical limitations to Eq. 25. It requires that the tip be placed exactly in the liquid surface or else immersed to a known depth so that extra pressure exerted by the added hydrostatic head can be accounted for. Brown[105] uses this technique although it involves a degree of measuring error similar to that encountered in single capillary rise experiments[94]. This criticism is overcome by comparing the excess pressure of two capillaries immersed to the same depth. Sugden[104] points out that the blown bubble never attains a truly spherical shape due to the hydrostatic head of the added bubble depth. Only with infinitely narrow bore capillaries does this error become negligible[104]. Sugden[104] considered both these criticisms and has constructed a set of correction tables.

As a consequence of Sugden's work, a simplified equation for the dual capillary technique was developed:

$$\gamma_{lv} = A(\Delta h \rho_m + 0.69\, r_1 \rho_1) \qquad \ldots 26$$

where r_1 = radius of large tube

ρ_1 = density of test liquid

Δh = $h_2 - h_1$

h_1, h_2 = manometer readings for large (r_1) and small (r_2) capillaries

A = calibration constant.

This equation is the most frequently used for surface tension determination using the dual capillary technique and is used in the present investigation. 'A' can be obtained by calibration against a liquid of known surface tension, e.g. water or benzene. The value of r_1 was determined by a cathetometer. Eq. 26 is valid for tubes up to several millimeters in diameter[104].

The tubes used should be as near circular as possible and the tips cut at right angles to the walls[104]. To avoid pressure fluctuations any variations in the tube diameter should be smooth. Avoiding all such variations by using a length of tubing of the required diameter would be best[42].

Equipment for the measurement of surface tension of various liquids is designed on the basis of Eqs. 23 and 24. The major consideration is that r_1 be small enough to register a measurable h_1 on the manometer under all conditions encountered. Letting $h_1 \approx 2$ cm on a water manometer ($\rho_m = 1.0$ gm.cm^{-3}), then for the lowest expected surface tension value for dodecylamine solutions of approximately 30 dynes.cm^{-1}, $r_1 \approx 0.01$ cm. Sugden, for instance, used tubes of $r_1 = 0.06$ cm and $r_2 = 0.0075$ cm for work on benzene (surface tension 28.2 dynes.cm^{-1} at 25° C[106]). Such tubes are not only difficult to draw accurately but are subject to chipping and dust-blockage[104].

If a bi-fluid manometer is used, larger bore tubes can be employed. Letting $\delta\rho_m$ equal the difference in density of the two manometer fluids, and H the difference in height measured on the bi-fluid manometer, then:

$$H\delta\rho_m = \Delta h\rho_m \quad \ldots 27$$

By choosing a small value of $\delta\rho_m$ a magnified reading is provided. Therefore, larger bore tubes can be used, which still give the required minimum reading of $h_1 \approx 2$ cm.

The two fluids must be immiscible and of low viscosity. A Shell pella oil (viscosity 4 c.p., density 0.8179 $gm.cm^{-3}$ at 25^{o} C) and water gave a $\delta\rho_m = 0.1821$ $gm.cm^{-3}$. Thus tubes approximately five times the diameter could be used. Commercially available 0.1 and 0.25 cm diameter tubes were selected. They are strong and free from dust-blockage problems. Such readily available tubing also enables a considerable length to be used, thus avoiding the pressure fluctuations associated with varying tube diameters[42].

Substitution of Eq. 27 into Eq. 26 yields:

$$\gamma_{lv} = A(H\delta\rho_m + 0.69\, r_1\rho_1) \quad \ldots 28$$

Eq. 28 is the basic equation for the present determinations.

has been shown that Eq. 29 is only valid if the r in the equation is actually r_n, the radius of this neck. In practice $r > r_n$ and so the large errors noted for the technique were explained[97]. The mass of the drop predicted by Eq. 29 is considered as that of the 'ideal' drop[97]. Experimentally, r_n is difficult to determine but Harkins and Brown[97] quite reasonably argued that the value of r_n would depend on r. This was done by noting that the mass of the falling drop would be a function of the drop diameter and drop length. The tip radius, r, can be used as a measure of the drop radius and $V^{1/3}$, where V is the volume of the drop, as a measure of the drop length. Eq. 29 becomes:

$$mg = 2\pi r \gamma_{lv} \psi(r/V^{1/3}) \qquad \ldots 30$$

where $\psi(r/V^{1/3})$ corrects for $r > r_n$ and thus indicates the fraction of the ideal drop which falls.

Harkins and Brown by using pure water and pure benzene and tips of various radii drew up tables correlating $\psi(r/V^{1/3})$ to $r/V^{1/3}$ over a range $0.3 \leq r/V^{1/3} \leq 1.6$. A graph of $\psi(r/V^{1/3})$ versus $r/V^{1/3}$ is given below (Fig. 10). Thus, by measuring r and V, $r/V^{1/3}$ and hence $\psi(r/V^{1/3})$ can be estimated and γ_{lv} found from:

$$\gamma_{lv} = \frac{mg}{2\pi r \psi(r/V^{1/3})} \qquad \ldots 31$$

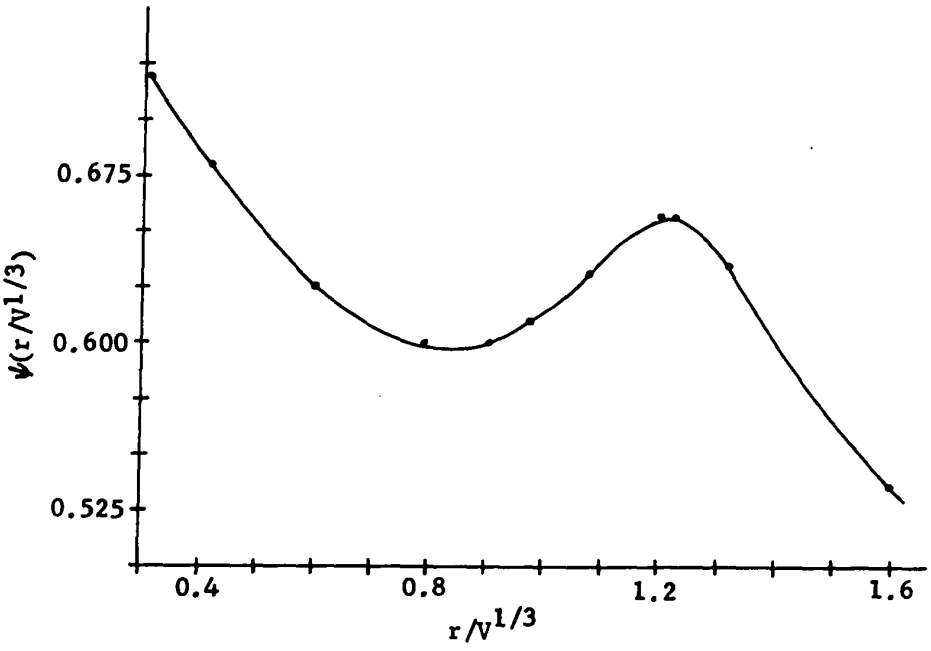

Figure 10. Drop Weight Correction Curve (after Harkins and Brown[97]).

The choice of tip will be influenced by Fig. 10 since over the range $0.65 \leq r/V^{1/3} \leq 1.05$ the value of $\phi(r/V^{1/3}) \approx 0.6$, thus slight errors in the $r/V^{1/3}$ value do not greatly distort the estimated $\phi(r/V^{1/3})$ value.

An important consideration that Harkins and Brown discovered was that the weight of the falling drop depended on the time taken to form the drop[97]. This is probably

due to physically 'over-shooting' the equilibrium mass by too rapid a growth rate. At least five minutes was specified as necessary to provide consistent data, a figure confirmed by Shergold and Mellgren[99].

Procedure and Apparatus

Certain aspects remained the same for each technique employed.

(i) A temperature of 25° C $\pm$ 1° was used. This temperature was maintained by using a constant temperature water bath in an air-conditioned room.

(ii) All apparatus which came into contact with dodecylamine solutions were cleaned in the following manner: standing in acid dichromate for four + hours and washing successively with tap water, distilled water, conductivity water and a small sample of test solution.

(iii) Sodium hydroxide and hydrochloric acid were used to control the pH.

(a) Capillary Rise

The equipment, shown in Fig. 11, was comprised of a beaker to hold the test solution sample and two capillaries dipped into the solution, supported vertically by a rubber stopper.

It was necessary to know accurately the radii of the two capillaries. This was computed by filling sections of each tube with triple distilled mercury and measuring the resulting length and weight of the mercury column. The length was measured at random locations over an approximate length of five inches. From the weight and average length

FIGURE 11

CAPILLARY RISE APPARATUS

of mercury, the radii of the two capillaries were calculated.

In order to employ Eq. 20, the capillaries must be completely wetted. This is aided by squeezing bulb B and forcing the liquid past the equilibrium level. Slow release of the pressure allows the liquid to fall to the equilibrium level, giving good opportunity for the walls to become wetted[97]. A cathetometer reading to 0.002 cm was used to measure the height difference, Δh. All the experiments were performed in duplicate.

(b) Maximum Bubble Pressure

The equipment, shown in Fig. 12, is in three sections: the bubbling unit, B; the bi-fluid manometer, M; and the pear-shaped funnel, F. The test solution is held in B to a level such that the tips r_1 and r_2 are immersed. By allowing water to drain from F via clip C, the pressure over the solution is lowered and air can enter, as indicated. Eventually a bubble will form either at r_1 or r_2, depending whether tap T is open or closed respectively. The maximum excess pressure is recorded on M, for both conditions, and hence H calculated. Readings were taken from a centimetre scale placed behind the manometer. Accuracy was to 0.02 cm using a hand lens. A notable feature of the present design is that the manometer

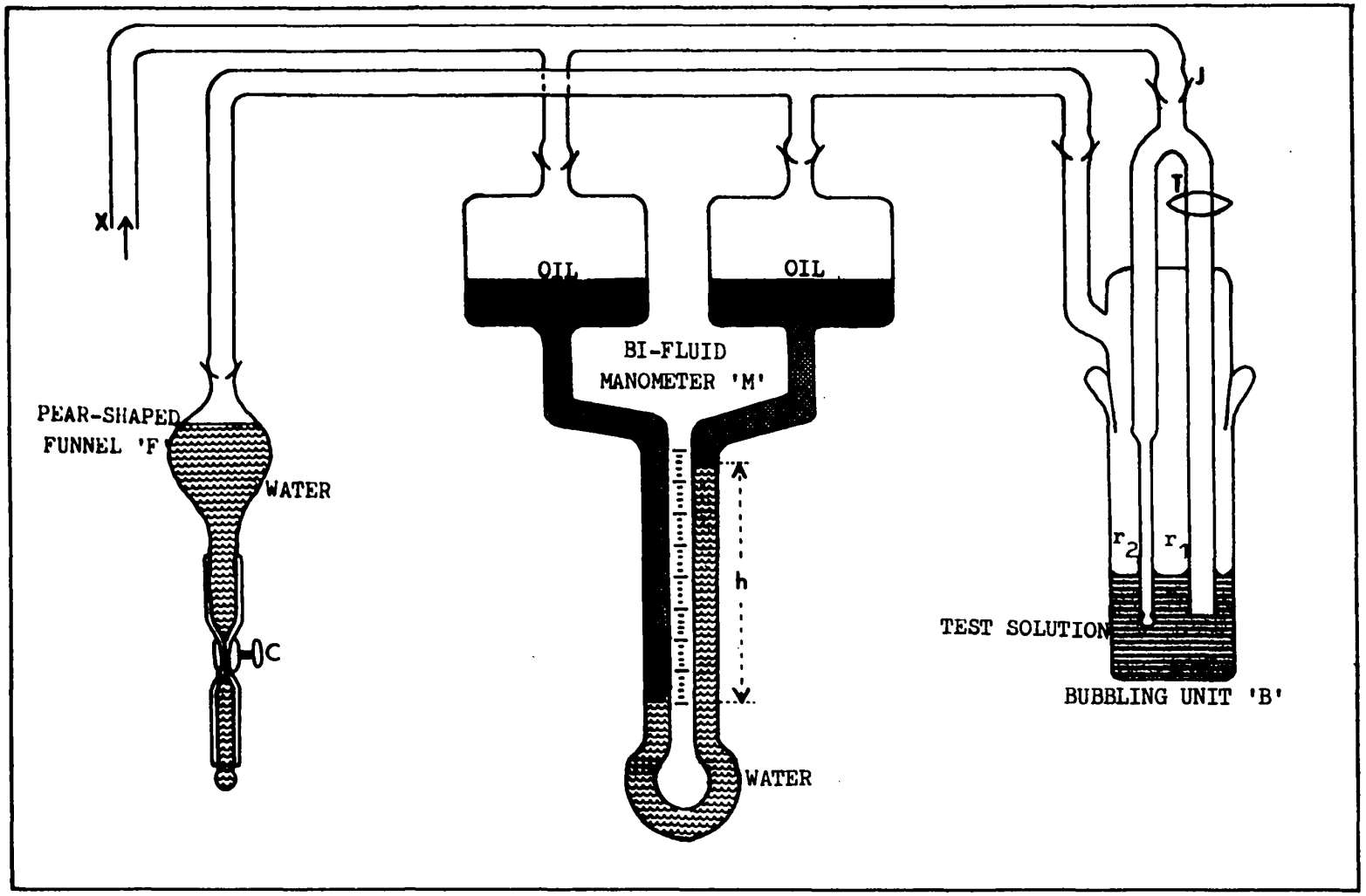
X
OIL
OIL
BI-FLUID
MANOMETER 'M'
PEAR-SHAPED
FUNNEL 'F'
WATER
C
h
WATER
J
T
r_2
r_1
TEST SOLUTION
BUBBLING UNIT 'B'

fluids and the test solutions are both completely enclosed, thus avoiding the substantial atmospheric contamination noted by Sugden[104].

The experiment was performed by first closing tap T and generating bubbles via r_2. Readings can be brought onto scale, if necessary, by altering the depth of solution in B. Using a fast bubbling rate the manometer meniscus was taken past the true equilibrium point. The manometer walls were thus wetted. The pressure was released via joint, J and the bubble rate slowed to approximately 1 in 10 seconds. The manometer reading was taken after roughly forty-five minutes. This was sufficient time for the solution to be at temperature and for the manometer to give steady, reproducible readings.

Joint J was again opened to release the pressure and tap T opened to allow air to exit via the large diameter capillary, r_1. After a further fifteen minutes a second manometer reading was taken. The operation was repeated to check the initial results.

(c) Drop Weight

The original technique of Harkins and Brown[97] was used and the equipment, shown in Fig. 13, is similar to their design. It consists of a holding cell, C_1, a

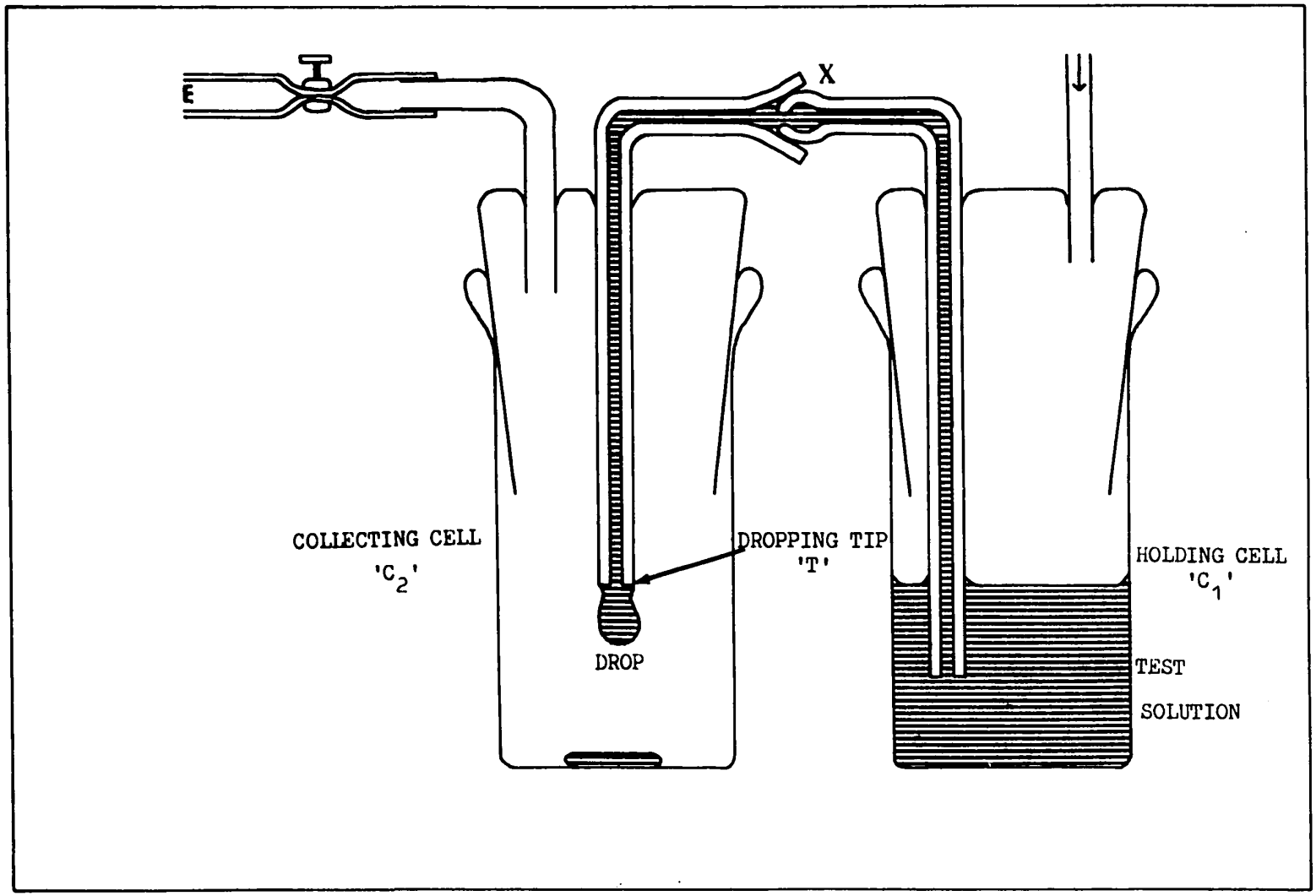
E
X
COLLECTING CELL
'C2'
DROPPING TIP
'T'
HOLDING CELL
'C1'
DROP
TEST
SOLUTION

collecting cell, C_2, connected by a glass capillary, X, with a dropping tip, T, held vertically in C_2.

Test solution was held in cell C_1 and initially allowed to drain freely via X (acting as a syphon), through the dropping tip, T. Eventually, (since there is only a finite quantity contained in C_1), drainage will slow, until the growth rate of an individual drop approaches the five minutes suggested by Harkins and Brown[97]. In the present investigation it proved sufficient to commence the experiments when there was no observable natural growth of the drop over a period of one minute.

At this juncture, a pre-weighed collecting cell, C_2, was carefully placed around the tip. The drop can be induced to form by slight suction on tube, E. A typical situation[78,97,100] is that approximately ninety per cent of the drop be thus drawn whilst the remaining ten per cent grow and fall naturally under gravity. So long as the drop falls naturally its weight will accurately reflect the surface tension according to Eq. 30.

An average of between eight and twenty drops was taken. The variation in the number of drops recorded was due to the varying surface tensions encountered, and indicates the delicate balance between the level of solution in C_1 and the ability to draw drops successfully. At the

end of the run, solution still held in the capillary syphon was forced back into the holding cell, C_1.

A number of factors can be considered to improve the accuracy of the technique. A tip, nominally 6 mm in diameter, was chosen because data presented by Harkins and Brown[97] indicates that, for water, a tip this size yields a value of $\psi(r/V^{1/3})$ of about 0.6. From Fig. 10 a value of this order is approximately constant over a wide range of $r/V^{1/3}$. Hence errors in $r/V^{1/3}$ will not cause significant errors in $\psi(r/V^{1/3})$.

Preparation of the tip is also important. All obvious flaws were removed by light polishing on 600 grit paper, which also provided the slight roughening to aid wetting of the tip[97]. After final preparation the tip radius was accurately determined using a cathetometer.

Eq. 31 indicates that the dropping tip should be held vertically. This is first considered in cutting and polishing the tip at right angles to the capillary walls, and secondly in supporting the tip in position by aligning visually with the support stand. Using this simple technique gave good reproducibility when tested with distilled water and was, therefore, deemed adequate.

From a knowledge of m and r, $r/V^{1/3}$ can be calculated, assuming that the specific gravity of

dodecylamine acetate solutions is 1.0[108]. Thus $\psi(r/V^{1/3})$ can be found and the surface tension calculated from Eq. 31. Duplicate tests were performed for each set of conditions.

Results

(a) Neutral Solutions

Agreement between the three techniques is good, the maximum bubble pressure tending to give the lowest surface tension values, as shown in Fig. 14. The maximum difference is about 5 dynes.cm^{-1}. Reproducibility of the results for individual methods is excellent, especially for the maximum bubble pressure and the drop weight. The capillary rise technique at 100 mg/l gives a scatter of nearly 5 dynes.cm^{-1}.

The shapes of the graphs are as expected from the theory. Initially there is little surface tension depression with increasing concentration. From 0 to 100 mg/l the surface tension has only dropped ~7 dynes.cm^{-1} to about 65 dynes.cm^{-1}. This corresponds to point A in Fig. 5. At concentrations greater than 100 mg/l the slope of the curves increases until the lowest surface tension value, approximately 28 dynes.cm^{-1}, is recorded at a concentration of 2850 mg/l (1.16 x 10^{-2}M). This corresponds to point B in Fig. 5, i.e. the critical micelle concentration or c.m.c. Agreement between the techniques on the c.m.c. is ± 200 mg/l. The measured surface tension at the c.m.c. varies from 27 dynes.cm^{-1} for the drop weight method to 30 dynes.cm^{-1} for the capillary rise technique. The surface tension increases slightly at concentrations greater than the c.m.c.,

FIGURE 14

SURFACE TENSION vs. DODECYLAMINE ACETATE
CONCENTRATION FOR NEUTRAL SOLUTIONS

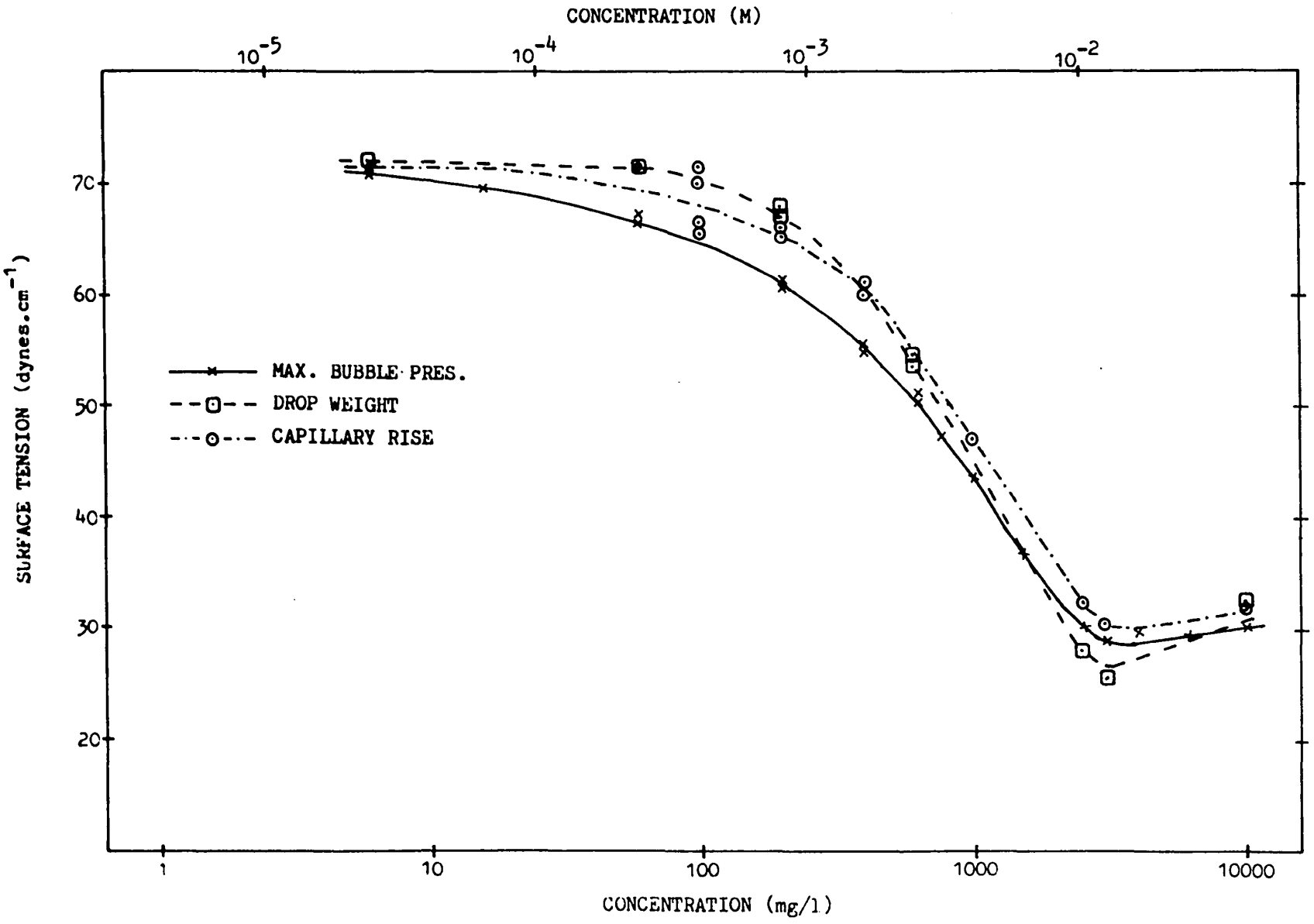
CONCENTRATION (M)
10^-5
10^-4
10^-3
10^-2
SURFACE TENSION (dynes.cm^-1)
70
60
50
40
30
20
MAX. BUBBLE PRES.
DROP WEIGHT
CAPILLARY RISE
1
10
100
1000
10000
CONCENTRATION (mg/l)

giving a value of 30 (maximum bubble pressure technique) to 32 dynes.cm^{-1} (capillary rise technique) at 10,000 mg/l. Thus, the surface tension - concentration curve suffers a minimum at the c.m.c.

(b) pH 4.1 ± 0.1 Solutions

The general shape of the curve and the agreement between the methods (see Fig. 15) is similar to that described for neutral solutions. Reproducibility is poorest for the capillary rise method. The difference between the curves at the two pH levels is a shift to higher concentrations in the case of pH 4.1 ± 0.1. This is demonstrated in the values of A and the c.m.c., which occur at about 250 dynes.cm^{-1} and at 3,800 mg/l (1.55 10^{-2}M) respectively. The c.m.c. again corresponds to the minimum surface tension measured, $\approx$ 30 dynes.cm^{-1} (given by all three techniques), and agreement between the methods at the c.m.c. is of the order of ± 200 mg/l.

(c) pH 9.5 ± 0.3 Solutions

Fig. 16 indicates that in comparison to pH 4.1 and neutral solutions, agreement between the methods is lacking at alkaline pH. The only similarity is that a significant surface tension depression is recorded at concentrations considerably less than are required for the equivalent effect

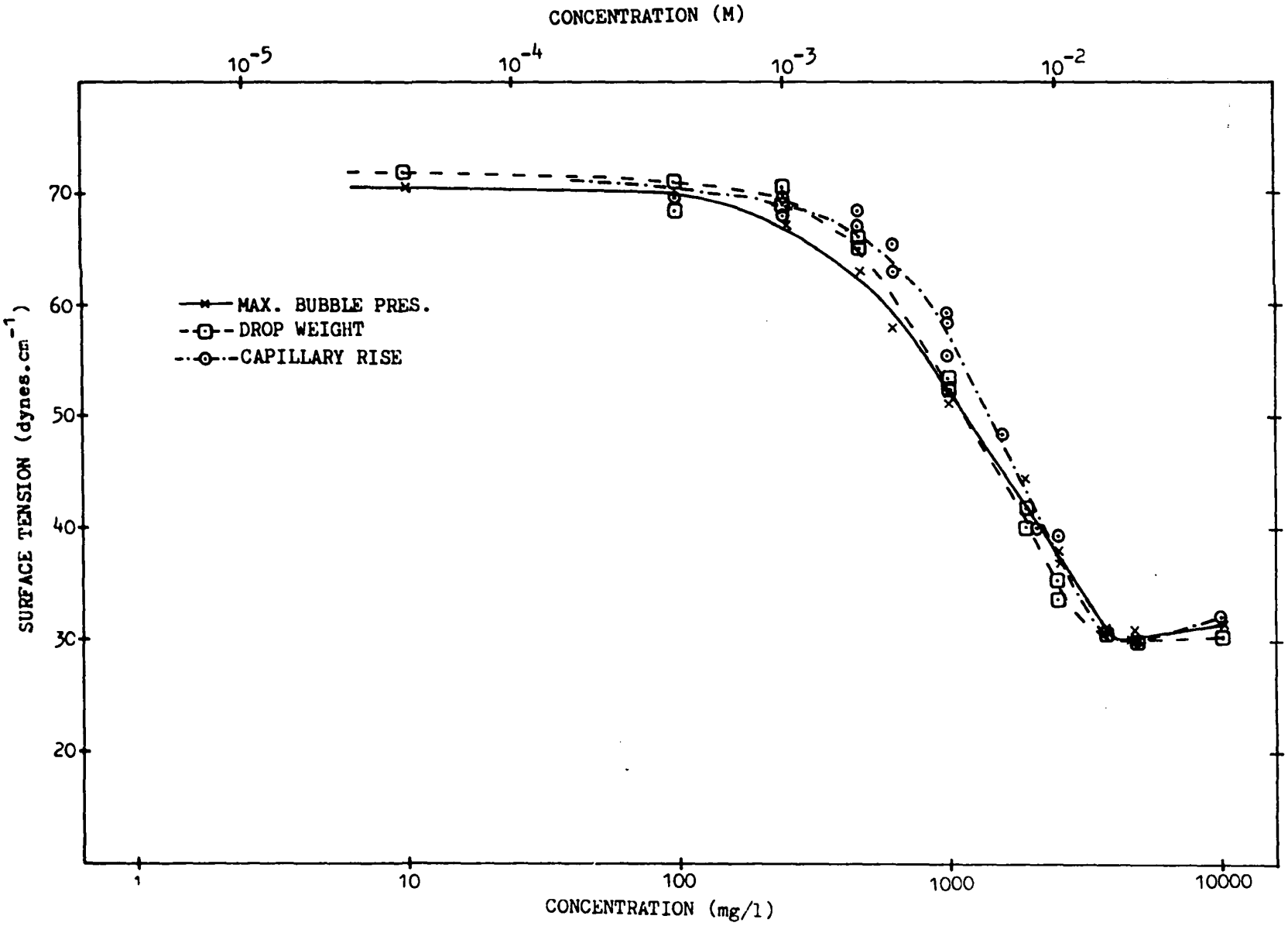
CONCENTRATION (M)
10^{-5}
10^{-4}
10^{-3}
10^{-2}
SURFACE TENSION (dynes.cm^{-1})
70
60
50
40
30
20
MAX. BUBBLE PRES.
DROP WEIGHT
CAPILLARY RISE
1
10
100
1000
10000
CONCENTRATION (mg/l)

FIGURE 16

SURFACE TENSION vs. DODECYLAMINE ACETATE CONCENTRATION FOR pH 9.5 ± 0.3 SOLUTIONS

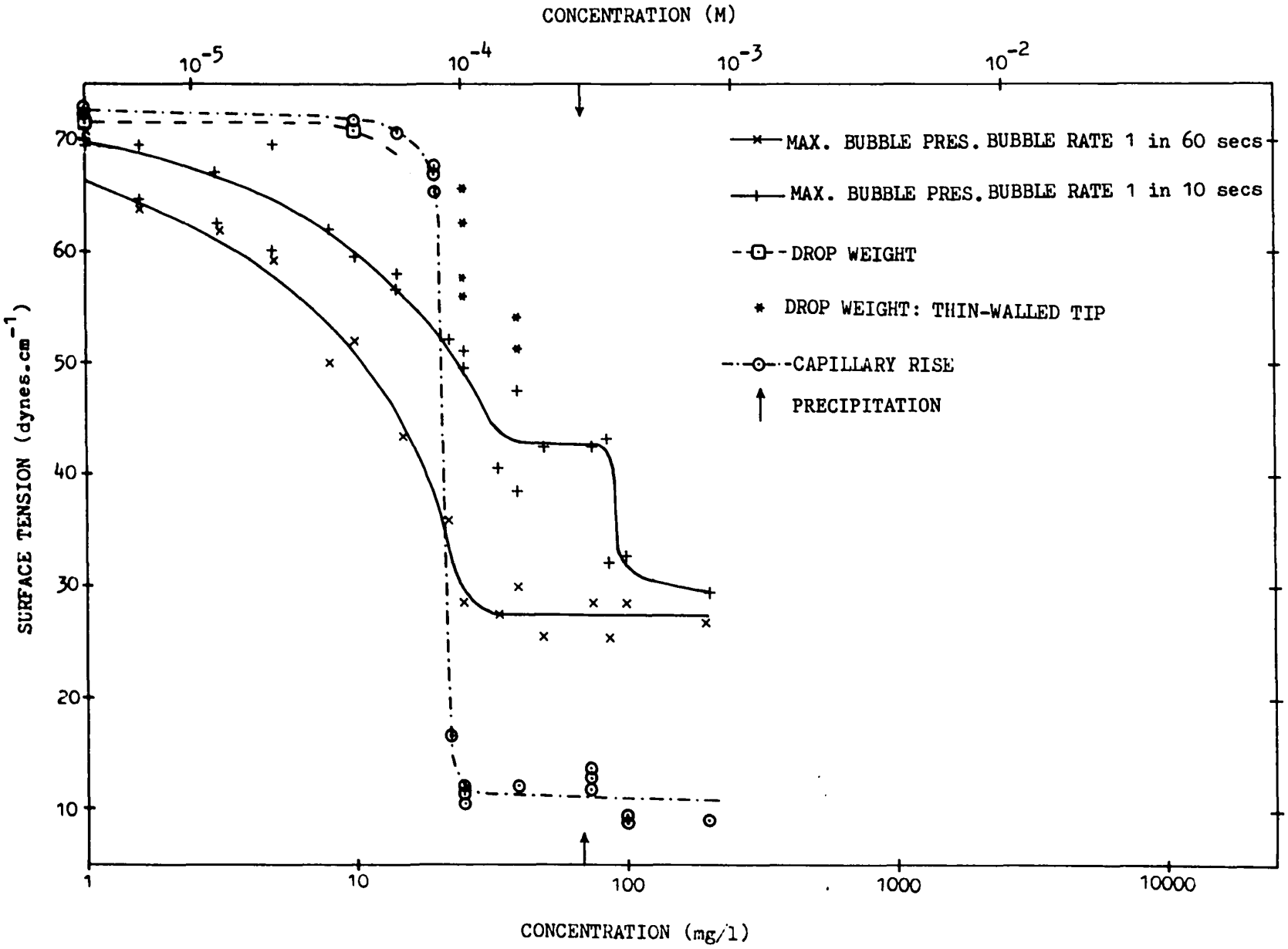
CONCENTRATION (M)
10^{-5}
10^{-4}
10^{-3}
10^{-2}
SURFACE TENSION (dynes.cm^{-1})
70
60
50
40
30
20
10
MAX. BUBBLE PRES. BUBBLE RATE 1 in 60 secs
MAX. BUBBLE PRES. BUBBLE RATE 1 in 10 secs
DROP WEIGHT
DROP WEIGHT: THIN-WALLED TIP
CAPILLARY RISE
PRECIPITATION
1
10
100
1000
10000
CONCENTRATION (mg/l)

in neutral or acid solutions. Concentrations up to only 200 mg/l were employed since considerable precipitation of free amine became visible. Precipitation is initiated at ~ 70 mg/l[64].

(i) Capillary Rise

There is negligible surface tension depression up to about 15 mg/l. Between 15 mg/l and 25 mg/l, the surface tension drops nearly 61 dynes.cm^{-1} to approximately 10 dynes.cm^{-1}. From the theory, 15 mg/l would appear to correspond to A and 25 mg/l to the c.m.c. At concentrations greater than the c.m.c., surface tension values appear constant. However, there is notable scatter of results.

(ii) Drop Weight

No measurements were taken at concentrations greater than 10 mg/l with the 6 mm diameter, thick-walled tip. The remaining values are measured by substituting a thin-walled tip. There is a significant scatter of these latter results. The indication is that little surface tension depression occurs below 10 mg/l, while between 10 mg/l and 20 mg/l a break in the curve occurs. In this respect the drop weight results are similar to those given by the capillary rise method. However, the results recorded by the thin-walled tip indicate much higher surface tension values in comparison to the capillary rise for the

same concentration levels.

(iii) Maximum Bubble Pressure

The value of the surface tension is dependent on the rate of bubbling. By bubbling slowly at 1 in 60 seconds the observed surface tension is up to 20 dynes.cm^{-1} less than that measured at the usual bubble rate of 1 in 10 seconds. However, reproducibility is not as good as that obtained at the lower pHs.

The 1 in 60 seconds curve and the 1 in 10 seconds curve have similar shapes. The value of A suggested is in the region of 1 mg/l, while interpreting the second change in slope as being the c.m.c. this latter value is about 30 - 35 mg/l (cf. capillary rise ~25 mg/l). The difference between the two curves is approximately 5 dynes.cm^{-1} at concentrations less than 10 mg/l, but scatter in the 1 in 10 seconds curve makes this unreliable. At concentrations greater than 10 mg/l the difference becomes more pronounced, and the scatter about each curve less. At roughly 25 mg/l the difference is about 20 dynes.cm^{-1} and this is maintained till about 80 - 100 mg/l. Thereafter, the indications are that the surface tension values are equivalent for both bubble rates.

$$\Gamma_{lv} = -\frac{1}{2.3RT}\frac{d\gamma_{lv}}{d \log c} \quad \ldots 11a$$

Hence, the observed increase in the slope between concentration 'A' and the critical micelle concentration is expected.

At the c.m.c., the solution surface is considered as saturated with a complete monolayer of surfactant species. By calculating the slope of the graph immediately prior to the c.m.c., a measure of the adsorption density of surfactant at the liquid - vapour interface is provided using Eq. 11a. Consequently the area occupied per dodecylamine species can be estimated. The values are given in Table 1.

TABLE 1

Solution pH	Adsorption density (10^{-10} moles.cm^{-2})	Area per molecule ($\AA^2$)
4.1 ± 0.1	6.9 ± 0.5	23.9 ± 2
neutral	6.4 ± 0.5	25.8 ± 2
9.5 ± 0.3		
a) 1 in 10 bubble rate	11.8 ± 1	14.0 ± 2
b) 1 in 60 bubble rate	9.0 ± 1	18.3 ± 2

The calculated area of 25.8 $\AA^2$/molecule agrees with the literature values quoted variously between 20.5 $\AA^2$/molecule[109]

and 30.0 A /molecule[110] for closely packed dodecylamine ions. Thus, at the c.m.c. a saturated monolayer coverage is approached. A possible conclusion is that micellisation occurs because the surfactant can no longer be accommodated in the interface.

The value of the c.m.c., $\sim 1.2 \times 10^{-2}$M, is the same as that given by Ralston[62], and the corresponding surface tension of 28 dynes.cm^{-1} given is of the same order as that obtained in the present investigation.

The tendency of the surface tension to increase at concentrations greater than the c.m.c. is generally ascribed to impurities[28,29,31]. However, the nature of the impurities is important since although this minimum is exaggerated by organic impurities[40,41], the same is not true for inorganic salt impurities[42,43]. Further, it appears that depression of the c.m.c. and lowering of the surface tension for a given concentration is a more pronounced aspect of the presence of impurities[40,42-44,111]. Considerable lowering of the c.m.c. of dodecylammonium chloride solutions is reported with 1-hexanol additions[44]. Since surface tension and c.m.c. depression is not reported along with noticeable surface tension rises, the case for impurities being responsible for the minimum in the surface tension - concentration curve is not entirely substantiated. The surface tension increase may be caused simply by the

presence of micelles in the solution interior.

Micelles, in comparison with the bulk solution, offer a greater attraction to the dodecylamine ions held at the surface. This is because the energy difference between the interface and the micelle is less than that between the interface and the solution bulk. Although this force might not actually promote negative adsorption, i.e. removal of solute from the interface, the effect of increased attraction into the solution will result in an increased surface tension. The attractive force will depend on the surface area of the micelles and their distance from the surface. As the concentration of solute increases, micelles become more numerous. Thus the surface area available increases and also the probability of more closely approaching the surface. The total attractive force will increase and an increase in surface tension will result.

Two operating problems were noted at this pH level:

(1) the difficulty in completely wetting the dropping tip at concentrations between 200 mg/l and 1,000 mg/l of dodecylamine acetate. This accounts for there being only one value obtained in this range, at 600 mg/l.

(2) the equilibrium time of up to sixty minutes found

in the capillary rise technique (see Fig. 17).

In the case of the dropping tip, the tendency to de-wet the glass (i.e. form a finite contact angle) corresponds to the development of a contact angle[6] and the floatability of quartz[112] in this concentration range. Thus the solution of dodecylamine acts as a de-wetting agent for the glass of the dropping tip.

The long equilibrium time noted for the capillary rise has been noted before[76] and is ascribed to surface aging[75,76]. This suggests that the solution surface is aging. Significant surface aging can be a property of surfactant solutions[47,50,58]. But, in the present case, the long equilibrium times involved in the capillary rise technique are not found in the other techniques and so it cannot be considered as a solution property alone. However, it is reasonable to suppose that the equilibrium time is due to a slow rate of solute accumulation at the surface. This may be due to the narrow capillaries in the equipment which contain the bulk solution from which the solute must be removed to the surface. Thus, the assumption that the bulk solution is an infinite source of solute, may not hold with this technique, except over extended times. This is not to say that the capillaries will actually affect the final equilibrium value, as very fine capillaries do[113-115] but might increase the time required to reach

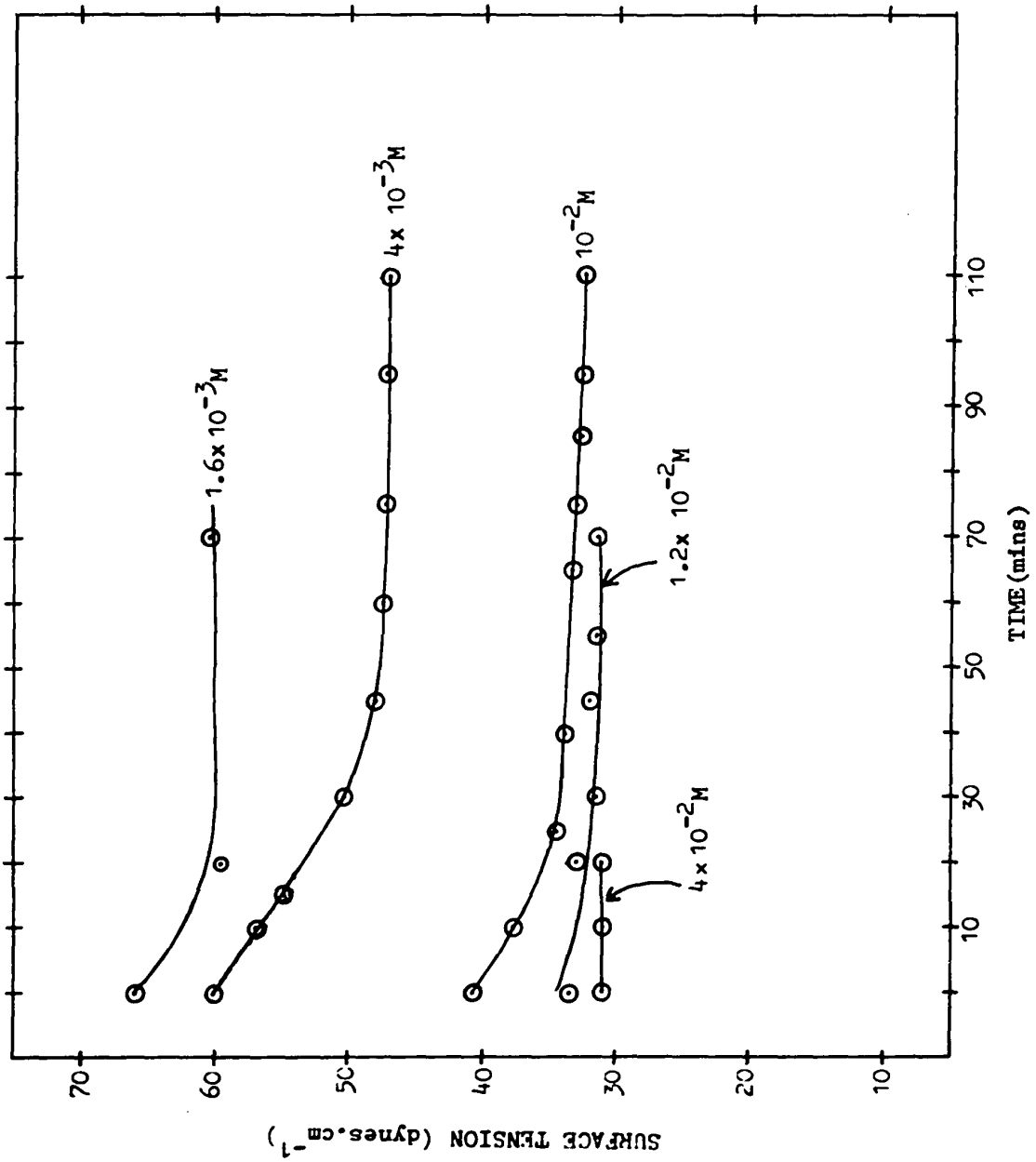
SURFACE TENSION (dynes.cm^{-1})
70
60
50
40
30
20
10
10
30
50
70
90
110
TIME (mins)
1.6x 10^{-3}M
4x 10^{-3}M
10^{-2}M
1.2x 10^{-2}M
4x 10^{-2}M

the equilibrium adsorption density demanded by the bulk concentration. This would lead to the pronounced equilibrium times observed. Because of this uncertainty, the tendency is to record surface tensions greater than the equilibrium value. The capillary rise does give consistently high values at concentrations less than the c.m.c. Also it is difficult to obtain good reproducibility when the time after surface formation is an unpredictable variable. Poor reproducibility, in comparison with the other two techniques, was observed in the present investigation as in previous work[76,82,83]. Tartar et al.[76] refer to 'mysterious fluctuations' in the capillary rise results 'which cannot be attributed to solution properties alone'.

The uncertainty in equilibrium time involved for any given solute concentration lends credence to the hypothesis of Adam and Shute[116] that the equilibrium surface tension value is the same for all concentrations, the latter only affecting the equilibrium time. This conclusion is discredited in results from the other techniques, but indicates the need to check the methods used.

A similar situation of physical restrictions on solute movement due to the equipment design may be present

in the drop weight technique. The solution is again held in a capillary tube. Although equilibrium times of such duration as found with the capillary rise technique are not indicated (reproducible results on drops only one minute old), it is notable that values tend to be high. This could indicate that the surface is not at equilibrium. The high values cannot be attributed to the method of drop formation, otherwise high values would be obtained for water; and, from Fig. 14, the highest surface tension recorded is 72 dynes.cm^{-1}. The good reproducibility in the technique also testifies to the success of the procedure.

In comparison, the maximum bubble pressure technique appears to be free of these design restrictions. The generation of the solution - gas interface is directly into the solution bulk, thus overcoming capillary restrictions being placed on the movement of the solute molecules.

The only feature which could be improved is the bi-fluid manometer. The experimental time per reading of about fifteen minutes was required due to a sluggish response on the part of the bi-fluid meniscus. This was due to preferential wetting of the glass walls by one of the fluids. A closer scrutiny of the wetting properties of the two fluids is required to overcome this phenomenon.

which gives rise to this effect on the surface tension at pH 4.1 is difficult to determine. It could be due to the increase in the hydrogen ion concentration, which enables the bulk solution to hold more dodecylamine ions, or it could be the reduced relative concentration of the free amine. If it is due to the latter, the extremely small concentration of free amine[66] indicates that the amine molecule plays an important role in determining the surface tension. Evidence presented at alkaline pH, where the concentration of amine molecules is comparable to the ionic concentration[64,66], does indicate the importance of the amine molecule.

The adsorption density was again determined prior to the c.m.c., and hence the area occupied per surfactant molecule. These figures are compared with those obtained at neutral pH in Table 1. There appears to be no significant pH effect. It is concluded, therefore, that the same surfactant species, in the same orientation, is present at the solution surface in both cases.

Testing at pH 4.1 ± 0.1 proved easier than in neutral solutions. This is especially true of the drop weight technique, where no de-wetting was encountered over the whole concentration range. This corresponds to the poor de-wetting characteristics of acid dodecylamine solutions

on oxides[6,27,117-119]. The capillary rise continued to give erratic readings although the equilibrium time is less evident. It is an interesting correlation that the decreased de-wetting power of the dodecylamine solutions corresponds to fewer operational difficulties as encountered at neutral pH. Overall, the drop weight and capillary rise still give higher results than the maximum bubble pressure method.

(c) pH 9.5 ± 0.3 Solutions

The extremely low concentration required to effect a noticeable surface tension depression ($\approx$ 10 mg/l) is due to the presence of the undissociated amine molecule, $C_{12}H_{25}NH_2$. The lack of a charged head group means that the hydrophobic alkyl chain, $C_{12}H_{25}$, predominates and adsorption at the liquid - vapour interface is strongly favoured. Even at 10 mg/l dodecyiamine acetate there is sufficient surfactant present to saturate the surface of a 0.25 cm diameter bubble blown into about 30 ml of solution, which corresponds to the present system using the large bore capillary.

Little previous work is available on the surface tension of alkali surfactant solutions. Manser[65] includes the surface tension - concentration curve for dodecylamine at pH 9.0 and Bartell[60] gives the curve for decylamine solutions at pH 10.2. Comparison of the present

data with that of decylamine solutions is valid since decylamine belongs to the same homologous series as dodecylamine. Both alkali solutions gave a shape of curve similar to those obtained at neutral pH in the present investigation. The only effect of increasing the pH was a lowering in surface tension for a given concentration. The minimum surface tension value is about 30 dynes.cm^{-1}, as with neutral pH[65]. This corresponds closely to the results for the maximum bubble pressure technique, using the 1 in 60 seconds bubbling rate. Assuming that no change in the shape of the curve will result from increasing the pH, several observations on the present data can be made.

(i) Capillary Rise

The sudden decrease in surface tension values between 15 and 25 mg/l is not characteristic of the solution alone. The indication is that at concentrations less than 15 mg/l, the surface tension observed is higher than the true equilibrium value, while at concentrations greater than 25 mg/l (c.m.c.) the surface tension is less than the equilibrium value. The former problem could be related to the restrictive effect of narrow capillaries proposed earlier. The latter is the result of contact angle development, so that $\gamma_{lv}\cos\theta$, the adhesion tension, is

being measured. Since $\cos\theta < 1$, $\gamma_{lv} \cos\theta < \gamma_{lv}$ and hence low values of calculated γ_{lv} are observed if cos θ is ignored. Contact angle development at pH 9.5 corresponds to the de-wetting power of alkali solutions of dodecylamine on oxide surfaces[6,27,117-119]. From a knowledge of $\gamma_{lv} \cos\theta$, with γ_{lv} known (determined by a method which is independent of contact angle considerations), θ can be calculated[27,81]. The development of the contact angle was much in evidence, with a notable straightening of the meniscus with time. Extrapolation of the results of Somasundaran[27] on the adhesion tension of dodecylamine against a glass capillary, indicate the same shape of graph, although at slightly elevated concentrations.

There was a tendency for some of the more concentrated solutions (> 40 mg/l) to give higher γ_{lv} values, indicating that θ was reducing. However, a decrease in pH was observed and was considered to be the cause of the increase in γ_{lv}.

(ii) Drop Weight

Concentrations between 0 and 10 mg/l give similar surface tension results to those from the capillary rise technique. At concentrations greater than 10 mg/l, it proved impossible to wet the dropping tip completely. After the formation and detachment of one drop, the following drop retreated from the edges of the tip, indicating a

significant, finite contact angle development. This phenomenon corresponds to the findings discussed at this concentration level in the capillary rise technique. The resulting drop weight will not accurately reflect the liquid surface tension according to Eq. 30, because 'r' is unknown. The effect of the contact angle in the capillary rise method can be estimated, but this is not so in the case of the drop weight, where the contact angle and 'r' will have a complex relationship. Therefore, the technique can be considered as having failed at concentrations greater than 10 mg/l. A thin-walled tip was substituted in an attempt to overcome the de-wetting problem, as suggested by Fowkes[78]. Drops were successfully drawn, but reproducibility was poor. A break in the curve between 10 and 20 mg/l is suggested but the surface tension value for concentrations greater than 20 mg/l are high when compared to equivalent concentration results given by the bubble pressure and capillary rise techniques. These observations indicate non-equilibrium conditions.

(iii) Maximum Bubble Pressure

The problem of decreasing pH, noted in the capillary rise experiments, became a major problem with the maximum bubble pressure technique. Unlike in the capillary rise and drop weight experiments, it was difficult

to obtain a γ_{lv} determination with the bubble pressure method using the procedure outlined without incurring a pH decrease. De Bruyn[66] noted this tendency of the pH to decrease and attributed it to the presence of the dodecylamine. Noting that work by Partridge[120] and Hendriks[121] in this laboratory at similar pH levels gave no pronounced pH drift when the solutions were held in air-free stoppered vials, atmospheric carbon dioxide is considered responsible. The act of bubbling air into the solution accounts for the significant pH drift which only occurred after long exposure to the atmosphere in the capillary rise experiments.

In an attempt to control this contamination, the pear-shaped funnel, F, was removed and the tube, X, connected to a pure nitrogen (99.99%) source (see Fig. 12). Monitoring of the solution pH still showed some drift; 9.5 ± 0.3 was the range inside which the experiments were conducted. Complete elimination of carbon dioxide is impossible since some air is left between joint J and the tip of the capillary in the bubbling unit after the unit is put in place. Further, the bubbling unit is open to the air via the tube previously connected to the pear-shaped funnel, F.

With this precaution, and testing only solutions which fell in the pH range 9.5 ± 0.3, it became clear that only by controlling the bubble rate could reproducibility

for decylamine solutions[60].

(2) Considering the curve resulting from a bubble rate of 1 in 60 seconds, the lowest surface tension value of approximately 26 dynes.cm^{-1} compares favourably with the minimum recorded at the other pHs[65]. Such an argument seems valid since, at the c.m.c., the surface is covered with a monolayer of surfactant. Therefore the surface tension measured is that of the surfactant itself. Consequently as the surface tension will be dominated by the hydrocarbon chain[58], the chain form should have little effect on the surface tension.

(3) From the 1 in 60 seconds curve, it is noted that for any given surface tension, the corresponding concentration at neutral pH is approximately one hundred times greater. The same relationship was found for decylamine[60].

Of the three techniques, therefore, the results of the maximum bubble pressure technique alone are free from interaction between the solution and the equipment. This bubble rate phenomenon must be interpreted as a dynamic surface tension effect, i.e. reproducible surface tension values which do not correspond to the equilibrium surface tension value[47].

Lange[47] noted two mechanisms which can give rise to a dynamic surface tension value; aging and the variable interface effect. By observation, bubble generation follows the sequence:

(1) The meniscus in the capillary develops the hemispherical shape, then remains unchanged;

(2) Rapid expansion of the surface as the bubble grows and breaks away.

Thus both the mechanisms described by Lange[47] occur; (1) indicating surface aging and (2) a variable interface. The present experiments indicated that process (2) was negligible in comparison to (1). The interface tended to adopt its final shape almost immediately, inside the capillary. Adsorption occured which reduced the surface tension until ΔP_{max} was sufficient to cause the bubble to grow rapidly and break away. Austin et al.[71], Kuffner[57] and Bendure[90] confirm these observations. The bubbling rate phenomenon is, therefore, indicative of a surface aging property. The bubbling rate of 1 in 10 seconds represents surfaces ten seconds old; 1 in 60 seconds, surfaces sixty seconds old. Fig. 18 is a graphical interpretation of the surface aging.

The apparent absence of surface aging at low pHs substantiates the work of Ralston[67], Morrow[6] and Somasundaran[27]. Recently, however, Kloubek[88] has

FIGURE 18

SURFACE AGING OF pH 9.5 ± 0.3
DODECYLAMINE ACETATE SOLUTIONS
- MAXIMUM BUBBLE PRESSURE METHOD

demonstrated that dodecylamine solutions do have an aging time. In a solution of 10^{-3}M dodecylamine at pH 4.0, the aging time was of the order of 10 seconds. Between 0 and 10 seconds the surface tension dropped about 9 dynes.cm^{-1} while from 10 to 1000 seconds a further drop of only about 1 dyne.cm^{-1} was recorded. Thus, on surfaces older than 10 seconds reproducibility to better than 1 dyne.cm^{-1} can be expected. This criterion applies to all the previous work, the surfaces on which measurements were made were older than ten seconds. Similarly with the present experiments, the capillary rise and drop weight methods measure the surface tension of surfaces at least one minute old, and in the maximum bubble pressure the use of a 1 in 10 second bubble rate indicates that the surfaces are 10 seconds old. Dodecylamine solutions do, therefore, possess a surface aging property. At alkaline pH the surface aging property becomes exaggerated. Surface aging is controlled either by the 'rate of diffusion' or the 'rate of real adsorption'. The presence in solution at pH 9.5 of a significant quantity of amine molecules, which is all that distinguishes the solution at pH 9.5 from the lower pH values, must reduce the rate of one or other of these mechanisms. This observation has not been made previously, although indirect evidence has been presented by Smith[123] in his paper on dynamic contact angles, the significance of which

will be discussed later.

Assuming diffusion control, the theory of Ward and Tordai[54] can be applied to the data. Taking a bulk concentration, C , of 10 mg/l (4×10^{-5}M) the calculated value of D is about 5×10^{-7} $cm^2.sec^{-1}$ (see Appendix III). This is close to the classical range, $10^{-6} - 10^{-5}$ $cm^2.sec^{-1}$. The implication is that the undissociated amine molecule diffuses more slowly than the aminium ion, yet previously it was shown to be more hydrophobic and, therefore, possess a greater tendency to reside in the liquid - vapour interface. Furthermore, the size of the free amine molecule and the ion are similar and according to the Stokes-Einstein[54] equation,should possess a similar diffusion coefficient. Defay and Hommelen[50] showed that an increase in chain length decreased the diffusion coefficient. It is possible that molecular aggregates or complexes form in alkaline dodecylamine solutions at concentrations less than the c.m.c.

Formation of molecular aggregates at concentrations less than the c.m.c. is not unknown[35]. Kung and Goddard[124] conclude that association of mixed long chain groups can occur from a differential thermal analysis on the binary system sodium dodecyl sulphate and dodecyl alcohol. Harkins et al.[44] found that alcohol additions to dodecylamine chloride solutions lowered the c.m.c.

which was explained by association between aminium ions and alcohol molecules. The changes in adsorption characteristics and flotation recovery occuring upon addition of polymers (e.g. ethylenadiamine) in the systems dodecylamine - quartz or magnetite was attributed by Ghigi[125,126] to complex formation. The presence of decyl alcohol was found by Fuerstenau et al.[127] to increase the flotation rate of corundum with trimethyldodecylammonium chloride as collector. Complex formation was considered to have occured, although Fuerstenau et al.[127] considered complex formation specifically at the solid - liquid interface. Similarly, Iwasaki et al.[128], Partridge[129] and Hendriks[121] conclude that complex formation occurs between dodecylamine ion and starches at the solid - liquid interface, in order to account for the amine adsorption characteristics in the hematite - dodecylamine - starch system. Complex formation in the solution bulk and subsequent adsorption at the solid - liquid interface would have the same effect.

Evidence for molecular aggregation is plentiful, including the dodecylamine system. In all cases a non-ionised molecule is involved. Since bringing ionic head groups together requires energy, complexing between ions and molecules or molecules and molecules is energetically

easier. The extension of the previous work is to suggest that dodecylamine ion or molecule can not only complex with alien molecules but with themselves. Ion-ion aggregates are unlikely due to the charged heads, but the presence of the undissociated amine molecule at pH 9.5 indicates that ion-molecule or molecule-molecule aggregation could occur. Thus complexing is favourable at alkaline pH, but not at neutral or acid pH, and as such could promote diffusion control of the surface aging observed at pH 9.5.

The structure of these complexes is not known, although the long hydrocarbon chains are believed to become interlinked. In this respect there are similarities to the proposed structure of micelles. From Fig. 16, clearly surface aging occurs at concentrations greater than the indicated c.m.c., in fact an increased surface aging is suggested. Micellar-like aggregates may form at concentrations less than the c.m.c. but not become a significant factor until the c.m.c. is reached. Surface aging may, therefore, result from the diffusion of micellar-like aggregates.

An added consideration at alkaline pH is that the free amine molecule is subject to complexing by reaction with carbon dioxide. Industrially, carbon dioxide is not removed from the air supply. As such the possibility of carbon dioxide promoting a surface aging property in

alkaline solutions of dodecylamine takes on greater significance.

The possibility of complex formation by reaction with carbon dioxide or molecular association can be checked. Firstly, elimination of all traces of carbon dioxide should eliminate the surface aging property. If not, careful measurement of the change in surface aging time for a given concentration at increasing pH would indicate consequent time variations. If amine molecule - amine ion association occurs the longest time would be at pH 10.7, when the concentration of amine molecule in solution is equal to that of the amine ion[66]. At higher pH the surface aging time should become less as the ratio of undissociated to dissociated amine becomes unfavourable to the latter. A continued increase in surface aging time would suggest that complex formation was occuring between undissociated amine molecules.

The rate of real adsorption concept has not been reduced to a general mathematical model. Its presence as the rate controlling mechanism is inferred if the calculated value of the diffusion coefficient is significantly less than 10^{-6} $cm^2.sec^{-1}$ [54]. Evaporation of a hydration layer which builds up around an ionised group in aqueous solution and an electrical energy barrier have been considered as giving rise to a reduced rate of real

adsorption. However, both are intimately connected to the presence of the ionic group. Since no surface aging is noted in solutions where the ionic form dominates (i.e. pH 4.1 and neutral pH) it is possible to eliminate these two processes as being responsible for pronounced surface aging at alkaline pH.

Randomly oriented molecules can also promote surface aging by reducing the rate of real adsorption[58]. In the present case free amine molecules, or the proposed complexes could randomly orientate at the surface. This is considered possible since the predominance of the hydrocarbon chain suggests that orientation in any direction, and not simply vertically, can be accommodated energetically. Since this applies to the proposed complexes too, disproving diffusion control does not eliminate complex formation as being responsible for the surface aging property.

Evidence for randomly oriented molecules at the liquid - vapour interface is given by the adsorption densities calculated from the 1 in 10 and 1 in 60 seconds bubble rate curves at concentrations just less than the c.m.c. The indication is that the adsorption density for a ten seconds old surface is greater than for a sixty seconds old surface. These apparently illogical results are supported by the observations of Addison[55] on

solutions of alcohols. Since surface tension decrease is related to the surface occupied by surfactant, the orientation of the surfactant molecules is important. Randomly oriented molecules occupy more surface area per molecule than vertically oriented molecules. Hence randomly oriented molecules will cause a greater surface tension decrease per molecule. Measuring the adsorption density from a surface tension decrease vs. concentration increase using the Gibbs adsorption equation will indicate a greater adsorption density for randomly oriented molecules than for vertically oriented molecules. The tendency for the adsorption density to be higher for the younger surface may be a reflection of random orientation at the liquid - vapour interface. As the surface ages, the molecules re-orientate such that at equilibrium the adsorption density is the same as that measured for neutral and acid pH. This trend is indicated in Table 1, the 1 in 60 curve tending to the adsorption density of surfactant calculated for neutral pH. Equilibrium surface tension measurements on decylamine solutions[60] indicate that the adsorption density at surfactant concentrations approaching the c.m.c. is the same at pH 10.2 as for neutral solutions.

It is impossible to conclude in favour of either rate controlling mechanism, diffusion or real adsorption. Much greater control over the bubble rate and pH drift is

FIGURE 19

PRECIPITATION AND CRITICAL MICELLE CONCENTRATION
vs. pH FOR DODECYLAMINE SOLUTIONS

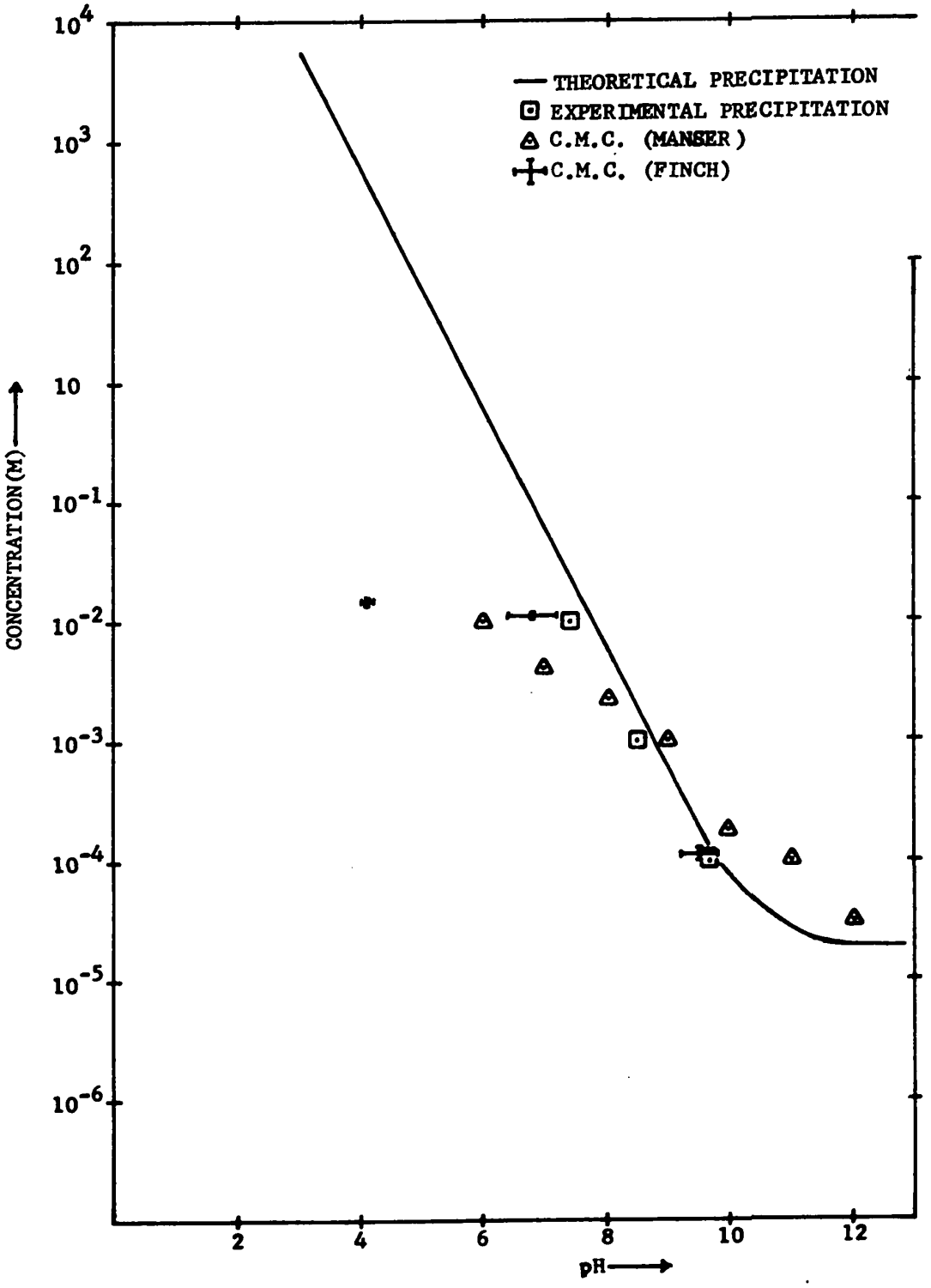
THEORETICAL PRECIPITATION
EXPERIMENTAL PRECIPITATION
C.M.C. (MANSER)
C.M.C. (FINCH)
CONCENTRATION (M)
pH
10^4
10^3
10^2
10
10^{-1}
10^{-2}
10^{-3}
10^{-4}
10^{-5}
10^{-6}
2
4
6
8
10
12

TABLE 2

Solution pH	c.m.c. (mg/l)
4.1 ± 0.1	3,800 ± 200
neutral	2,850 ± 200
9.5 ± 0.3	30 ± 5

The present data indicate a reasonable correlation between the c.m.c. and the precipitation curve at pH greater than 7. At pH 4.1, however, there appears to be no comparable relationship. As the pH increases, it becomes difficult to distinguish the c.m.c. from the precipitation curve. This is accentuated by the coincidence of the c.m.c. determined in the present investigation at pH 9.5 and the experimental precipitation pH of 9.7 - 9.8 obtained by Partridge for a 10^{-4}M solution of dodecylamine. Further, Manser[65] indicates c.m.c. values at concentrations greater than the precipitation point for pH values greater than ~8.5.* This is especially noticeable at pH 11 and 12. No mechanism is apparent to explain micelle formation at concentrations greater than are required to form a precipitate. Ignoring adsorption of amine on the glass walls of any containing vessels would lead to over-estimating the bulk solution concentration.

*Manser gives no details on the surface tension technique employed for determining the c.m.c.

The possibility that the c.m.c. value obtained at alkaline pH by the discontinuity in the surface tension vs. concentration curve is actually a phase transition (i.e. amine precipitation) cannot be ruled out. Bartell[60] concluded that for solutions of decylamine at pH 10.2 precipitation occured before the c.m.c. was reached. Decylamine is some ten times as soluble as dodecylamine, so the likelihood of precipitation with the latter is greater.

Conclusions

(1) The method employed for surface tension determination can affect the observed results.

(2) The maximum bubble pressure technique is free from interaction between the equipment and the test solutions of dodecylamine acetate.

(3) Dodecylamine solutions possess a surface aging property which becomes more pronounced at pH 9.5 in comparison with pH 4.1 or neutral solution.

(4) The presence of undissociated amine molecules is responsible for the surface aging effect. It is not proven whether the surface aging is due to a reduction in the rate of real adsorption (randomly oriented lone molecules or complexes) or a reduction in the rate of diffusion through the bulk solution (complexes). The complexes could be due to amine molecule - ion association or reaction between undissociated amine and carbon dioxide to form carbonates or carbamates.

(5) The area occupied per molecule at the liquid - vapour interface at equilibrium is unaffected by pH and has a value of approximately 25 $Å^2$/molecule.

(6) The c.m.c. values change little in the acid region, but reduce considerably in alkaline solutions. Measurements of the c.m.c. in alkaline solutions are difficult to distinguish from the precipitation point.

CHAPTER THREE

CONTACT ANGLE

Theory

A contact angle occurs whenever three phases meet along a common boundary. The magnitude of the contact angle is a measure of the balance between the three interfacial tensions and indicates the ease with which one phase will replace another. In flotation, the three phases are: vapour (moisture-laden air), liquid (collector solution), and solid (mineral particle). Considering the mineral substrate as inflexible, the contact angle, θ, measured by convention through the liquid phase, develops as shown in Fig. 20.

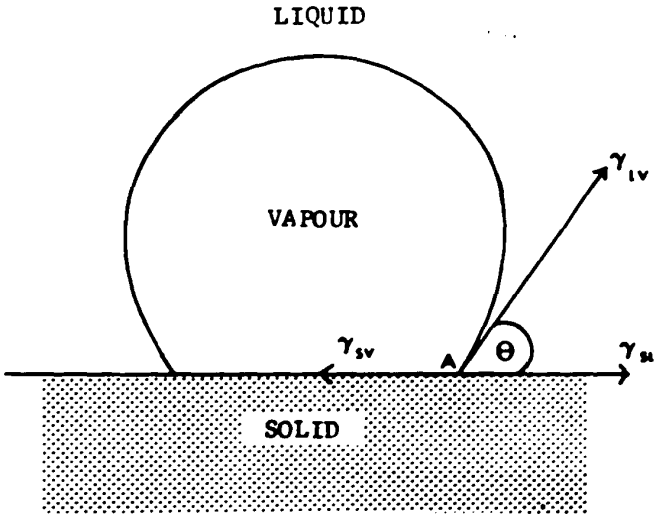

Figure 20. Bubble - Solid Equilibrium.

Thus, θ measures the ability of the vapour phase to replace the liquid phase. As θ increases the vapour phase becomes more energetically favoured at the mineral surface. Assuming equilibrium at **A** (a point along the common boundary), the Young equation (Eq. 5) can be derived:

$$\gamma_{sv} - \gamma_{sl} = \gamma_{lv} \cos \theta \qquad \ldots 5$$

For finite contact angle development:

$$\gamma_{sv} - \gamma_{sl} < \gamma_{lv} \qquad \ldots 32$$

Eq. 32 indicates that for flotation, it is desirable that γ_{lv} should be large, γ_{sl} large and γ_{sv} small. Under equilibrium conditions, the Gibbs adsorption equation applies to all the interfaces; solid - vapour, solid - liquid and liquid - vapour[26-28]. To meet the above requirements, therefore, adsorption of surfactant at the solid - vapour interface is desirable but not at the other two interfaces. Overbeek et al.[26] showed this mathematically, indicating that $\Gamma_{sv} > \Gamma_{sl}$ holds for finite contact angle development. Aplan and de Bruyn[130], Somasundaran[27], Smolders[28], and Sandvik and Digrè[69] have demonstrated that $\Gamma_{lv} > \Gamma_{sl}$ occurs in contact angle development, and that $\Gamma_{sv} > \Gamma_{lv}$ often occurs at low surfactant concentrations[27,28,69].

Little attention has been given to the dependence of contact angle (and hence floatability) on the relative adsorption densities of surfactant at the three interfaces.

However, substantial investigation into the relationship between contact angle and mineral floatability has been carried out[6,123,131-136]. An increase in θ indicates that the presence of the vapour phase is energetically favoured at the mineral surface and thus flotation is promoted. Attempts to verify this correlation have had varied success[135]. A tentative conclusion is that development of a contact angle is a pre-requisite to flotation, and that for $\theta > 40^{o}$ flotation recovery is good[119]. However, Kim[117,137] demonstrated that 100% recovery of magnetite in alkaline dodecylamine solution was possible at concentrations greater than 2×10^{-4}M, when the measured contact angle was zero. Similarly, Iwasaki et al.[138] observed zero contact angle on goethite with dodecylamine solutions under conditions yielding 100% flotation recovery.

(a) Relationship between θ and γ_{lv}

The variation in θ with γ_{sl}, γ_{sv} and γ_{lv} is impossible to determine because of the non-measurable terms γ_{sl} and γ_{sv}. However, the effect of varying γ_{lv} on θ can be investigated. Zisman[15] has studied this relationship for low surface energy solids. These are solids which naturally form a finite contact angle with pure water, as opposed to the high surface energy solids generally

encountered in flotation, where water naturally wets the solid surface. Zisman showed that for a given solid, tested against pure liquids of known surface tension γ_{lv}, the resulting cosine of the contact angle varied as in Fig. 21.

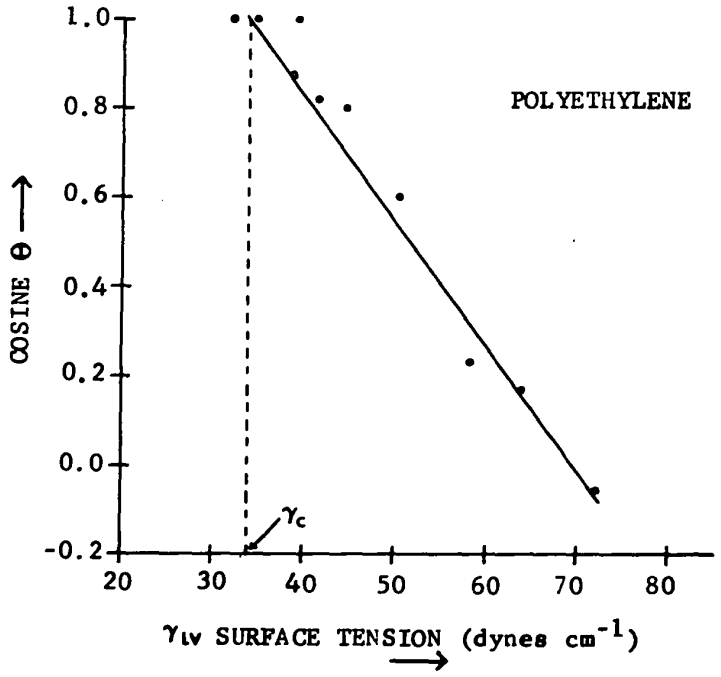

Figure 21. Variation of $\cos\theta$ with γ_{lv} for a Low Surface Energy Solid (after Zisman[15]).

The straight line intercepted cos θ = 1 (i.e. θ = 0) at a value of γ_{lv} which was characteristic of the solid surface[15]. This value of γ_{lv} he termed the 'critical surface tension' of wetting, γ_c. A finite contact angle will develop on a solid if $\gamma_{lv} > \gamma_c$. If $\gamma_{lv} < \gamma_c$, the

liquid wets the solid.

The physical significance of γ_c is not known[20]. Attempts have been made to relate γ_c to the surface tension of the solid. It is proposed that $\gamma_c = \gamma^d$, the dispersion force contribution to the solid surface tension[20]. For most minerals in flotation systems, γ_c is greater than the surface tension of water. The addition of surfactant reagents results in the formation of a contact angle. From Zisman's model, this is interpreted as indicating that the effective γ_c has been reduced such that $\gamma_{lv} > \gamma_c$ holds. Adsorption of the low surface energy surfactant at the solid surface must occur, progressively converting the high surface energy solid into a low surface energy solid, and consequently reducing the γ_c. Thus, $(\gamma_{lv} - \gamma_c) > 0$ is equivalent to the mineral surface being rendered hydrophobic. Any factors which affect the relative values of γ_{lv} and γ_c will affect the mineral's susceptibility to flotation. The effect of the solution surface tension on the magnitude of θ, although implied[119], has received little attention in flotation studies.

(b) Contact Angle Hysteresis

The value of the measured contact angle depends on the relative motion of the liquid - vapour interface with respect to the solid substrate. If the liquid is advancing

to wet a previously non-wetted (or de-wetted) surface the measured contact angle is called an "advancing" contact angle, θ_A. As the liquid phase retreats to expose fresh surface to the vapour phase, the resulting contact angle is a "retreating" contact angle, θ_R. The general observation is that $\theta_A > \theta_R$ [15,113,139-146]. The difference ($\theta_A - \theta_R$) is termed "contact angle hysteresis".

Both an advancing and a retreating liquid - vapour interface occur in flotation. In order to achieve replacement of the liquid by vapour, the liquid - vapour interface must retreat. This is governed by θ_R. Similarly the liquid must be prevented from advancing to re-wet the surface, and this is governed by θ_A. Fig. 22 indicates the physical interpretation of the phenomenon, $\theta_A > \theta_R$.

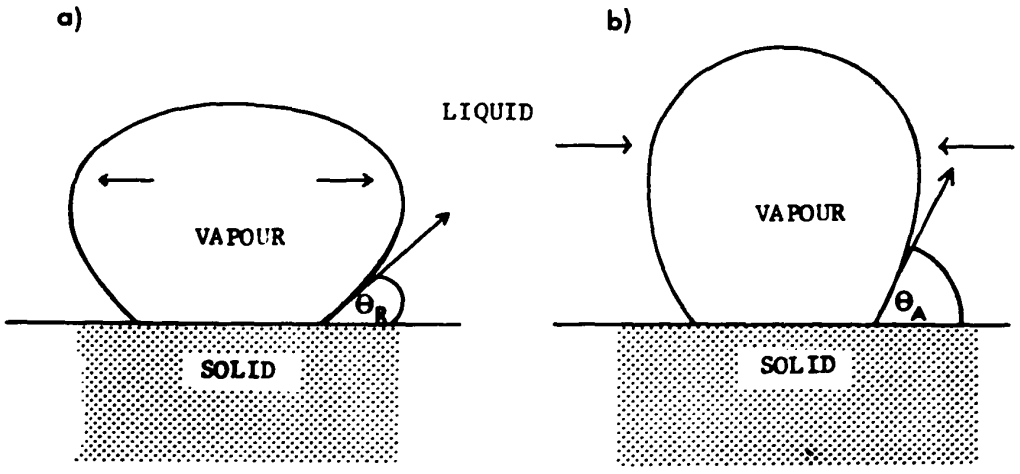

Figure 22. Physical Significance of $\theta_A > \theta_R$.

Condition (a) represents the vapour phase attempting to spread, i.e. generation of θ_R. Condition (b) represents the converse, with consequent development of θ_A. $\theta_A > \theta_R$ follows if the three-phase boundary of contact does not move, indicating that it is difficult to re-wet a surface once the liquid has retreated[113].

The stability of the three-phase perimeter of contact can be the result of differences in the adsorption density between the wetted and non-wetted surfaces[135,147]. Variations in surfactant adsorption density at the three interfaces were considered earlier. Somasundaran[27] and Sandvik and Digre[69] have shown that in flotation systems, $\Gamma_{sv} > \Gamma_{sl}$ holds.

Adam and Jessop[148] considered that contact angle hysterisis was due to frictional forces. From this assumption they showed:

$$2 \cos \theta_E = \cos \theta_A + \cos \theta_R \qquad \ldots 33$$

where θ_E is the so-called equilibrium contact angle. For angles between 45° and 135° an error of only 2° arises if Eq. 33 is reduced to:

$$\theta_E = (\theta_A + \theta_R)/2 \qquad \ldots 34$$

Observed variations in the measured contact angle, notably in the captive bubble technique, are averaged and

θ_E taken as representative[135].

Harkins and Fowkes[149] support the concept of frictional forces, noting that contact angle hysteresis was destroyed after carefully polishing the solid substrate. However, MacDougall and Okrent[143] indicate that θ_A is equal to θ_E, and recently Morrow et al.[144] have verified the equality. This implies that quoted contact angle variations[135] are the result of random variations about a mean (i.e. θ_A) and not due to contact angle hysterisis. Contact angle data derived from the captive bubble technique indicates the energy available to prevent re-wetting of the solid. The energy change involved in replacement of the liquid (i.e. the first stage in successful flotation) is not assessed.

Shuttleworth and Bailey[150] considered that contact angle hysteresis was due to surface roughness. No surface on which contact angle measurements are made is truly smooth. A rough surface has a greater surface area than a smooth surface. The vapour phase can readily occupy the entire, true surface available (f_1), while the liquid phase occupies only an apparent surface area (f_2), where $f_1 > f_2$. On replacing the liquid at the mineral surface, it appears that added surface is generated, ($f_1 - f_2$). Wenzel[151] showed that:

$$\cos \theta^1 = r \cos \theta \quad \ldots 35$$

where $r = f_1/f_2$ and θ^1 is the 'apparent' contact angle as opposed to θ, the 'real' contact angle. The 'real' contact angle will only be obtained by close examination of an element of the surface which appears smooth[141]. The measurement appears to be somewhat arbitrary since on a molecular level, the surface can never be smooth. Cassie[140] considered that the inability to repeat surface preparation resulted in the many different published values for the contact angle of a given liquid and solid.

The rough nature of the solid surface hinders movement of the liquid - vapour interface across the solid surface. Lack of such movement causes $\theta_A > \theta_R$, i.e. contact angle hysteresis[135]. Thus surface roughness aids the maintenance of bubble - particle contact but hinders the actual development of bubble - particle contact. The latter was observed by Mitrofanov[152,153] who concluded that isolated pockets of liquid are left behind due to surface roughness and consequently the surface tends to remain wetted. Measurement of surface roughness and, therefore, determination of its role in flotation, is extremely difficult. Certainly, mineral particles to be floated will always possess a considerable degree of roughness, which will interfere with the correlation of floatability with contact angles derived from carefully

polished specimens[144,154].

Contact angle hysteresis is believed to occur whenever successful flotation occurs[135]. Several workers have attempted to relate θ_A, θ_R and $(\theta_A - \theta_R)$ to mineral floatability[133,155,156]. However, Cassie[140] and MacDougall and Okent[143] have demonstrated that θ_R is a variable quantity, implying that $(\theta_A - \theta_R)$ is impossible to quantify. Gaudin[135] considered that contact angle hysteresis was simply another product of the same factors which promoted flotation. Recently, Morrow et al.[144], using the suction potential technique, showed that a measure of θ_R was obtained in the galena - xanthate system, yielding $\theta_R \approx 1/3\ \theta_A$, suggesting a reliable measure of θ_R could be made, and hence $(\theta_A - \theta_R)$ calculated.

(c) Dynamic Contact Angles

Using the captive bubble technique, Smith and Lai[123] have reported a phenomenon they term a "dynamic contact angle". In 10^{-4}M dodecylamine solutions at pH $>$ 9.1, contact angles on carefully prepared silica substrates were found to be about 80^o at the onset of bubble - particle contact. The magnitude of the contact angle was then observed to decrease to zero after about 100 to 120 seconds. Also reported was that, if the bubble was allowed to age in the solution prior to contacting the

silica surface, the resulting contact angle was negligible, or even zero.

Smith and Lai indicate that from the Young equation, a decreasing surface tension over this period of time (i.e. surface aging) would account for the observations. They claimed this could not be the case since γ_{lv} does not reduce sufficiently to give rise to a contact angle decreasing from 80^{o} to zero. Assuming γ_{sl} and γ_{sv} to be unchanged over the time interval considered, then a drop in surface tension from 70 dynes.cm^{-1} to the minimum of 30 dynes.cm^{-1} is indeed insufficient. Further, they observe that since the phenomenon does not occur below about pH 9.1, surface aging of the solution must be ruled out, the implication being that surface aging will be unaffected by pH. They concluded that the bubble 'stripped off' some of the surfactant adhering to the solid, so that γ_{sv} tended to increase. From the Young equation, a large value of γ_{sv} is detrimental to bubble - particle contact.

The observations of Smith and Lai are not unique. Wark[157] in 1936 reported that an aged bubble exhibited a smaller contact angle than a fresh bubble. He considered that an increase in the adsorption density of ionised surfactant had occured at the bubble surface (i.e. liquid - vapour interface). The bubble became charged and consequently less able to accommodate itself on the surfactant-coated

mineral surface. The term, 'bubble armouring', was adopted to describe this aged bubble effect[158,159]. Rogers et al.[160] in 1946 reported a similar non-contact when the bubble had aged in the solution. Rogers considered a wetting layer developed on the aged bubble, preventing adherence to solid, and showed that, if the bubbles were fresh, flotation recovery was improved[161]. The observations of Wark[157] and Rogers[160] were not pursued because the phenomenon only occured in concentrated collector solutions, outside the concentration range required for successful flotation. In the case of Smith and Lai[123], the concentrations considered are close to those used for flotation.

In a discussion of this paper of Smith and Lai, Leja[162] stated that he and Schulman had observed similar dynamic contact angle effects with both alkylamine hydrochloride and salts of alkyl sulphates at concentrations just below the c.m.c.[163]. Leja observed that only the liquid - vapour interface was capable of the rapid changes in surfactant adsorption density required to account for the dynamic contact angle effect. Noting that dynamic contact angles were found only in alkaline solutions, the undissociated amine was considered to be able to pack closer in the liquid surface since the repulsive force of the charged head group is absent. 'Progressive condensation'

occured giving a decreasing surface tension with time [162]. No proof of surface aging in alkaline alkylamine solutions was given.

The occurrence of a dynamic contact angle in a system will have a profound effect on mineral floatability. The fresh air bubble will initially contact yielding a high contact angle and thus promote flotation. Since flotation of a single particle occurs over a very short time period (of the order of a few seconds), the contact angle will not diminish appreciably. Measurements of the contact angle taken at conditions approaching equilibrium, which is the usual procedure, will give little indication of this floatability.

(d) Methods

(i) Review

In 1941, Ferguson [164] reviewed the methods available for contact angle measurement, and divided them into three categories:

(1) Direct estimation of θ;

(2) Simultaneous determination of γ_{lv} and $\gamma_{lv} \cos \theta$;

(3) Measurement of $\cos \theta$, with γ_{lv} for the system known.

Category (1) has received the widest attention in all fields relating to contact angle behaviour. Its major

advantage is that only one variable is involved. The most frequently used in this group is the sessile drop technique. Zisman[15] uses this technique on low surface energy solids (e.g. Teflon) and such data have helped to lay a foundation to the understanding of wetting and adhesion[9,15,20]. Taggart et al.[165] noted that such a procedure does not correspond to the flotation system. Hence Taggart, Taylor and Ince developed a 'captive bubble technique', which involved inducing a bubble of vapour to attach to a flat, prepared mineral surface submerged in the test solution. Results from the captive bubble technique have been shown to be different from those obtained using the sessile drop[166]. This suggests that data from the captive bubble technique give information peculiar to the flotation system.

The captive bubble technique has been widely used[6,82,83,117,123,132,138]. The bubble is introduced via a capillary tube so that it grows to touch the prepared mineral surface. The bubble is viewed through a microscope with a built-in protractor and adjustable cross-hairs, enabling a direct estimation of θ. Alternatives are either to photograph the bubble or project its image onto a screen with subsequent measurement of θ. From this record of the bubble shape and dimensions, the treatment of Mack and Lee[167-169] can be utilised. The latter yields a value of θ computed from all points of contact, thus averaging out

random variations. In the design used by Kim[137] the bubble is allowed to leave the capillary and rise to impinge on an inverted mineral surface.

Although the captive bubble technique has been widely used, certain criticisms can be made:

(1) There is no distinction between θ_A and θ_R. It is assumed that the measured angle is θ_E, as defined by Adam and Jessop[148]. Gaudin et al.[145] suggest that θ_A and θ_R can be developed by leaving the bubble in contact with the capillary (a frequent procedure) and dragging the bubble across the solid. However, Ablett[141,170] and Riddiford[171,172] have demonstrated that, depending on the force applied to move the liquid - vapour interface, the resultant contact angle would alter. As the force increased the measured contact angle increased. Because no control is given for the force applied in the procedure by Gaudin[145], the measured contact angle is not a true indication of θ_A and θ_R. There is also no correlation with the forces involved in movement of the liquid - vapour interface relative to the mineral surface as experienced under flotation conditions.

(2) Interference occurs due to the presence of the bubble-generating capillary. This is a similar

problem to that outlined above, but applies to any circumstances where the capillary is left in contact with the bubble. There is no control over any impressed motion generated. The procedure of Kim had advantages in this respect. However, Gaudin[173] notes that with the bubble being below the mineral, the direction of the interfacial tension forces maintaining the system does not correspond to that operating in actual flotation.

(3) There is little control over the size of the bubble used, although variation of θ with bubble diameter is reported[174,175].

(4) The preparation of the mineral surface is much more rigorous than that received by mineral particles prior to successful flotation[144,154]. The excessive polishing recommended[165] could lead to changes in crystal form at the surface. The formation of an amorphous surface layer has been mooted[176,177].

(5) The relative size of the bubble and mineral are completely different from that experienced in flotation.

Another direct evaluation of θ procedure is the tilting plate of Nietz[178]. It can be designed to enable the specimen to be moved in and out of the liquid - vapour

interface, to simulate θ_R and θ_A respectively[149]. However, the surface preparation is just as tedious and the operation more complex than that of the captive bubble technique[149,179]. As such it has received little use in flotation studies.

In categories (2) and (3), the general criticism is that a magnetite specimen cannot be obtained in the desired shape. This is true of the cylinder required in the technique by Ablett[170] and the capillary tube required by Sentis[81]. However one technique, which falls into category (3), is the suction potential technique, developed by Morrow et al.[144] for investigating the contact angle on granular materials held in a loosely-packed bed. The technique offers several advantages:

(1) The solids for contact angle determination and flotation testing can be the same size and be prepared in the same manner.

(2) The value of θ obtained represents the mean of many measurements on newly broken surfaces.

(3) Depending on whether the liquid is entering the packed bed of material or leaving, θ_A and θ_R are obtained respectively.

(4) The bed throughout the test is surrounded by either liquid or saturated vapour so that non-reproducible contact angles due to air drying are eliminated.

There are, however, three disadvantages:

(1) The equipment is more elaborate and the procedure is longer than with the other methods. Morrow[144] indicates a minimum of four working days are required.

(2) Atmospheric variations will affect the applied suction potential. Isolation from the atmosphere is considered by Jowett[180] but he concludes it is not a straightforward problem. Therefore, constant monitoring of the suction potential is necessary.

(3) A theoretical disadvantage is suggested by the work of Chahal and Yong[181,182]. They demonstrated that, depending whether the moisture is removed from the bed by suction or pressure, a different potential versus moisture elimination curve results. However, the discrepancy is small and certainly will not conceal the effect of increasing dodecylamine concentration.

The technique has been successfully employed for measuring contact angles of xanthate solutions with galena[144] and of water on naturally floatable coals[154]. Primarily because of the first three advantages, the method was selected for determining contact angle data on magnetite. A comparison with contact angle data derived from the captive bubble technique[117,137] is available.

(ii) Suction Potential Technique

Bartell[183] in the late '20s developed a technique for measuring the contact angle developed on a powdered solid since known as the 'Bartell technique' or 'displacement technique'. Bartell assumed the powdered solid, when held in a packed bed, to act as a bundle of capillaries. Fig. 23 represents the equilibrium condition, y, for one such capillary:

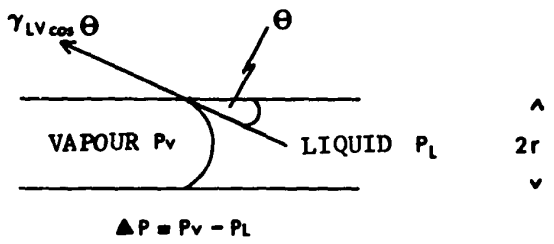

Figure 23. Equilibrium Conditions for Liquid - Vapour - Solid Contact in a Capillary.

At equilibrium:

$$\Delta P_y = \frac{2(\gamma_{lv})_y \cos\theta_y}{r} \quad \ldots 36$$

$$\cos\theta_y = \frac{\Delta P_y r}{2(\gamma_{lv})_y} \quad \ldots 37$$

A measure of ΔP, if r and γ_{lv} are known, gives a measure of $\cos\theta_y$. The surface tension, γ_{lv}, of the liquid can be found independently but r for the packed bed has to be

determined indirectly. From Eq. 37, if $\theta = 0$, i.e. the liquid completely wets the solid, then:

$$1 = \frac{(\Delta P_x)r}{2(\gamma_{lv})_x} \qquad \ldots 38$$

where the subscript x represents the new condition of complete wetting.

Thus, substituting Eq. 38 into Eq. 37 gives:

$$\cos \theta_y = \frac{(\Delta P_y)(\gamma_{lv})_x}{(\Delta P_x)(\gamma_{lv})_y} \qquad \ldots 39$$

The values of $(\gamma_{lv})_x$, $(\gamma_{lv})_y$ are known and ΔP_y and ΔP_x can be measured. Assuming no change in 'r', θ_y can be evaluated.

This technique has been widely used[184-187] but Haines[188] has demonstrated that a complex relationship exists between the equilibrium pressure, ΔP, and the moisture content of the soil bed. The latter parameter was measured as a per cent saturation, s, the water content of the bed at a particular instant as a per cent of the total amount of moisture the bed could hold under the same conditions. If a steadily increasing negative pressure, or suction potential, is applied to a packed bed saturated with moisture, the decrease in s against ΔP follows curve R_o,

the 'primary desaturation' curve, shown in Fig. 24.

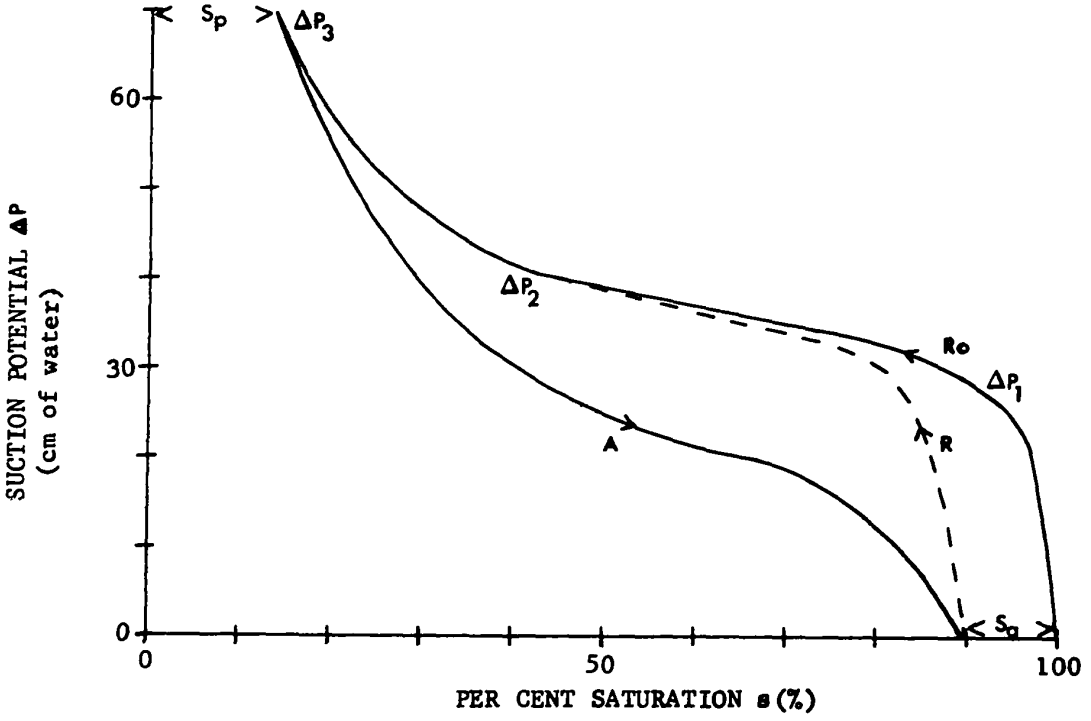

Figure 24. Primary Desaturation - Secondary Desaturation - Pendular Imbibition, or R_o - R - A, Curves for Conductivity Water in a Packed Bed of High Surface Energy Solids.

This indicates that a suction potential greater than ΔP_1 is required to reduce the saturation noticeably. Moisture is then readily removed, flowing as a continuous liquid channel through the capillaries. Above ΔP_2 the moisture level is insufficient to maintain this continuous liquid channel and moisture is left in isolated pockets surrounding the particles. The 'irreducible minimum water content', s_p,

corresponds to the value of s at ΔP_3 [144]. If now the suction potential is continuously reduced, the bed takes up moisture according to curve A. Curve A is called the 'pendular imbibition' curve. The moisture level never returns to 100% saturation. The difference, s_a, represents the maximum volume of entrapped air resulting from the removal of moisture. It is possible to repeat the desaturation giving curve R, the 'secondary desaturation' curve. Curve R and curve R_o should coincide at roughly ΔP_1 [144]. The graphical presentation given in Fig. 24 indicates the complex relationship observed by Haines [188].

An extensive mathematical treatment of the curves of Fig. 24 is given by Morrow et al. [144] and others [189-191]. The relevant equation, however, can be deduced from an extension of the treatment offered by Bartell [183]. For each equilibrium point, i.e. position on the curves, the suction potential, ΔP, is related to the surface tension γ_{lv}, capillary radius r, and contact angle θ, as indicated in Eq. 36. Considering a bed for which 'r' is constant, then the R - A cycle for two different liquids can be idealised as in Fig. 25. If the full line represents the condition x, where the liquid completely wets the bed (cf. Bartell) and the broken line the condition y, where a finite contact angle is developed, then for any value of s on curve R:

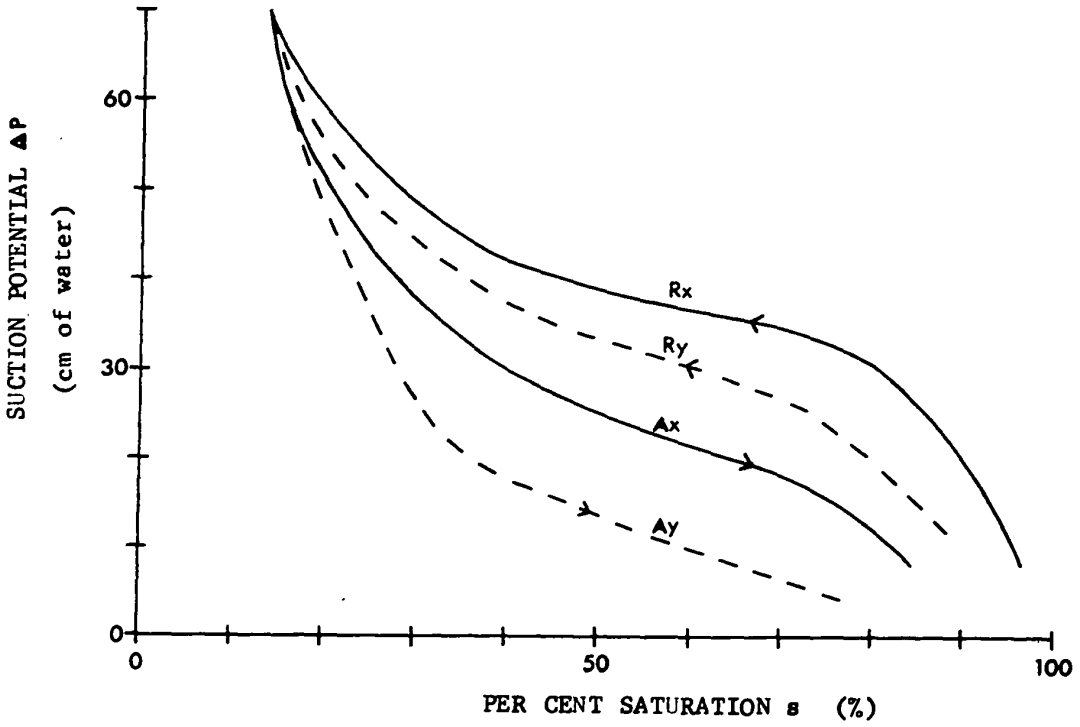

Figure 25. Comparison of R - A Cycle for Water and a Surfactant Solution Yielding a Finite Contact Angle on a High Surface Energy Solid.

$$\cos \theta_y = \frac{\Delta P_y}{\Delta P_x} \frac{(\gamma_{lv})_x}{(\gamma_{lv})_y} \qquad \ldots 40$$

A similar equation can be derived for curve A. This means that two contact angle measurements are given. This is the unique advantage of the technique. Curve R represents the dynamic equilibrium between the retreating liquid - vapour interface and a solid substrate, while curve A represents the dynamic equilibrium between an advancing liquid - vapour

interface and solid substrate. Thus curve R represents the retreating angle and curve A the advancing angle. Using R and A as subscripts gives the equations as used:

$$(\cos \theta_y)_R = \left(\frac{\Delta P_y}{\Delta P_x}\right)_R \frac{(\gamma_{lv})_x}{(\gamma_{lv})_y} \qquad \ldots 41$$

and

$$(\cos \theta_y)_A = \left(\frac{\Delta P_y}{\Delta P_x}\right)_A \frac{(\gamma_{lv})_x}{(\gamma_{lv})_y} \qquad \ldots 41a$$

The equations are valid for all values of s. Morrow[144] and Bailey et al.[154] suggest the use of s = 50% as representative of the contact angle formed in order to facilitate comparison with data derived by alternative techniques. Thus:

$$(\cos \theta_y)_R = \left(\frac{h_y}{h_x}\right)_R \frac{(\gamma_{lv})_x}{(\gamma_{lv})_y} \qquad \ldots 42$$

and

$$(\cos \theta_y)_A = \left(\frac{h_y}{h_x}\right)_A \frac{(\gamma_{lv})_x}{(\gamma_{lv})_y} \qquad \ldots 42a$$

where h_y = suction potential in cm of water at s = 50% for condition y

and h_x = suction potential in cm of water at s = 50% for condition x.

The values of h_x and h_y are given on the R - A cycle curves.

The major problem is to ensure that for successive tests 'r' does not alter. Bartell[183] was forced to use packing pressures up to 2,500 p.s.i. to obtain reproducible beds. Such packing pressures cannot be used in the suction potential technique and Morrow[144] was forced to measure 'r' for each bed. However, a recent modification by Jowett[180] has enabled the same, undisturbed bed to be used for successive tests. The modification is to hold the bed in place by means of a tight-fitting piece of screen cloth. Thus, washing the bed with test solution does not disturb the bed and cause changes in 'r'. Unfortunately this leads to a problem concerning water retention by the screen cloth, over and above that held by the bed. Jowett[180] found that if the sample was supported 5 cm above the measuring tube, then sufficient head was provided to remove moisture from a 35 mesh screen gauze. The bed is not appreciably affected by this added head, as shown in Fig. 24.

In order to calculate θ_A and θ_R, therefore, it is necessary to establish a base R - A curve for water, which naturally wets magnetite, and then compare the R - A curve for various test solutions at 50% saturation.

( )

Apparatus and Procedure

The essential features of the apparatus, shown diagrammatically in Fig. 26, are:

(1) The Suction Head. A filter funnel of cross-sectional area 9.6 cm^2 and guaranteed maximum pore size 1.4 μ was used. The fine pores are required to prevent air being drawn into the system. The sample is placed evenly on the fritted glass in a thin layer[144], and held by a piece of tight-fitting 35-mesh screen gauze[180]. About 12 gm of water-saturated magnetite, spread evenly, gave a bed depth of ~0.5 cm, approximately the condition recommended by Morrow et al.[144]. The suction head was enclosed in an inverted beaker to maintain a saturated atmosphere above the magnetite (see Fig.27).

(2) The Calibrated Measuring Tube. A tube of uniform internal diameter, 0.4 cm, was selected to measure the moisture loss from the bed. As suction is applied to the bed, moisture reports to the measuring tube; and readings of length, l, of the water column against suction potential, ΔP, were made. At the end of all testing an actual value of moisture content of the bed was determined for a known value of 'l'. Knowing the internal tube diameter, the relationship between 'l' and

FIGURE 26

SUCTION POTENTIAL APPARATUS

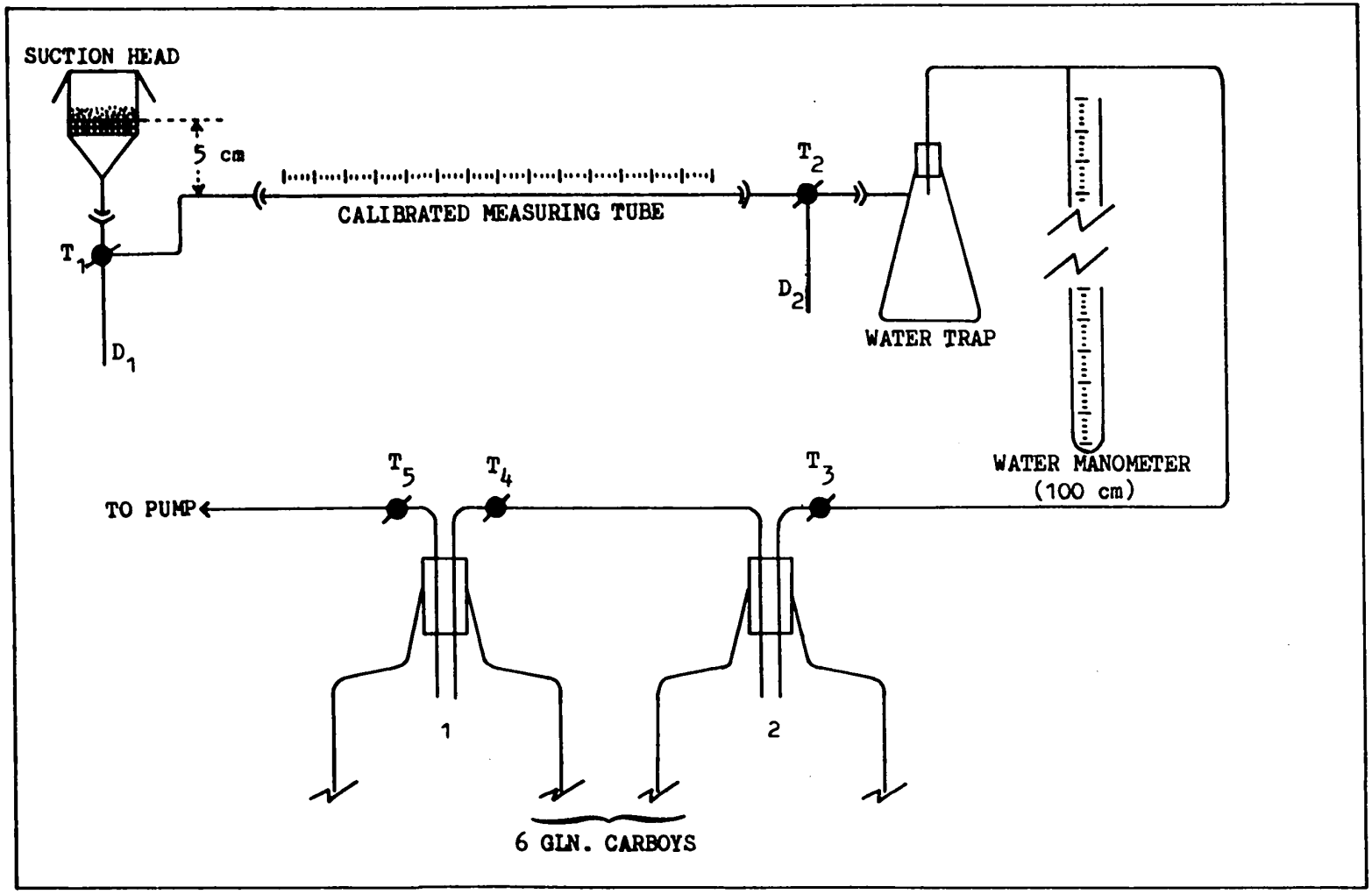
SUCTION HEAD
5 cm
CALIBRATED MEASURING TUBE
T_1
T_2
D_1
D_2
WATER TRAP
WATER MANOMETER
(100 cm)
T_5
T_4
T_3
TO PUMP
1
2
6 GLN. CARBOYS

FIGURE 27

SUCTION HEAD ASSEMBLY

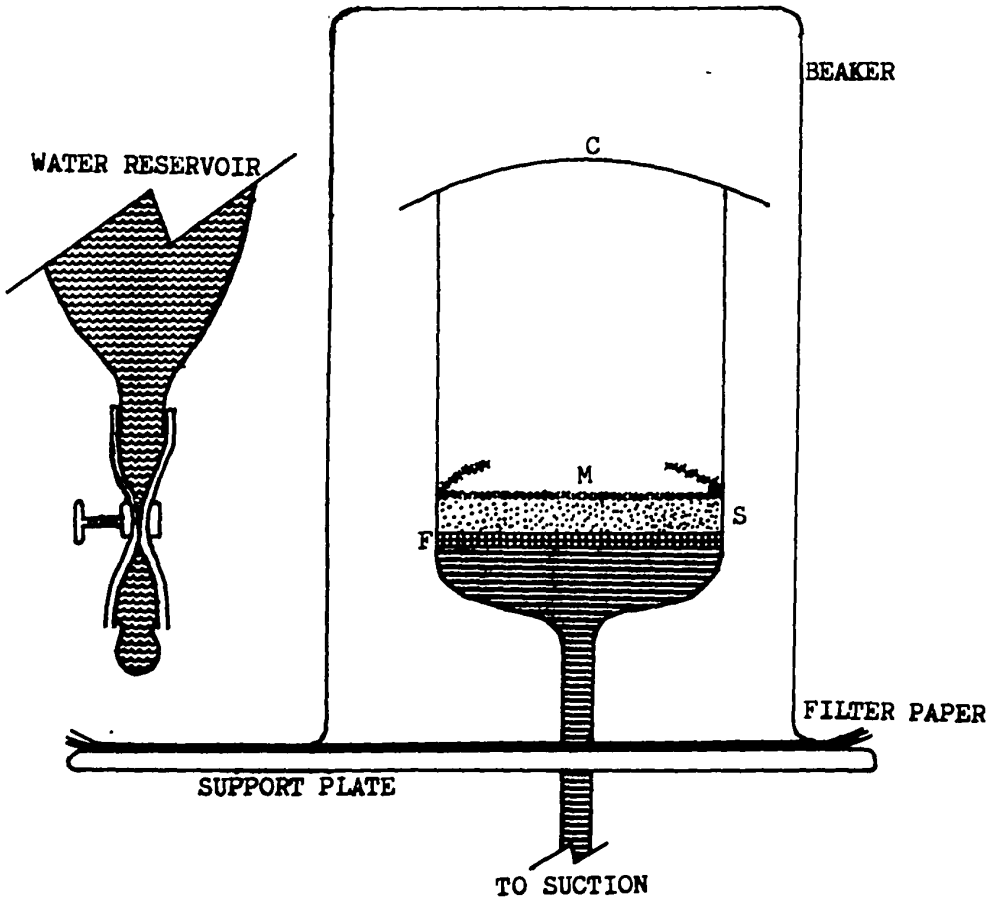

Key S: MAGNETITE SAMPLE
F: 1.5μ FRITTED GLASS
M: 35 MESH SCREEN GAUZE
C: COVER GLASS

% saturation, s, can be calculated (see Appendix IV).

(3) The Water Manometer. From the data of Morrow et al.[144] a 100 cm water manometer is suitable for use with -65 +80 mesh material.

(4) The Two Carboys. These provide for a carefully controlled variation in the suction potential, which Morrow recommends to be in increments of 4 cm of water[144]. Carboy 1 was first evacuated by means of a pump and then carboy 2 allowed to drain, in controlled increments, into carboy 1 via tap T_4.

All the glassware, excluding the carboys, was cleaned with acid dichromate solution and carefully rinsed. Special care was required to ensure that all acid was removed from the fritted glass. The measuring tube was treated with a solution of 'Dri-cote' to provide a non-wettable surface[180]. The joints were ball and socket type and were lightly greased. Tygon tubing was used to connect to the vacuum assembly. All seals were made with a resin glue. After initial testing, the equipment was observed to be air-tight.

The suction head assembly, up to the measuring tube, was filled with water and the sample added. The procedure was as follows:

(1) Tap T_2 was opened to connect the measuring tube to the atmosphere via drain D_2. Tap T_1 was turned to connect the suction head to the measuring tube. Excess moisture can drain naturally from the bed and be observed in the measuring tube. The 100% saturation point was taken when, over a period of one hour, no further movement of the liquid column in the measuring tube was noted.

(2) Tap T_2 was left open to the atmosphere and tap T_1 turned so that the liquid held in the measuring tube could empty via drain D_1. The meniscus can be adjusted to read zero on the scale.

(3) Tap T_1 was turned to re-connect the suction head to the measuring tube.

(4) Tap T_4 was closed, tap T_5 opened and the pump connected. Carboy 1 was evacuated and tap T_5 was then closed.

(5) Taps T_1, T_2 and T_3 were turned to connect carboy 2 to the suction head via the water manometer and calibrated measuring tube.

(6) Tap T_4 was opened, the desired suction potential recorded on the water manometer, and then tap T_4 was closed.

(7) The system was left until movement of the liquid column in the measuring tube ceased. Equilibrium

dodecylamine solutions were compared to a base R - A cycle for water determined under the same conditions.

With the base curve established, alkaline (pH = 9.5) solutions of dodecylamine, in increments up to 35 mg/l, were tested. After the final solution of 35 mg/l had been tested, conductivity water was again flushed through the bed. The irreducible minimum water content was established and, with the bed still under suction and 'l' noted, the moisture content of the bed was determined. The calibration curve of 's' against 'l' was then constructed (see Appendix IV).

Results

Fig. 28 shows the primary saturation - secondary desaturation - pendular imbibition cycle, or R_o - R - A, for conductivity water. The primary desaturation curve rises sharply from 100% saturation (s = 100%), tends to the horizontal at about 80% saturation and a suction potential of 25 cm of water (ΔP_1, see Fig. 24), and rises sharply again at 20% saturation and a suction potential of 40 cm of water (ΔP_2). Thus, as the suction potential, ΔP, varies from 25 to 40 cm of water, the % saturation, s, diminishes from 80% to 20%. The minimum water content, s_p, is about 9% saturation. The pendular imbibition curve follows a similar trend but the suction potential is lower for any given degree of saturation. The corresponding changes in slope occur at 70% saturation and a suction potential of 11 cm of water, and 22% saturation and a suction potential of 25 cm of water. Thus, as the suction potential varies from 25 to 11 cm of water, the % saturation increases from 22% to 70%. The maximum volume of entrapped air, s_a, is about 12% saturation. The secondary desaturation curve is similar to the primary desaturation curve, rising steeply to within 5% of the primary desaturation curve at a suction potential of 25 cm of water (ΔP_1). The primary and secondary desaturation curves are coincident at a suction potential of 34 cm of water and 40% saturation. At 50%

FIGURE 28

PRIMARY DESATURATION - SECONDARY DESATURATION - PENDULAR IMBIBITION CYCLE, R_o - R - A, FOR CONDUCTIVITY WATER IN A LOOSELY PACKED BED OF -65 +80 MESH MAGNETITE

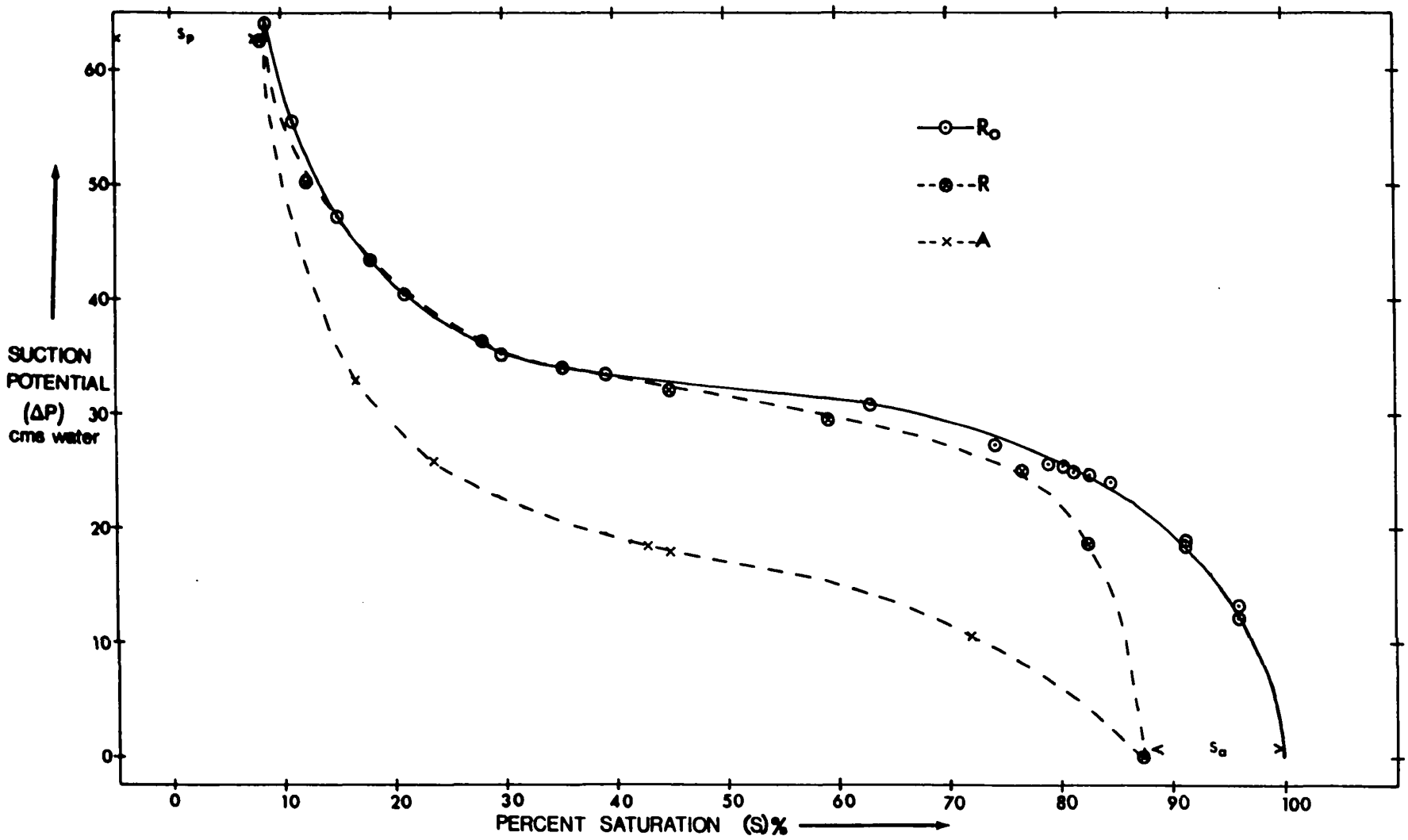
S_p
R_o
R
A
S_a
SUCTION POTENTIAL (ΔP) cms water
PERCENT SATURATION (S)%
0
10
20
30
40
50
60
70
80
90
100

saturation (the % saturation at which h_x, h_y are taken), the difference between the primary and secondary desaturation curves is less than 2%.

Fig. 29 compares the secondary desaturation - pendular imbibition cycle, R - A, obtained for separate tests with conductivity water. The secondary desaturation curves are virtually coincident, the pendular imbibition curves showing a tendency to separate. At 50% saturation the error involved in the pendular imbibition curves is about 5%. The average of these two cycles was taken as the base R - A cycle (i.e. condition x).

Figs. 30 - 36 compare the R - A cycle developed from flushing the bed with test solution (i.e. condition y) with the base R - A cycle. The solute concentrations range from 0.1 mg/l to 35 mg/l dodecylamine acetate. Between concentrations 0.1 mg/l and 1 mg/l little variation occurs. At 10 mg/l, the R - A cycle separates noticeably from the base R - A cycle, the former having a lower value of suction potential for any given degree of saturation. From 15 to 35 mg/l, the magnitude of this separation remains fairly constant but tends to reduce between 25 and 35 mg/l.

Fig. 37 shows the effect of final re-washing of the bed with conductivity water. Compared to 35 mg/l, it indicates that the R curve tends to return to the base

FIGURE 29

COMPARISON OF TWO R - A CYCLES
USING CONDUCTIVITY WATER TO OBTAIN
THE BASE R - A CYCLE

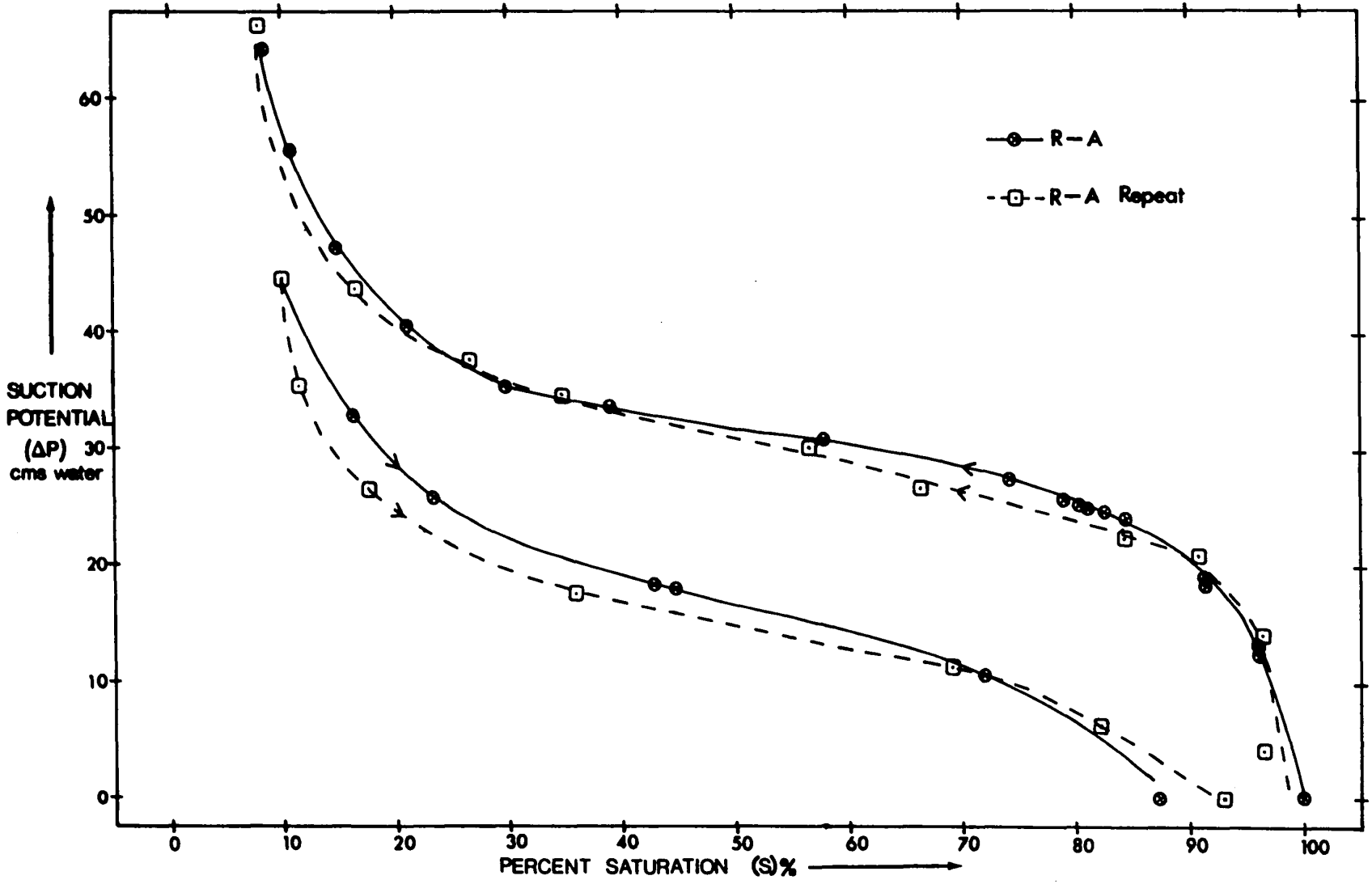
R—A
R—A Repeat
SUCTION POTENTIAL (ΔP) cms water
0
10
20
30
40
50
60
70
80
90
100
PERCENT SATURATION (S)%

FIGURES 30 - 36

R - A CYCLES FOR SOLUTIONS OF DODECYLAMINE ACETATE

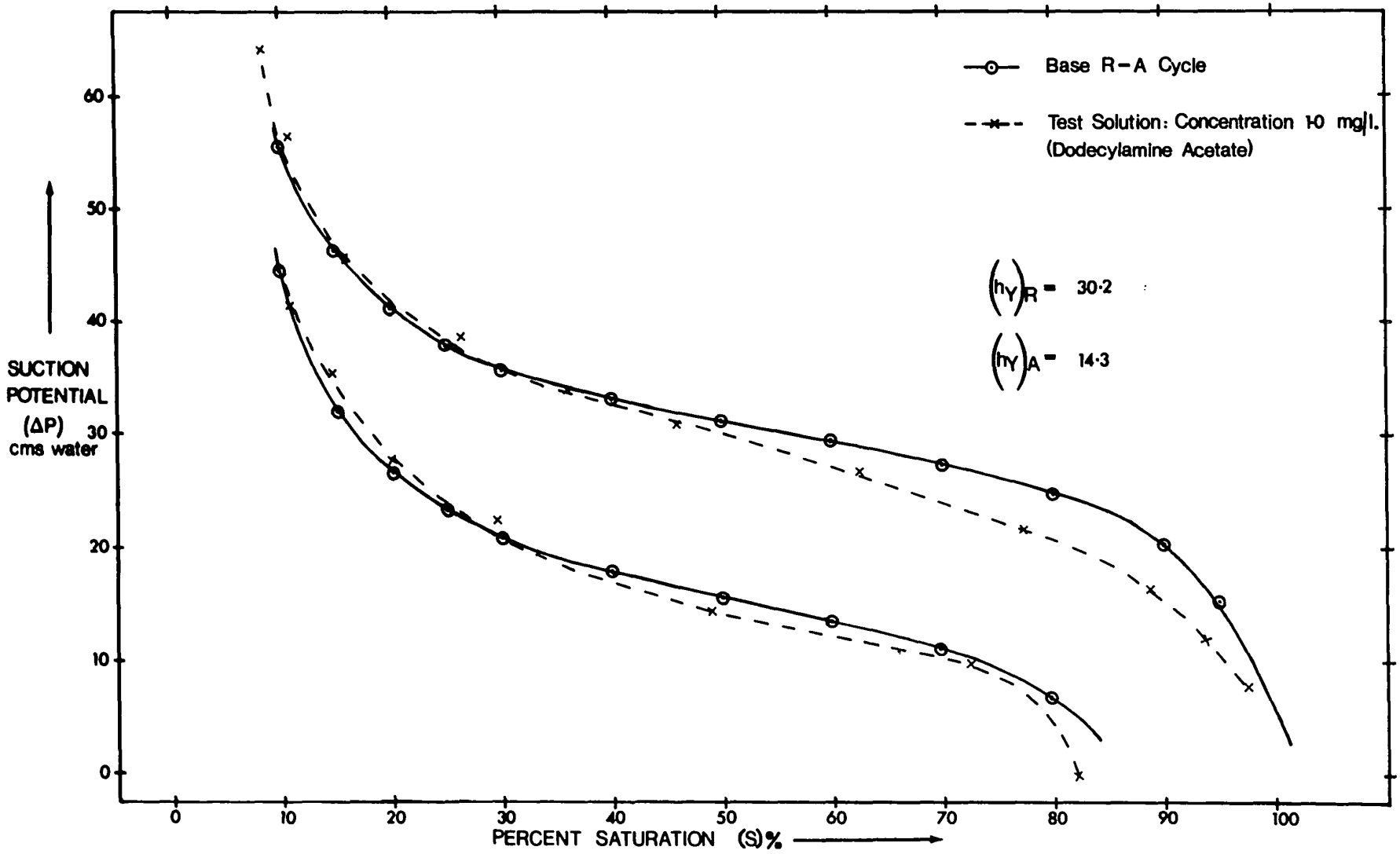
Base R–A Cycle
Test Solution: Concentration 1·0 mg/l.
(Dodecylamine Acetate)
$(h_Y)_R$ = 30·2
$(h_Y)_A$ = 14·3
SUCTION POTENTIAL (ΔP) cms water
PERCENT SATURATION (S)%
0
10
20
30
40
50
60
70
80
90
100

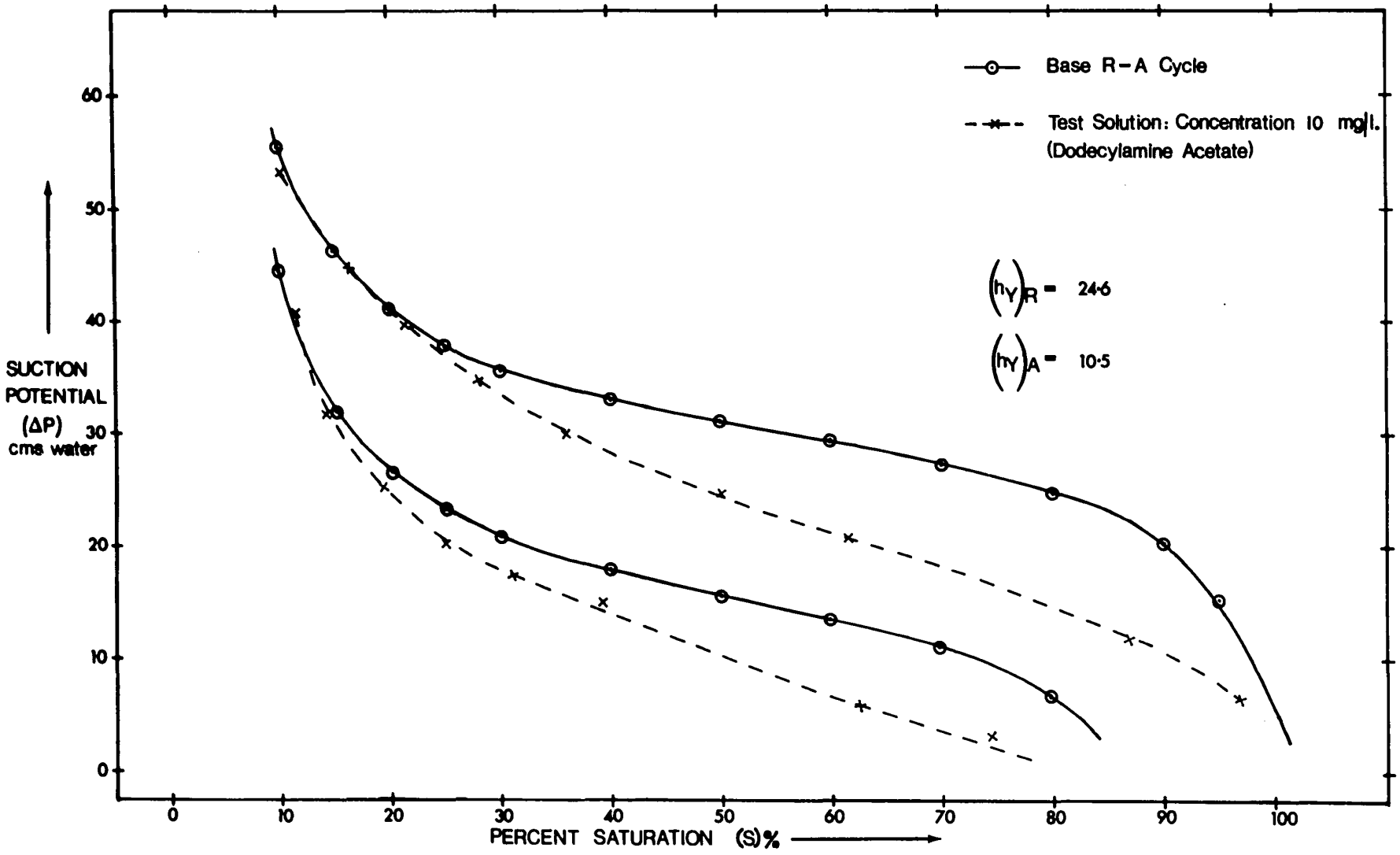
Base R-A Cycle
Test Solution: Concentration 10 mg/l.
(Dodecylamine Acetate)
$(h\gamma)_R$ = 24·6
$(h\gamma)_A$ = 10·5
SUCTION POTENTIAL (ΔP) cms water
PERCENT SATURATION (S)%
0
10
20
30
40
50
60
70
80
90
100

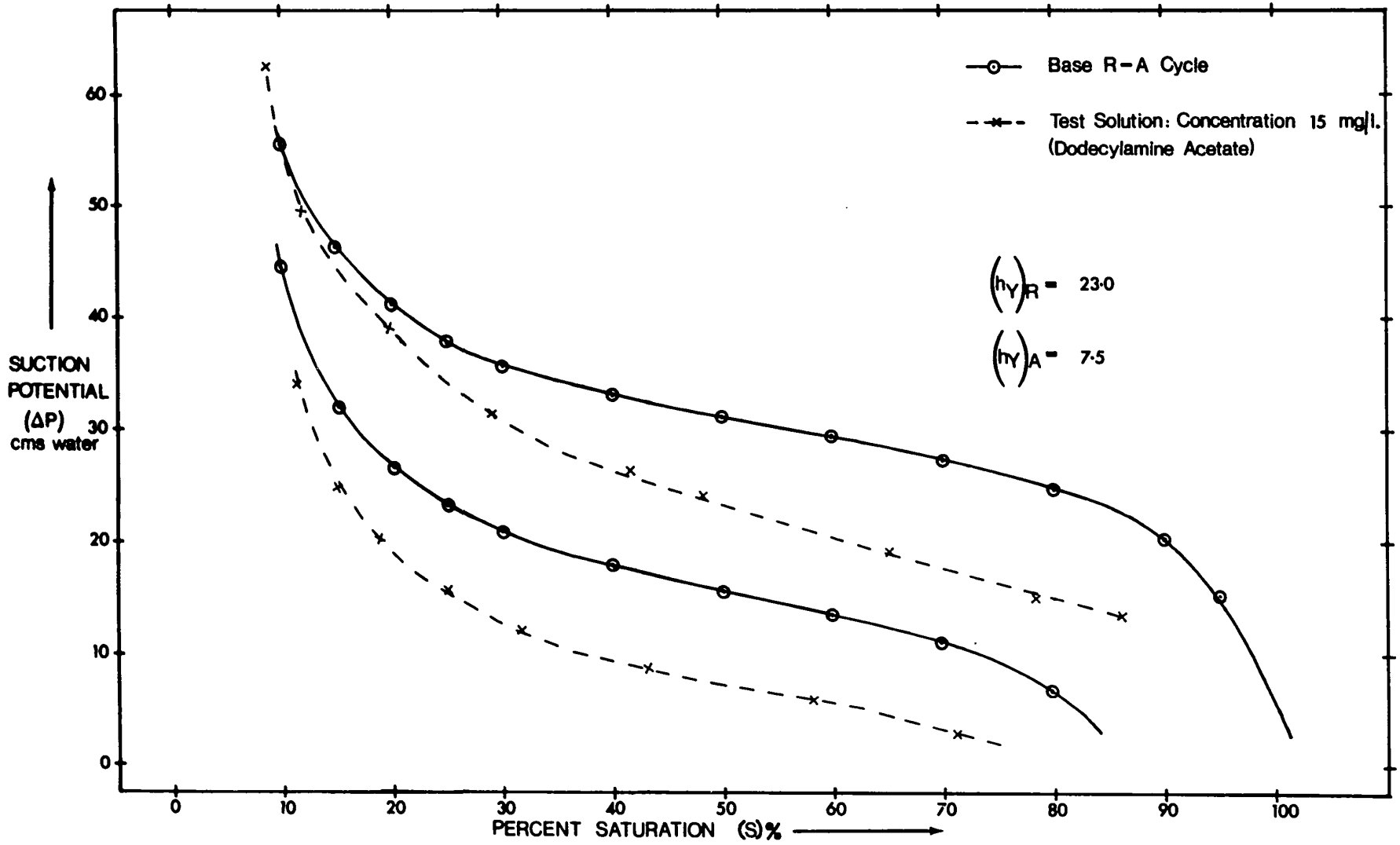
Base R-A Cycle
Test Solution: Concentration 15 mg/l.
(Dodecylamine Acetate)
$(h\gamma)_R$ = 23·0
$(h\gamma)_A$ = 7·5
SUCTION POTENTIAL (ΔP) cms water
PERCENT SATURATION (S)%
0
10
20
30
40
50
60
70
80
90
100

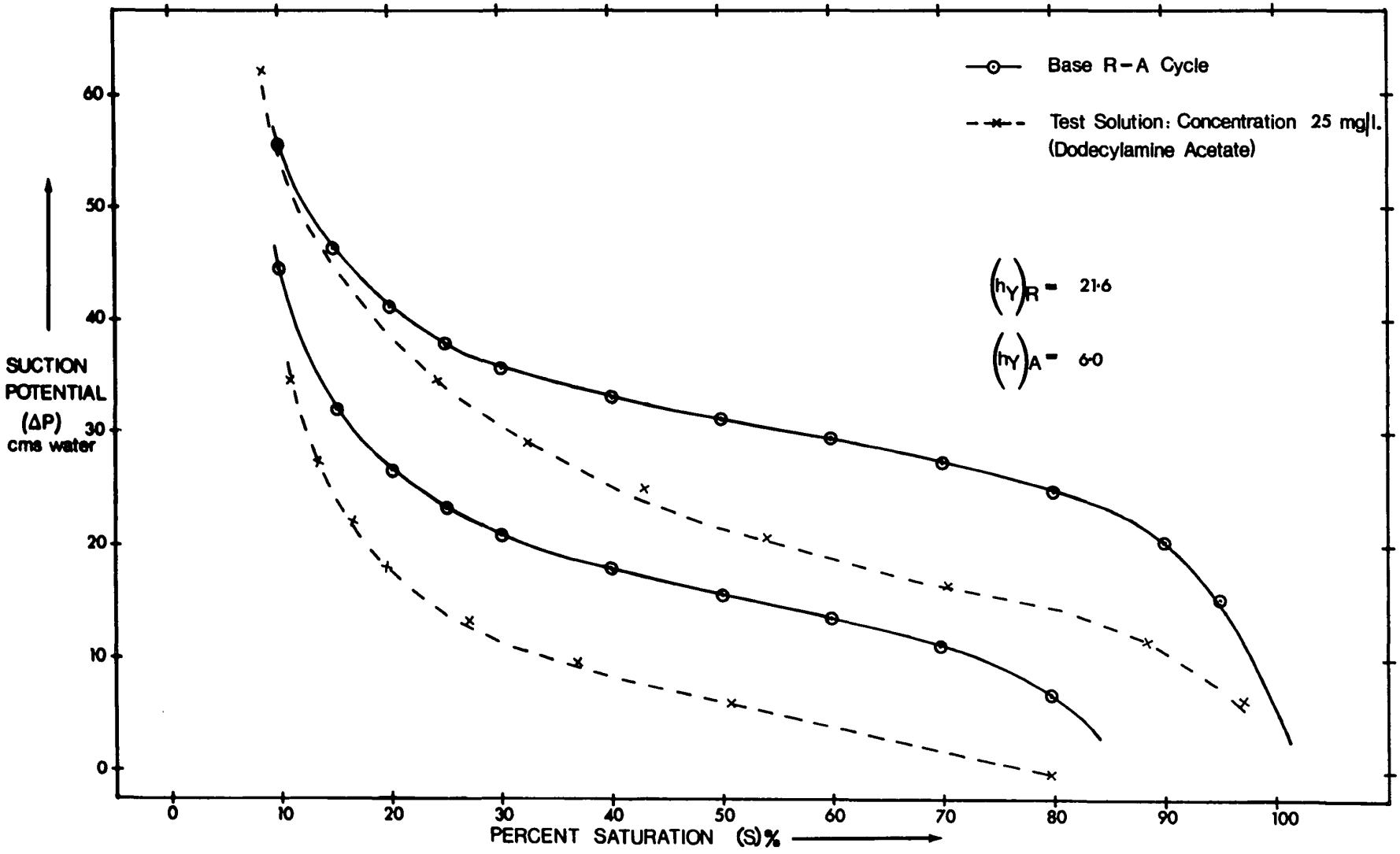
Base R-A Cycle
Test Solution: Concentration 25 mg/l.
(Dodecylamine Acetate)
$(h\gamma)_R$ = 21·6
$(h\gamma)_A$ = 6·0
SUCTION POTENTIAL (ΔP) cms water
PERCENT SATURATION (S)%
0
10
20
30
40
50
60
70
80
90
100

FIGURE 37

R - A CYCLE AFTER RE-WASHING
WITH CONDUCTIVITY WATER

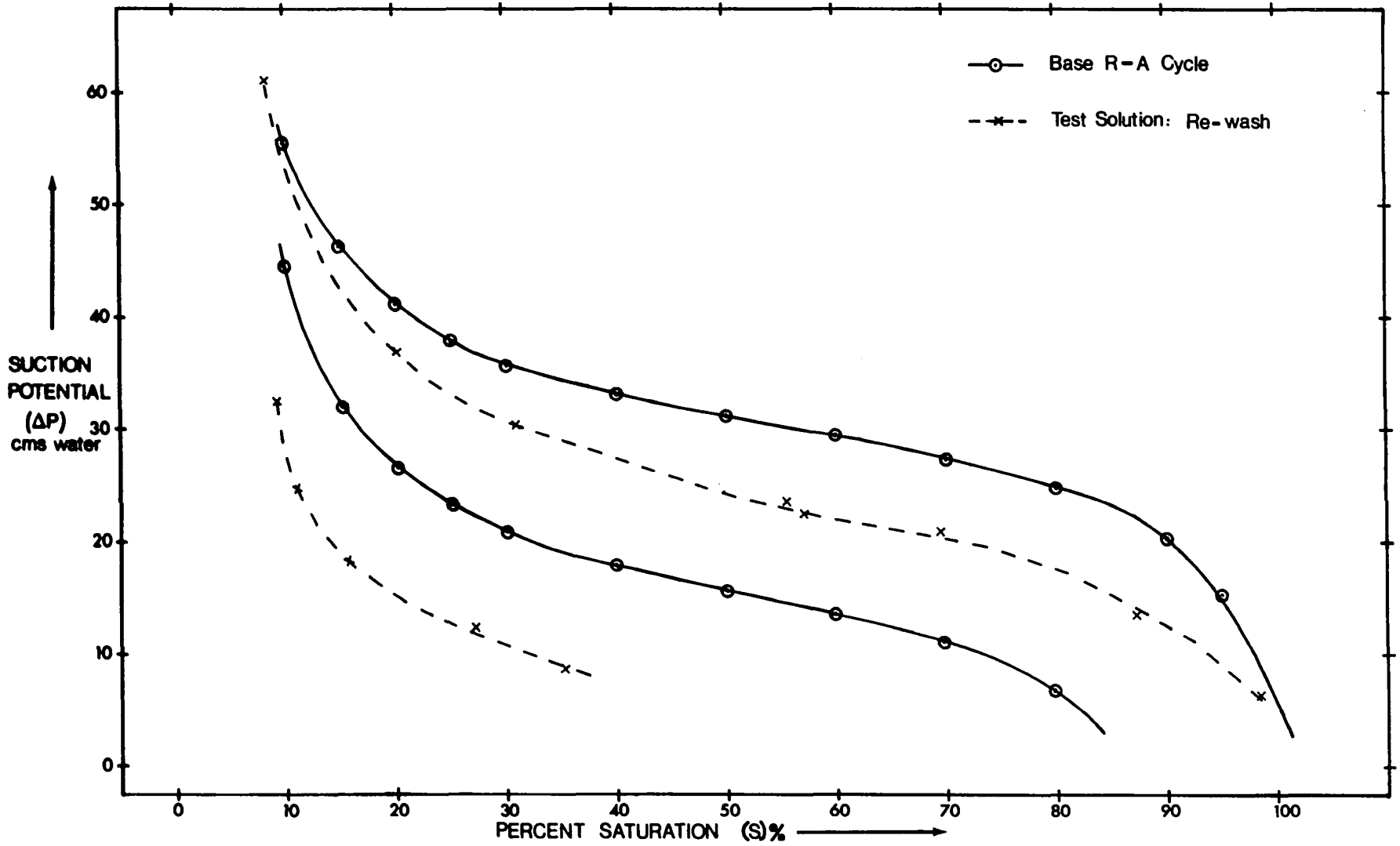
Base R-A Cycle
Test Solution: Re-wash
SUCTION POTENTIAL (ΔP) cms water
0
10
20
30
40
50
60
0
10
20
30
40
50
60
70
80
90
100
PERCENT SATURATION (S)%

R curve, although the A curve appears unaffected.

Fig. 38 indicates the variation of θ_A and θ_R (determined at s = 50%) with dodecylamine acetate concentration compared to the variation in θ_E as determined by Kim[117,137] using the captive bubble technique. It shows that θ_A is zero at concentrations less than about 5 mg/l, rising to a maximum of about 40° between 14.0 and 18.0 mg/l, declining to zero again at about 35.0 mg/l. Accuracy is about ± 6°. The value of θ_R is zero at all concentrations. Contact angle values of θ_E follow the same trend as θ_A but over an extended region, giving finite values over a range 1.0 to 80.0 mg/l. The maximum value of 60° occurs at about 25.0 mg/l.

FIGURE 38

CONTACT ANGLE vs.

DODECYLAMINE ACETATE CONCENTRATION

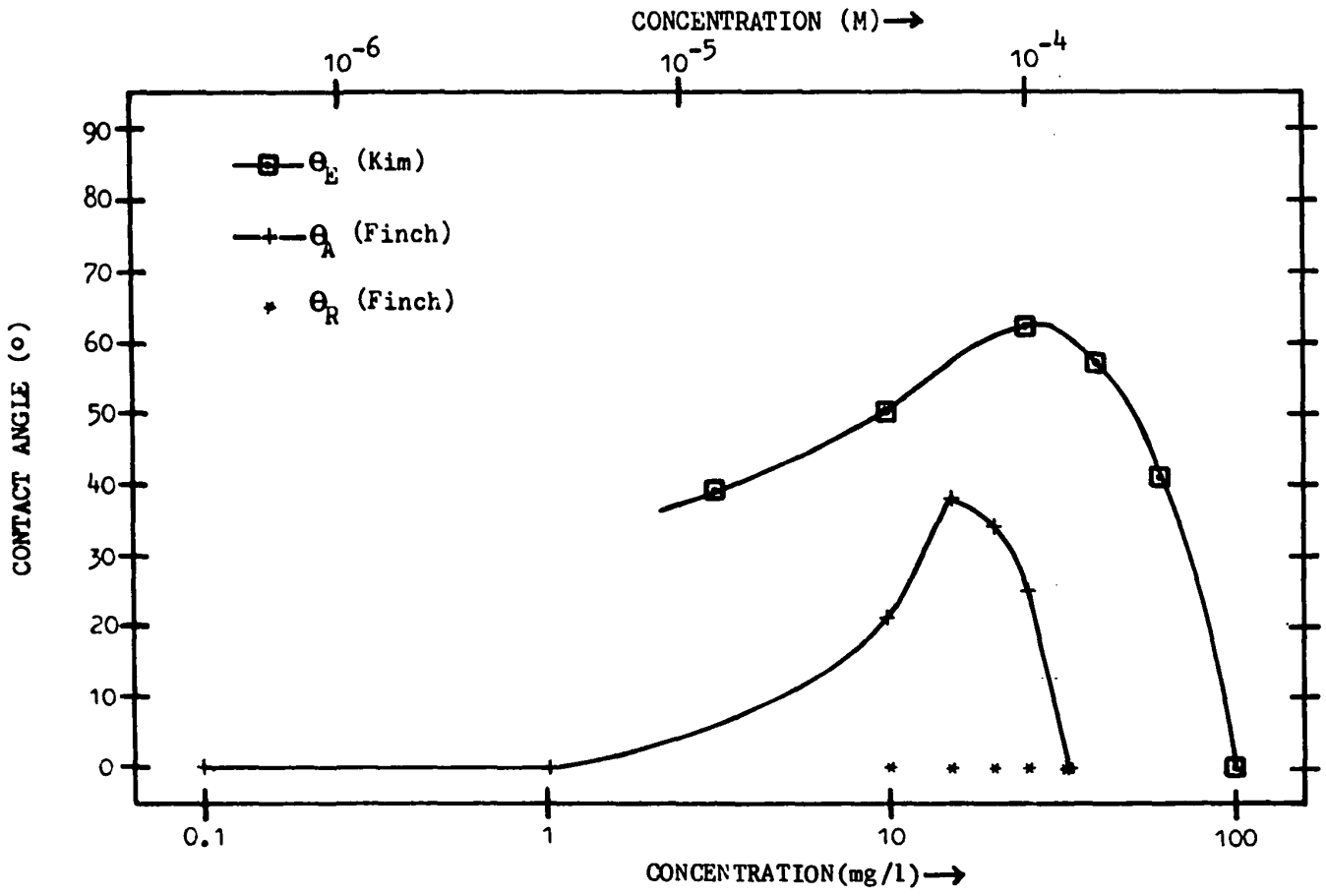
CONCENTRATION (M)→
10^-6
10^-5
10^-4
θE (Kim)
θA (Finch)
θR (Finch)
CONTACT ANGLE (o)
90
80
70
60
50
40
30
20
10
0
0.1
1
10
100
CONCENTRATION(mg/l)→

Discussion

The R_o - R - A cycle for conductivity water shown in Fig. 26 is similar to that obtained by Morrow[144] using -60 +72 mesh galena. The changes in slope correspond to those of Morrow, as do the values of s_p and s_a. The R - A curves resulting from test solutions indicate the same type of deviation from the base R - A curves. Before discussing the resulting contact angle data, several experimental points should be noted.

(1) After the initial test with pure water it was noted that a moisture loss had occurred by evaporation from the bed. A watch glass cover for the suction head was provided and then the suction head was surrounded by an inverted beaker. The air inside the beaker was kept saturated by allowing water to drain continually on to filter paper inserted under the beaker (see Fig. 27).

(2) It proved impossible to drain all the moisture from the 35 mesh screen gauze even with the 5 cm head difference, as revealed by a tendency for the R - A cycle to shift to reduced saturation levels. All curves were corrected to the initial s_a value obtained in the first run before the screen gauze had become wet, i.e. prior to the first bed washing. Such a correction is justified since the development

of a contact angle does not affect the irreducible minimum water content, s_p[144,192-4]. Further experimentation is required to overcome this problem of excess water retention.

(3) The R curves for the test solutions have an indefinite starting point, the start lying between s_a for pure water and s = 100%. This arises from conditioning the bed in situ, the trapped air being partially replaced upon washing the bed. The value of $s_a \approx 12\%$ agrees well with values for irregular shaped particles[194].

(4) Towards the end of the series of nine tests, the sides of the measuring tube started to wet. This will affect the R - A cycles of the later tests. Jowett[180] claims that the measuring tube will need treating only very infrequently. From the present work, about eight tests is the maximum before the measuring tube should be re-treated.

The above problems arise from the modifications of Jowett, although more rapid testing is promoted. The original method of Morrow[144] appears to allow better control of the system.

(5) A pronounced pH drift was observed, as noted previously in the surface tension work. Throughout the bed conditioning period the pH was monitored and

adjusted to hold 9.5 ± 0.3. Kim[137] did not note any comparable drift. Once the R - A cycle is entered, any pH variation cannot be controlled. The problems of pH drift must be solved before further work in alkaline regions is attempted. Noting that Kim's data took only about 30 minutes to obtain, any pH drift will probably have a minor effect. In this respect, the captive bubble technique has an advantage at pH 9.5.

(6) The initial bed conditioning can cause problems. Morrow et al.[144] conditioned the galena sample in 500 ml of xanthate solution for ten minutes. Conditioning in situ[180] has the added advantage of prolonging exposure, approximately two days in the present investigation. Work in this laboratory indicates that 50 ml of dodecylamine acetate solution is sufficient to condition two gram samples of -325 +400 mesh hematite and quartz in six hours[120] and ten hours[121] respectively. Since the magnetite sample used in the present investigation is much coarser (-65 +80 mesh), the total surface area is smaller and complete conditioning can be assumed.

(7) The necessary four to five days required to establish the R - A cycle for a given dodecylamine concentration meant that the time required to test the entire amine concentration range covered in the

surface tension work would be prohibitive. The alkaline region, pH 9.5, was selected since it enabled the full surface tension variation to be utilised with solute strengths up to only 35 mg/l. At concentrations greater than this, precipitation of undissociated amine would change the bed characteristics. A comparison with captive bubble contact angle data at this pH is available from the work of Kim[117,137]. Kim also notes that ~ pH 9.5 represents a good region for flotation, as it is for most oxides using dodecylamine[119]. Therefore, the work of adhesion formula is well tested at this pH level.

(8) Deterioration of the dodecylamine acetate over such extended time periods as used in the suction potential technique was considered. The acetate is susceptible to conversion to the acetamide[158]. Subsequent flotation testing using solutions of different age revealed no differences. Therefore, deterioration was not considered important.

(9) The final re-wash of the bed, using conductivity water at neutral pH (Fig. 37), did not return the R - A cycle to the base condition, x. However in a similar experiment, Morrow and Gaudin[6] required over 500 ml of conductivity water to remove adsorbed dodecylamine from a hematite surface. After 50 ml,

desorption was less than 25% complete. Janis[195] determined the desorption characteristics of dodecylamine adsorbed on silicates, and found that at pH 11.0, 70% desorption was the maximum attainable. Janis measured the adsorbed species on the solid surface as opposed to Morrow and Gaudin, who determined the presence of dodecylamine in the wash solution. Either of these previous observations account for the results shown in Fig. 37. If Janis is correct, then adsorbed amine is still present at the magnetite surface and will affect the R - A curve, as was observed.

(a) Advancing Contact Angles

From Figs. 30 - 36, θ_A and θ_R were calculated at s = 50% saturation according to Eqs. 43 and 43a, and are plotted in Fig. 38. The 50% saturation level corresponds to the horizontal section of the R - A cycle. The estimated error of $\pm 6^\circ$ is due to the 5% deviation encountered in establishing the base R - A cycle (Fig. 29) and from an estimated 5% error in the value of the equilibrium surface tension. From the surface tension work, it is noted that at pH 9.5 a significant surface aging time was involved. However, all the liquid - vapour interfaces in the mineral bed must be considered as older than one

minute, and, therefore, at equilibrium. Errors of $\pm 6^{o}$ are not uncommon in this technique[154], and reflect the uncertainty of measuring contact angles, especially with rough-surfaced particles as used in flotation.

It follows from the contact angle values of θ_A and θ_R, given in Fig. 38, that $\theta_A > \theta_R$. This implies that, energetically, it is more difficult to create bubble - particle attachment than it is to maintain the attachment once it has been achieved. Morrow[144] observed that $\theta_A > \theta_R$ and concluded that $\theta_A = \theta_E$ (as measured in the captive bubble technique). From the present data, the variation in θ_A and θ_E are similar, but the latter tends to be some 20^{o} higher and covers a wider concentration range.

Two possible explanations are available:

(1) Fig. 39 indicates the variation of θ_A with dodecylamine concentration at various saturation levels. As the % saturation increases, the measured contact angle increases. It is well known that some mineral particles will not float while others do. A wide variation in contact angle values is indicated, and the noted variation of contact angle with % saturation may be a reflection of this.

FIGURE 39

VARIATION IN CONTACT ANGLE

WITH % SATURATION OF MAGNETITE BED

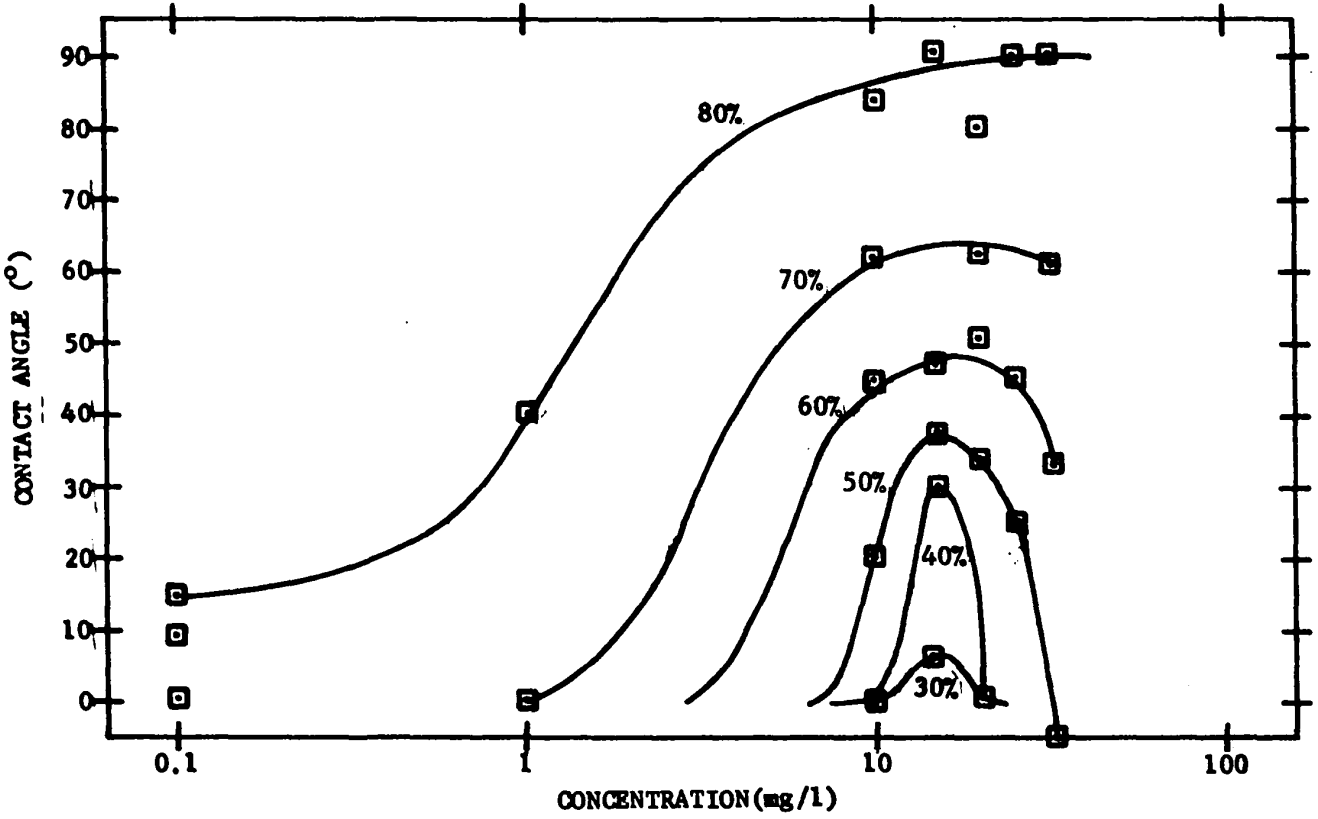
90
80
70
60
50
40
30
20
10
0
CONTACT ANGLE (°)
80%
70%
60%
50%
40%
30%
0.1
1
10
100
CONCENTRATION (mg/l)

The variation of θ_A at s = 70% closely corresponds to the contact angle data given by Kim[117]. The possibility that the relative quantities of vapour and liquid in contact angle measurements may affect the result has not been considered in captive bubble tests. Kabanov and Ivanishchenko[175] note that the measured contact angle increases with a decreasing diameter of attached bubble, but capillary pressure inside the bubble, and not the vapour - liquid ratio, is considered the determining factor[174]. Certainly in most captive bubble testing, the liquid phase covers more of the solid than the vapour phase, i.e. the % saturation is greater than 50%. That the contact angle should become larger as the vapour phase becomes less abundant appears contradictory, although the observations of Kabanov and Ivanishchenko[175] are effectively the same. Morrow and Jowett[144] note an increase in contact angle with % saturation, although it is not so marked as in the present investigation.

(2) Smith and Lai[123] observed that alkaline dodecylamine solutions gave large dynamic contact angles on quartz surfaces. According to Leja[162], the reason was surface aging of the solution. Thus dynamic contact angles can exist in the dodecylamine - magnetite system. The liquid - vapour interface once established in contact with a solid tends to

remain stable. Such factors as surface roughness help promote the stability of the bubble perimeter of contact with the solid. It is quite possible that the initially large contact angle value noted by Smith and Lai could become metastable under conditions which dictate a much smaller, or even zero, contact angle. A dynamic contact angle, metastable for any length of time, may explain why dynamic contact angles have been so rarely observed. In the present investigation, the prolonged contact between the three phases means that true equilibrium is more nearly approached. Lower values of the contact angle would result.

The variations in θ_A and θ_E, shown in Fig. 38, indicate that under equilibrium conditions, finite contact angle development occurs over a limited concentration range. If the rule $\theta > 40^\circ$ for successful flotation is applied [119], this concentration range is even more restricted. The range depends on whether the θ_A or θ_E variation is considered. The latter gives about twice the range. From Fig. 39, an increase in saturation of the magnetite bed also gives an increase in the amine concentration range. However, in all cases, the shape of the curves is similar; a maximum value of contact angle between 10.0 and 25.0 mg/l with a rapid decrease in contact angle at concentrations outside this range. Therefore, dodecylamine solutions

exhibit maximum de-wetting power on magnetite surfaces at concentrations between 10.0 and 25.0 mg/l.

The Young equation states that for finite contact angle development:

$$\gamma_{sv} - \gamma_{sl} < \gamma_{lv}$$

At amine concentrations between 10.0 and 25.0 mg/l, $\gamma_{lv} - (\gamma_{sv} - \gamma_{sl})$ must be a maximum. Since, from the surface tension of dodecylamine solutions at pH 9.5 (see Fig. 16), concentrations 10.0 to 25.0 mg/l indicate a decreasing γ_{lv}, a reduction in $(\gamma_{sv} - \gamma_{sl})$ must also have occurred.

The theory introduced by Zisman[15] enables the quantities, γ_{sv} and γ_{sl}, to be eliminated in favour of the single parameter γ_c, the critical surface tension of wetting. A finite contact angle occurs if:

$$\gamma_{lv} - \gamma_c > 0.$$

At amine concentrations between 10.0 and 25.0 mg/l $(\gamma_{lv} - \gamma_c)$ must be a maximum. Because the value of γ_{lv} reduces over this range, a reduction in γ_c of the solid surface must have occurred.

Adsorption of dodecylamine at the solid surface and liquid - vapour interface controls γ_c and γ_{lv} respectively

and hence the condition $(\gamma_{lv} - \gamma_c) > 0$. When no dodecylamine is present, water completely wets a magnetite surface. Since γ_{lv} for water is $\sim$72 dynes.cm^{-1}, γ_c must be greater than 72 dynes.cm^{-1} for a clean magnetite surface. Upon addition of dodecylamine, positive adsorption at the interfaces occurs[26] and γ_{lv} and γ_c reduce. The mechanism proposed is that at concentrations less than a value characteristic of the system, adsorption at the solid surface is insufficient to yield $\gamma_{lv} > \gamma_c$, and so a contact angle does not develop. In the present system, the concentration at which a contact angle is first formed is in the region of 1 to 5 mg/l. At concentrations greater than this characteristic value, $(\gamma_{lv} - \gamma_c) > 0$ holds. Adsorption at the solid must be such that a rapid reduction in γ_c occurs. This indicates that a greater adsorption density at the solid surface than at the liquid - vapour interface is required. Recently, Somasundaran[27], Sandvik and Digrè[69] and Ter-Minassian-Seraga[195] have reported that, in the presence of a gas phase, adsorption at the solid surface is greater than at the liquid - vapour interface. In contact angle determinations, a gas phase must always be present. From the observations of Somasundaran, Sandvik and Digrè and Ter-Minassian-Seraga, a reduction in γ_c, greater than that in γ_{lv} for a given amine concentration increase, is possible.

At concentrations 10.0 mg/l to 25.0 mg/l, the reduction in γ_{lv} and γ_c is such that $(\gamma_{lv} - \gamma_c)$ is a maximum, and contact angle development most pronounced. As the concentration is taken beyond 25.0 mg/l, γ_{lv} continues to reduce, but γ_c approaches a lower limiting value. Thus, $\gamma_{lv} \rightarrow \gamma_c$ at concentrations greater than 25.0 mg/l. Consequently the mineral surface appears hydrophyllic in relation to the dodecylamine solution and the contact angle is zero. It is notable that the inside walls of the calibrated measuring tubes started to wet at the end of the experiments, indicating the dodecylamine solutions were no longer rendering the silica surface hydrophobic.

The lower limiting value of γ_c will approach that of a dodecylamine surface as the magnetite surface is progressively covered by adsorbed amine, and monolayer coverage is approached. The value of γ_c for dodecylamine can be found experimentally[15,196]. Fowkes[20] has indicated that, within experimental error, $\gamma_c = \gamma^d$, the dispersion force contribution to the surface tension. Since dodecylamine is a hydrocarbon, $\gamma^d = \gamma_{DDA}$, the surface tension of dodecylamine[9]. From the surface tension work, the liquid - vapour interface at concentrations approaching the c.m.c. tended to a monolayer coverage of dodecylamine. Therefore, the surface tension of dodecylamine, i.e.

$\gamma_{DDA} \approx 28$ dynes.cm^{-1}. Thus γ_c has a lower limiting value of ~28 dynes.cm^{-1}. At concentrations greater than 25.0 mg/l, γ_{lv} approaches 28 dynes.cm^{-1} and hence the de-wetting power of the solution diminishes.

The general trend observed in the surface tension vs. amine concentration fits the observed variation in contact angle vs. amine concentration, regardless of the actual contact angle values considered. Conflicting data are given by the capillary rise technique, since a finite contact angle appears to hold at concentrations greater than 25 mg/l. A rise in surface tension results was observed, but was attributed to the decrease in pH which occurs in alkaline amine solutions. Somasundaran[27] indicates that the surface tension, using the capillary rise technique, does increase. The problem of obtaining satisfactory equilibrium conditions possibly masked γ_{lv} variations.

The surface tension of the solution in which the magnetite is immersed plays an important role in determining the wetting characteristics of the system. It is not sufficient to consider a surface being rendered hydrophobic by adsorption of surfactant at the solid - liquid interface without regard for the adsorption occuring at the liquid - vapour interface.

The reducing values of γ_{lv} and γ_c and the

development of $(\gamma_{lv} - \gamma_c) > 0$ are shown in Fig. 40.

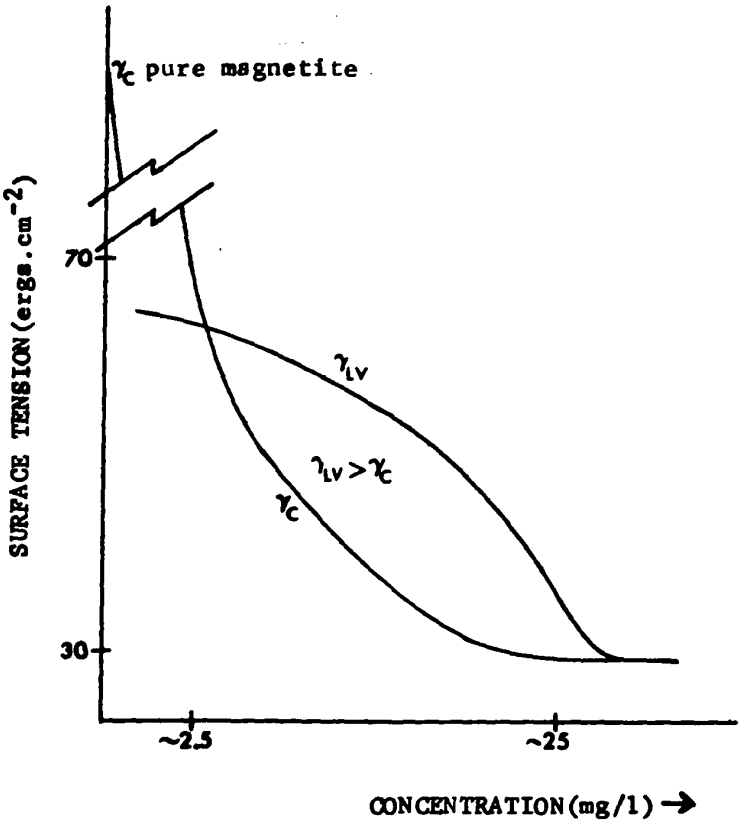

Figure 40. Variation in γ_{lv} and γ_c with Dodecylamine Acetate Concentration.

The diversity of the contact angle data for this system is surprising since contact angles are considered as characteristic of a given system. However, differing

results obtained from equilibrium conditions indicate that initiation of bubble - magnetite contact does not depend on the wetting properties of the solution. Bubble - particle collision kinetics or bubble surface charge may be controlling contact. However, flotation conditions are not at equilibrium, and as such $\theta_R = 0$ could be true for the system at equilibrium but not reflect the system under flotation conditions. Once contact is achieved, the resulting advancing contact angle, θ_A, can be explained in terms of the wetting properties of the equilibrated system.

Conclusions

(1) The suction potential technique and the captive bubble technique must be considered as complementary. The former yields both θ_A and θ_R and gives such values at truly equilibrated surfaces. The latter, if carefully handled, will yield dynamic contact angle values. The worth of either to any given system has to be assessed.

(2) The modification of Jowett[180] may result in operational difficulties. Also, it can not be satisfactorily demonstrated that the bed pore radius, r, does not vary after repeated use of the same bed.

(3) The general observation that $\theta_A > \theta_R$, is substantiated.

(4) Over all finite values, θ_A (as measured at s = 50%) is lower than θ_E. The value of θ_A at s = 70% approaches θ_E, suggesting that the ratio of liquid to vapour is important. Alternatively, θ_E may be high, since a metastable, dynamic contact angle can exist in this system.

(5) The variation of θ_A with concentration of dodecylamine acetate at all saturation levels is similar to that of θ_E.

(6) The dependence of the absolute value of θ_A on the

% saturation may indicate that a true contact angle value cannot be applied to flotation systems.

(7) Theoretically, surface roughness can promote a variety of contact angle values, by the stability it imparts to the triple point, liquid - vapour - solid.

(8) The variation in θ_A (and θ_E) can be explained in terms of the variation in $(\gamma_{lv} - \gamma_c)$ with increasing amine concentration. The contact angle approaches zero when $\gamma_{lv} \rightarrow \gamma_c \rightarrow \sim 28$ dynes.cm^{-1}.

(9) $\theta_R = 0$ for all conditions of concentration and % saturation, indicating that, for equilibrium conditions, replacement of dodecylamine solution at the solid surface by vapour is not spontaneous. $\theta_R = 0$ is possibly due to surface roughness.

FIGURE 41

WORK OF ADHESION

vs. DODECYLAMINE ACETATE CONCENTRATION

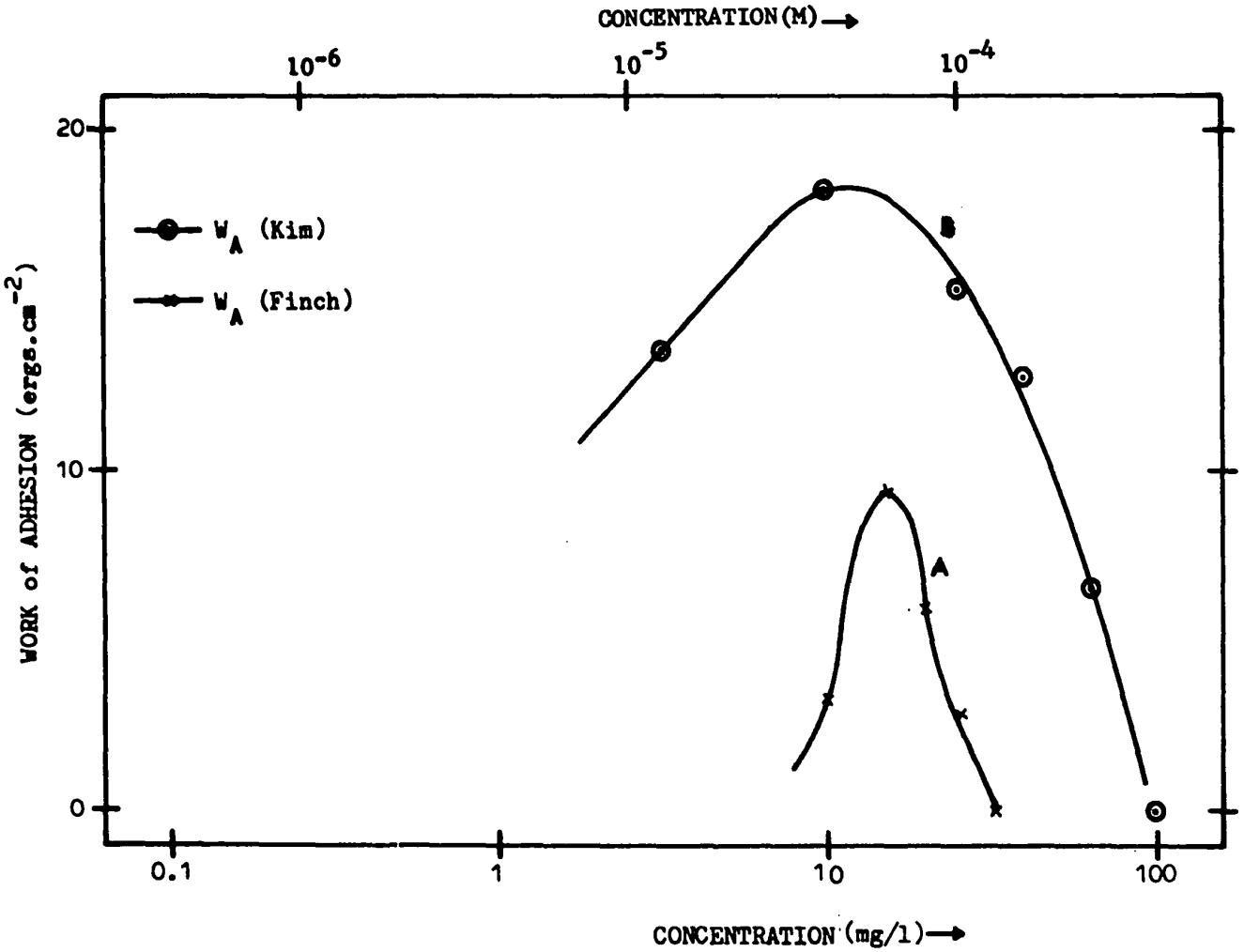
CONCENTRATION (M) →
10^-6
10^-5
10^-4
20
10
0
W_A (Kim)
W_A (Finch)
WORK of ADHESION (ergs.cm^-2)
B
A
0.1
1
10
100
CONCENTRATION (mg/l) →

is zero at concentrations less than about 8 mg/l and greater than 30 mg/l. Kim's data show a greater spread, the work of adhesion being finite in the range 1 mg/l to 80 mg/l. The maximum value of approximately 18 ergs.cm^{-2} occurs at about 10 mg/l. In both cases, work of adhesion reduces rapidly at concentrations outside the range corresponding to the maximum work of adhesion.

In order to test the calculated work of adhesion variation under flotation conditions, flotation tests were carried out on magnetite in dodecylamine solutions at pH 9.5 over the concentration range covered by the work of adhesion curves.

Flotation

(a) Apparatus and Procedure

The cell used was one previously developed and tested in this laboratory[120,129]. A full description of the apparatus, design and operation is given in a recent paper[198]. The design of the stirrer was improved to provide better agitation as the particle sizes to be tested, -65 +100 mesh, were much coarser than the samples originally tested, -325 +400 mesh. Also, a higher nitrogen flowrate was used, 100 ml/min. (at 76 cm of mercury) as opposed to 20 ml/min.[120].

The -65 +100 mesh magnetite sample was prepared and stored under distilled water. It was from this sample that the -65 +80 mesh material used for contact angle work was isolated. Flotation testing was carried out on approximately 1 gm of dry magnetite, delivered by a specially designed scoop[199]. In order to provide a measure of the importance of the solid - liquid interface to flotation, two sets of flotation tests were performed, one with zero conditioning time, the other using a thirty minute conditioning time, as recommended by Kim[137].

For zero conditioning time, the 1 gm sample was placed directly into the cell, the desired solution added and flotation performed for thirty seconds[120]. In the

case of thirty minutes conditioning time, the sample was first placed in a 50 ml vial, which was filled with test solution and stoppered with a rubber serum cap. Air was carefully removed by means of a hypodermic syringe[120], and the vial rotated end over end for thirty minutes. The total vial contents were then added to the cell and the flotation test performed.

The recovery was calculated by collecting, drying and weighing both the float and sink products. All the flotation tests were performed in duplicate.

(b) Results

Fig. 42 shows flotation recovery versus concentration of dodecylamine acetate. At concentrations less than 10 mg/l recovery is zero, for both conditioned and non-conditioned samples. Between 10 and 30 mg/l, the recovery for the conditioned magnetite rises sharply, being 100% at concentrations greater than 30 mg/l up to at least 200 mg/l. The recovery curve is less reproducible for the non-conditioned magnetite, but 100% recovery is observed at concentrations greater than 100 mg/l.

Fig. 43 compares the recovery of magnetite from the conditioned sample to the variation in work of adhesion according to the captive bubble data of Kim[117,137] and the present suction potential investigation, based on a

50% saturation level.

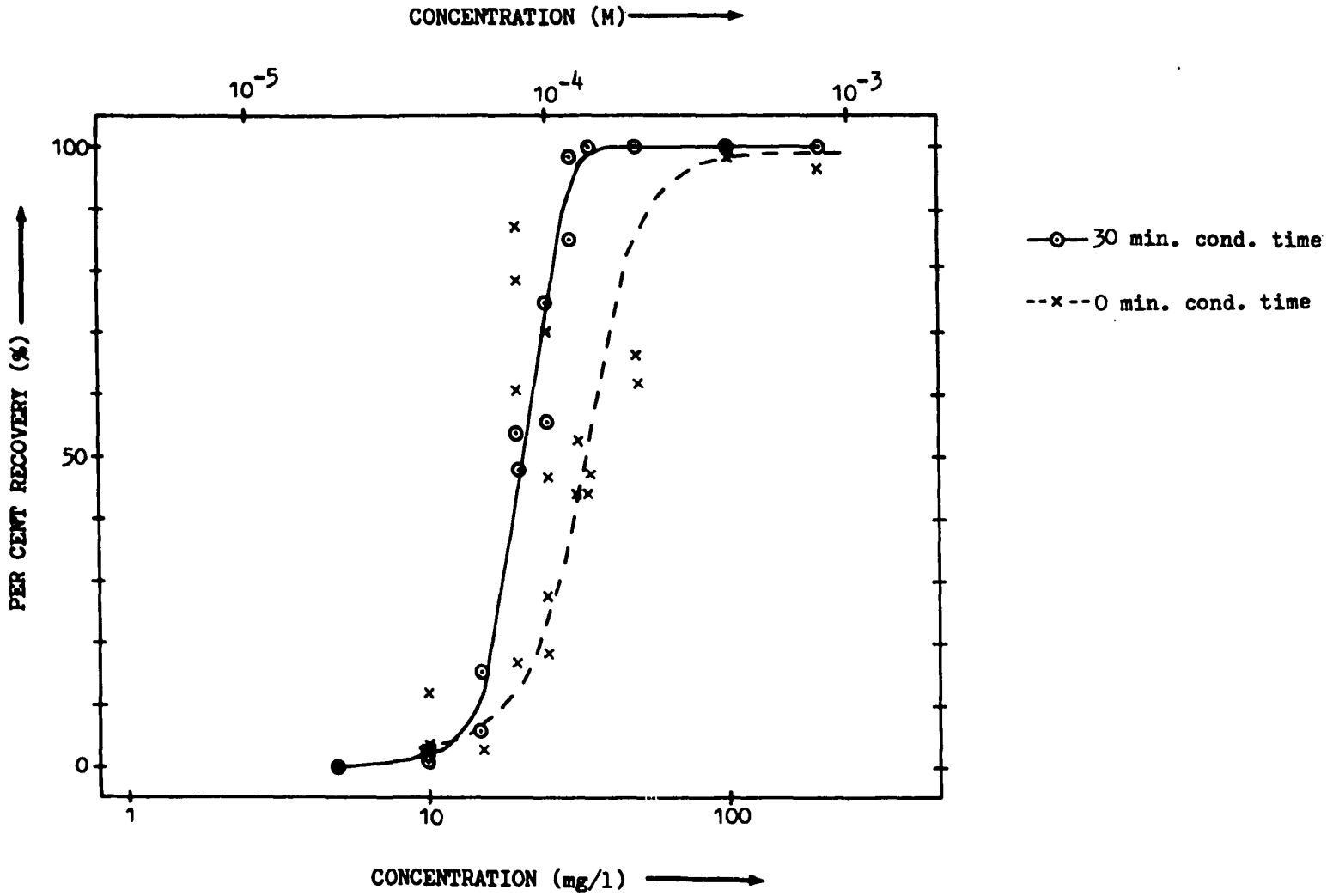
CONCENTRATION (M)
10^{-5}
10^{-4}
10^{-3}
100
50
0
PER CENT RECOVERY (%)
1
10
100
CONCENTRATION (mg/l)
30 min. cond. time
0 min. cond. time

FIGURE 43

MAGNETITE RECOVERY AND WORK OF ADHESION
vs. DODECYLAMINE ACETATE CONCENTRATION

GENERAL DISCUSSION

From Fig. 42, magnetite recovery for conditioned and non-conditioned surfaces commences at about 10 mg/l. According to Fig. 43, 10 mg/l corresponds to the maximum work of adhesion, W_A. At concentrations between 10 and 25 mg/l, the contact angle development was maximum, which was interpreted as the maximisation of $(\gamma_{lv} - \gamma_c)$. Thus, the initiation of magnetite flotation corresponds to the maximum measured hydrophobicity of the mineral in alkaline dodecylamine acetate solutions determined under equilibrium conditions. Flotation only occurs when the contact angle reaches a certain value, in fact its maximum value. 'Good' flotation is noted above $\theta = 40^o$ (119), suggesting that a certain contact angle must be reached.

Two notable features in the surface tension determination at pH 9.5 were the 'failure' of the drop weight technique at concentrations between 10 and 20 mg/l, and the sharp decrease in measured surface tension using the capillary rise technique at concentrations between 15 and 25 mg/l. Both were explained by the glass surfaces of the equipment being rendered hydrophobic under the action of the dodecylamine acetate solution. The subsequent contact angle work on magnetite revealed maximum hydrophobicity for the system at similar concentrations. This

correlation between magnetite and silica surfaces indicates that the amine solution chemistry controls the hydrophobicity of the two oxides. Under equilibrium conditions, therefore, solutions of dodecylamine acetate, at concentrations between 10 and 25 mg/l, at pH 9.5, can render silica and magnetite surfaces hydrophobic.

At concentrations greater than 25 mg/l, flotation recovery continues to increase, but the work of adhesion diminishes. Fig. 38 shows that the contact angle also diminishes above 25 mg/l, becoming zero at about 35 mg/l in the present investigation. Fuerstenau[134] demonstrated that flotation recovery and contact angle in the hematite - dodecylamine system increase together. This is clearly not the case with magnetite in alkaline dodecylamine solutions, regardless of the contact angle data chosen. An increase in % saturation of the magnetite bed in the suction potential technique indicated an increase in contact angle. Most flotation occurs with the liquid phase predominating. However, at $s \leq 70\%$, the contact angle trend does not support the noted flotation. At $s = 80\%$, the trend can only be inferred by comparing to the curves at lower % saturation. However, all the curves being of one family, it is reasonable to assume that the trend will be similar. Measurements at $s = 80\%$ are in doubt due to difficulty in reading the R - A cycle[144].

From the Young equation and the Zisman model, a high value of γ_{lv} promotes contact angle development and hence floatability:

$$\gamma_{lv} - (\gamma_{sv} - \gamma_{sl}) > 0 \qquad \text{...Young}$$

$$(\gamma_{lv} - \gamma_c) > 0 \qquad \text{...Zisman}$$

The surface tension determination, using the maximum bubble pressure technique, indicated that alkaline solutions of dodecylamine acetate are subject to pronounced surface aging. The surface tension in the few seconds required for flotation can be some 10 to 20 dynes.cm^{-1} greater than values of surface tension recorded at equilibrium. The surface aging phenomenon is, therefore, advantageous to flotation in this system. Therefore, the equilibrium measurements of θ_A and θ_R cannot be applied to the flotation condition. In this case, $\theta_R = 0$ may not be applicable to flotation, and spontaneous replacement of the solution at the solid surface may be possible.

The work of Smith and Lai[123] has shown that dynamic contact angles exist in alkaline dodecylamine acetate solutions above pH 9.1. Without a knowledge of the surface aging effect in these solutions, a metastable dynamic contact angle could be postulated as responsible

for the observed flotation. Leja[162] proposed that the dynamic contact angle was due to a surface aging effect. This is supported by the present observations. Leja considered "progressive condensation" occured, the non-charged amine molecule tending to pack closer into the solution surface. This should show itself in an increased equilibrium adsorption density and a lower minimum surface tension, in comparison to neutral solutions. Neither of these observations were made in the present investigation, nor by Manser[65] and Bartell[60] on alkaline dodecylamine and decylamine solutions respectively.

The correlation between the reported dynamic contact angle and surface aging is substantial. Both occur over the same time period, 0 - 100 seconds (within experimental error), and at similar concentrations and pH levels. Leja reported that dynamic contact angles occured at concentrations 'just less than' the c.m.c. The c.m.c. of alkaline dodecylamine is not clearly defined, but the sharp change in slope of the surface tension vs. concentration curve, interpreted as the c.m.c., corresponds to the maximum surface aging effect.

Smith and Lai, although considering surface aging as a possible explanation for dynamic contact angles, raised the objection that γ_{lv} can never reduce sufficiently

to effect a contact angle decrease from 80^{o} to zero, without change in γ_{sv} and/or γ_{sl}. Assuming an initial γ_{lv} of 70 dynes.cm^{-1}, a final value of 12.5 dynes.cm^{-1} is required, which is much lower than is observed. However, using the Zisman model[15], contact angle development is related to the value of $(\gamma_{lv} - \gamma_{c})$. When $\gamma_{lv} = \gamma_{c}$, contact angle development ceases. Smith and Lai used 25 mg/l dodecylamine solutions. The present investigation has indicated that at concentrations greater than about 30 mg/l, at equilibrium, $\gamma_{lv} = \gamma_{c} \approx 28$ dynes.cm^{-1}. Thus, the observation that the dynamic contact angle reduces to zero can be explained entirely by a reducing value of surface tension.

The concept of $(\gamma_{lv} - \gamma_{c})$ controlling contact angle formation was seen to be useful in describing contact angle vs. concentration curves in the equilibrated system. Adsorption of surfactant occurs at the bubble surface and the solid surface, changing the relative values of γ_{lv} and γ_{c}. Under flotation conditions adsorption at these surfaces again takes place, but with time as an added parameter. Conditioning of the mineral surface enables γ_{c} to approach the equilibrium value. A low value of γ_{c} is useful in promoting hydrophobicity and this is demonstrated in the improvement in flotation recovery which occurs when the magnetite is conditioned for thirty minutes. Upon the

introduction of a fresh air bubble, γ_{lv} is larger than the equilibrium value. A large value of γ_{lv} is useful for promoting hydrophobicity, as the flotation recovery demonstrates in comparison to the contact angle data, where all the surfaces involved have 'aged'. Thus, the concept of $(\gamma_{lv} - \gamma_c)$ is useful in describing the flotation regime used in the present investigation.

Although $(\gamma_{lv} - \gamma_c)$ has proven extremely useful, the concept of γ_c remains abstract. From a plot of γ_{lv} vs. $\cos\theta$ (Fig. 21), γ_c is envisaged as being the value of γ_{lv} at $\theta = 0$, if the solid could be isolated from the surfactant solution. Like the values of γ_{sv} and γ_{sl}, γ_c is virtually impossible to measure, but unlike γ_{sv} and γ_{sl}, γ_c has the physical significance indicated by Fig. 21 and, therefore, is easier to conceive and work with. The concept of γ_c was derived from data on low surface energy solids, and as such the applicability to high surface energy oxides can be questioned. However, the art of flotation is to render the solid hydrophobic, which is the property of a low surface energy solid. Thus, if flotation occurs, the floated material can be considered a low surface energy solid.

Accepting the concept of γ_c, two inferences arise:

(1) The surface tension of the solution is important in controlling flotation. As γ_{lv} approaches γ_c,

contact angle development and flotation cease.

(2) Adsorption of surfactant at the solid surface must be greater than at the liquid - vapour interface, as indicated in Fig. 40. Adsorption at the solid surface can be either via the solid - liquid interface or the solid - vapour interface.

The first inference is that surface tension is important in determining mineral floatability. A low value of γ_{lv} is detrimental to contact angle development and flotation. From the present investigation a low value of γ_{lv} can occur by allowing the liquid - vapour interface to approach equilibrium, by employing a high surfactant concentration, or using a high pH. In the present investigation, allowing γ_{lv} to decrease by permitting equilibrium to be approached was seen to be detrimental to magnetite floatability. Similarly, the observations of Smith and Lai[123], Leja and Shulman[163], Wark[157] and Rogers[160] can be explained by 'aging' of liquid - vapour interfaces involved. In the flotation systems employing amines, it is a frequent observation that at high surfactant concentration or high pH, mineral floatability is decreased[6,119,134]. Reverse orientation of the adsorbed layer, rendering the surface hydrophyllic, is considered a possible cause[200]. However, both high amine concentration and high pH tend to give low values of γ_{lv}, indicating that γ_{lv} approaches γ_c and

hence accounting for the poor floatability. In general, the surface tension of the collector solution has been of limited interest with respect to actual flotation. The present investigation indicates that surface tension may play an important role.

The second inference is the subject of recent reports by Somasundaran[27], Sandvik and Digrè[69] and Wada[201] and by implication, Zisman[15] and Ter-Minassian-Seraga[169]. They observe, in dilute solutions in the presence of a gaseous phase, increased adsorption at the solid surface. In contact angle work and flotation, a gaseous phase must be present. Approximately 30% greater adsorption density has been noted at the solid surface in comparison with the liquid - vapour interface[69]. The gaseous phase is considered as a transporting agent, promoting adsorption at the solid - vapour interface[27,69,201]. Fig. 42 indicates that, although conditioning time improved flotation, it was not necessary to achieve at least some flotation. In view of the experiments of Sandvik and Digre etc., the presence of the gaseous phase itself is probably more than just an agent for transporting the mineral particle to the solution surface. Since flotation does not rely entirely on adsorption at the solid - liquid interface, long, equilibrium adsorption tests in the absence of a gas phase, which is the usual technique[6,66,121,129], must be considered of

limited applicability.

The object of the present research was to investigate the poor correlation between work of adhesion and floatability. The most important factor is time. Measurements performed on the equilibrium system do not relate to the floatability exhibited by magnetite in alkaline dodecylamine solutions. Flotation is a dynamic process and this must be considered in flotation testing. The time required for the flotation of a mineral particle must be known, and contact angle and surface tension data determined for surfaces which have aged for this time. An improved correlation between work of adhesion and flotation should follow.

The work of adhesion formula could be re-written to include the time variable:

$$\gamma_{lv} = f_1(t)$$

$$\text{and } \cos\theta = f_2(t)$$

$$\text{Thus } W_A(t) = f_1(t)\left[1 - f_2(t)\right] \qquad \ldots 43$$

The average work of adhesion, $\bar{W}_A$, over the time T for flotation of a mineral particle is:

$$\bar{W}_A = \frac{\int_o^T W_A(t)dt}{\int_o^T dt}$$

$$= \frac{\int_o^T f_1(t)\left[1 - f_2(t)\right]dt}{\int_o^T dt} \qquad \ldots 44$$

The known values are:

$$f_1(0) = 72$$

$$f_2(0) = 0.17^*$$

Determining $\theta = f_2(t)$ would present difficult control problems, especially the roughness of the surface on which experiments are to be conducted. If $\overline{W}_A$ could be determined according to Eq. 44, its relevance to the present flotation system would be improved, and probably to all flotation systems.

*From the observations of Smith and Lai on quartz[123].

CONCLUSIONS

(1) The relative decrease of γ_{lv} and γ_c with increasing amine concentration controls the value of $(\gamma_{lv} - \gamma_c)$ and flotation commences when $(\gamma_{lv} - \gamma_c)$ is maximum.

(2) Allowing the solid - liquid interface to reach equilibrium allows the equilibrium value of γ_c to be approached, increasing $(\gamma_{lv} - \gamma_c)$, and promoting flotation.

(3) The presence of the gas phase promotes the attainment of the equilibrium value of γ_c, further increasing $(\gamma_{lv} - \gamma_c)$.

(4) Surface aging of alkaline dodecylamine solutions gives a high value of γ_{lv} at the initiation of bubble - particle contact, increasing $(\gamma_{lv} - \gamma_c)$, and promoting flotation.

(5) The observed surface aging of alkaline dodecylamine solutions substantiates the proposal of Leja[162] to account for the dynamic contact angle of Smith and Lai[123].

(6) Work of adhesion calculations based on γ_{lv} and θ obtained from interfaces at equilibrium, do not correspond to the dynamic conditions of flotation. A 'true' contact angle value may not be applicable to flotation

systems.

(7) The time factor, introduced in Eq. 44, adds a new variable to the understanding of flotation. It may play an important role in determining flotation in certain systems. The use of equilibrium conditions to investigate flotation is questioned.

SUGGESTIONS FOR FURTHER WORK

(1) The important role of surface aging in the dodecylamine - magnetite system requires further investigation. Surface aging in general should be investigated. Correlation between the age of the bubble and flotation recovery should be possible.

(2) The mechanism controlling surface aging should be determined. Knowledge of the mechanism may aid the understanding of adsorption at the solid surface and the role of neutral molecules which enhance flotation.

(3) The relationship (if any) between Eq.44 and flotation recovery should be investigated.

(4) The role of the solution surface tension, shown here to be a controlling factor, should be investigated for other systems. This can possibly be done by analysing previous contact angle and flotation data.

(5) The concept of γ_c was shown to be useful in explaining floatability. The value of γ_c for a dodecylamine surface can be found experimentally, and hence the predicted relationship, $\gamma_c = \gamma_{DDA} = 28$ dynes.cm^{-1}, can be tested.

(6) Recent work, including this study, has suggested that

the bubble is an important agent for transfering surfactant to the solid surface, specifically to the solid - vapour interface. This observation needs further investigation. Of particular interest is the possibility of reducing conditioning time by introduction of a gaseous phase.

Dodecylamine Acetate

The dodecylamine acetate used was from a batch previously prepared in this laboratory[129]. A melting point determination indicated the dodecylamine acetate to be of high purity[129].

Two stock solutions were made up by dissolving a known weight of dodecylamine acetate in conductivity water. Tests using dodecylamine acetate involved both stock solutions, thus affording a check on the results obtained. All concentrations are quoted in mg/l of dodecylamine acetate.

Conductivity Water

Distilled water from a 'Precision' brand laboratory still was re-distilled in an all-Pyrex Yoe-type still (Corning model AG-2). The pH was adjusted, and maintained at ~7 by flushing with high purity nitrogen.

Nitrogen

Certified 99.99% nitrogen (Grade L, Canadian Liquid Air Ltd.) was used with no further purification.

Magnetite

A sample of -65 +100 mesh magnetite was isolated

from a California magnetite beach sand supplied by Ward's Natural Science Establishment, Inc. The procedure was:

(1) Screening through 20 mesh and 65 mesh screens, the former to remove coarse silica sand (identified by visual inspection), the latter to remove unwanted fines.

(2) Electrostatic precipitation to remove silica.

(3) Successive washings in a Ding magnetic separator until no non-magnetics were obtained.

(4) Batch grinding under water in an agate mortor and wet screening to yield -65 +100 mesh material.

(5) Tumble washing in distilled water to remove fines.

(6) Storage under distilled water.

The sample used in the suction potential technique was obtained by wet screening at -65 +80 mesh.

APPENDIX II

SURFACE TENSION

A: CAPILLARY RISE

CALIBRATION EQUATION

$$\gamma_{lv} = \frac{1}{2} \rho g \frac{r_1 r_2}{r_1 - r_2} \Delta h$$

$$= K \Delta h$$

where $$K = \frac{1}{2} \rho g \frac{r_1 r_2}{r_1 - r_2}$$

ρ = 1.000 $gm.cm^{-3}$

g = 980.6 $cm.sec^{-2}$

r_1 = radius of large bore

r_2 = radius of small bore

Determination of r_1 and r_2:

Length of mercury column = l.

Weight of mercury column = w.

Specific gravity of mercury = ρ_{Hg}.

$$r = \left(\frac{w}{l \rho_{Hg} \pi} \right)^{\frac{1}{2}}$$

where ρ_{Hg} = 13.5303 (26.5° C) (202)

		Large Bore	Small Bore
l	(cm)	5.640 ± 0.006	7.123 ± 0.010
w	(gm)	0.5452 ± 0.001	0.2135 ± 0.0001
r_1	(cm)	$0.0476_8 \pm 0.0003$	
r_2	(cm)		$0.0265_5 \pm 0.0003$

$$\text{Hence } K = 29.37 \pm 0.15$$

Since the error in Δh is negligible in comparison to the error in K:

$$\underline{\gamma_{lv} = 29.37\ \Delta h \pm 0.15}$$

RESULTS

TABLE 3

SURFACE TENSION vs. DODECYLAMINE ACETATE CONCENTRATION

pH 4.1 ± 0.1

DDA Conc'n (mg/l)	Height Difference, Δh (cm)	Surface Tension, γ_{lv} (dynes.cm^{-1})
10	2.421	71.1
	2.424	71.2
	2.460	72.2
	2.452	72.0
100	2.372	69.7
	2.364	69.4
	2.363	69.4
	2.358	69.2
250	2.351	69.0
	2.330	68.4
	2.358	69.2
	2.359	69.3
	2.280	67.8
475	2.328	68.4
	2.285	67.1
	2.287	67.2
500	2.221	65.2
	2.344	68.8
625	2.193	64.4
	2.166	63.6
	2.245	65.9
	2.258	66.3
	2.253	66.2
1000	2.020	59.1
	2.029	59.6
	2.011	59.1

TABLE 3 (continued)

DDA Conc'n (mg/l)	Height Difference, Δh (cm)	Surface Tension, γ_{lv} (dynes.cm^{-1})
1600	1.651	48.5
2000	1.353	39.7
2500	1.324	38.9
	1.311	38.5
5000	1.027	30.2
	1.019	29.9
10000	1.028	30.2
	1.045	30.7
	1.048	30.8
	1.053	30.9
	Neutral	
0	2.470	72.5
	2.467	72.4
	2.474	72.6
	2.468	72.4
	2.467	72.4
	2.463	72.3
10	2.443	71.7
	2.438	71.6
100	2.388	70.1
	2.370	69.6
	2.276	66.8
	2.221	65.2
400	2.054	60.3
	2.084	61.2
1000	1.604	47.1
2500	1.105	32.4

TABLE 3 (continued)

DDA Conc'n (mg/l)	Height Difference, Δh (cm)	Surface Tension, γ_{lv} (dynes.cm^{-1})
3000	1.074	31.5
	1.027	30.2
10000	1.064	31.2
	1.090	32.0
	pH 9.5 ± 0.3	
1	2.483	72.9
	2.500	73.4
	2.495	73.3
10	2.407	70.8
15	2.411	71.0
20	2.218	65.1
	2.293	67.3
	2.318	68.1
22.5	0.548	16.1
25	0.391	11.5
	0.366	10.7
	0.405	11.9
40	0.419	12.3
	0.559	16.4
75	0.394	11.6
	0.427	12.5
100	0.329	9.7
	0.321	9.4

TABLE 4

EQUILIBRATION TIMES FOR NEUTRAL DODECYLAMINE ACETATE SOLUTIONS

DDA Conc'n 400 mg/l			DDA Conc'n 1000 mg/l		
Time (mins)	Δh (cm)	γ_{lv} (dynes.cm^{-1})	Time (mins)	Δh (cm)	γ_{lv} (dynes.cm^{-1})
0	2.229	65.5	0	2.057	60.4
20	2.026	59.5	10	1.941	57.0
60	2.054	60.3	15	1.874	55.0
			30	1.706	50.1
			45	1.642	48.2
			60	1.627	47.8
			75	1.616	47.5
			85	1.607	47.2
			100	1.604	47.1

TABLE 4 (continued)

DDA Conc'n 2,500 mg/l			DDA Conc'n 3,000 mg/l			DDA Conc'n 10,000 mg/l		
Time (mins)	Δh (cm)	γ_{lv} (dynes.cm^{-1})	Time (mins)	Δh (cm)	γ_{lv} (dynes.cm^{-1})	Time (mins)	Δh (cm)	γ_{lv} (dynes.cm^{-1})
0	1.373	40.3	0	1.151	33.8	0	1.066	31.3
10	1.285	37.7	20	1.124	33.0	10	1.056	31.0
25	1.167	34.3	30	1.076	31.6	20	1.064	31.2
40	1.153	33.8	45	1.094	32.1			
65	1.124	33.0	55	1.079	31.7			
75	1.120	32.9	70	1.074	31.5			
85	1.111	32.6						
95	1.105	32.4						

B: DROP WEIGHT

CALIBRATION EQUATION

$$\gamma_{lv} = \frac{mg}{2\pi r\ \psi(r/V^{1/3})}$$

$$= K \frac{m}{\psi(r/V^{1/3})}$$

where $K = \frac{g}{2\pi r}$

	Thick-Walled Tip (cm)	Thin-Walled Tip (cm)
r =	$0.376_1 \pm 0.005$	$0.200_0 \pm 0.003$
K =	$414.9_1 \pm 0.5$	$780._2 \pm 1.2$

Since error in m and $\psi(r/V^{1/3})$ is negligible,

Thick-walled tip:

$$\gamma_{lv} = 414.9 \times \frac{m}{\psi(r/V^{1/3})} \pm 0.5$$

Thin-walled tip:

$$\gamma_{lv} = 780.0 \times \frac{m}{\psi(r/V^{1/3})} \pm 1.2$$

RESULTS

TABLE 5

SURFACE TENSION vs. DODECYLAMINE ACETATE CONCENTRATION

DDA Conc'n (mg/l)	Drop Weight, m (gm)	$V^{1/3}$ (cm)	$r/V^{1/3}$	$\psi(r/V^{1/3})$	Surface Tension, γ_{lv} (dynes.cm^{-1})
		pH 4.1 ± 0.1			
10	0.10400	0.4703	0.7998	0.6000	71.9
	0.10420	0.4706	0.7992	0.6000	72.1
100	0.09854	0.4619	0.8143	0.6002	68.1
	0.10233	0.4677	0.8041	0.6000	70.8
250	0.09895	0.4625	0.8131	0.5999	68.4
	0.10211	0.4674	0.8047	0.6000	70.6
	0.10144	0.4664	0.8064	0.5999	70.1
475	0.09443	0.4554	0.8259	0.5996	65.3
	0.09530	0.4568	0.8234	0.5996	65.9
1000	0.07597	0.4235	0.8880	0.5997	52.6
	0.07695	0.4253	0.8842	0.5996	53.2
	0.07640	0.4243	0.8863	0.5997	52.9
1875	0.05930	0.3900	0.9645	0.6053	40.6
	0.05994	0.3914	0.9610	0.6048	41.1
2500	0.05012	0.3687	1.0201	0.6130	33.9
	0.04949	0.3671	1.0244	0.6138	33.4
	0.04904	0.3660	1.0275	0.6142	33.1
	0.05191	0.3730	1.0082	0.6110	35.2
3750	0.04496	0.3556	1.0577	0.6195	30.1
	0.04521	0.3562	1.0557	0.6191	30.3
5000	0.04464	0.3547	1.0602	0.6199	29.9
	0.04466	0.3548	1.0600	0.6199	29.9
10000	0.04499	0.3554	1.0582	0.6195	30.1
	0.04494	0.3555	1.0578	0.6195	30.1

TABLE 5 (continued)

DDA Conc'n (mg/l)	Drop Weight, m (gm)	$V^{1/3}$ (cm)	$r/V^{1/3}$	$\psi(r/V^{1/3})$	Surface Tension, γ_{lv} (dynes.cm^{-1})
		Neutral			
0	0.10374	0.4699	0.8004	0.6000	71.7
	0.10362	0.4697	0.8007	0.6000	71.7
6	0.10402	0.4703	0.7997	0.6000	71.9
	0.10417	0.4705	0.7993	0.6000	72.0
60	0.10334	0.4693	0.8015	0.6000	71.5
	0.10358	0.4696	0.8008	0.6000	71.6
200	0.09691	0.4393	0.8188	0.5998	67.0
	0.09757	0.4604	0.8170	0.5998	67.5
600	0.07741	0.4262	0.8825	0.5995	53.6
	0.07854	0.4282	0.8782	0.5995	54.4
1000	0.06851	0.4092	0.9191	0.6005	47.2
	0.06808	0.4083	0.9211	0.6005	47.0
2500	0.04204	0.3477	1.0816	0.6259	27.9
	0.04224	0.3483	1.0799	0.6259	28.0
3000	0.03923	0.3398	1.1069	0.6293	25.9
	0.03925	0.3398	1.1067	0.6293	25.9
6000	0.04428	0.3538	1.0631	0.6199	29.6
	0.04431	0.3539	1.0628	0.6199	29.7
10000	0.04896	0.3658	1.0281	0.6259	32.5
	0.04948	0.3671	1.0245	0.6249	32.8

TABLE 5 (continued)

DDA Conc'n (mg/l)	Drop Weight, m (gm)	$V^{1/3}$ (cm)	$r/V^{1/3}$	$\psi(r/V^{1/3})$	Surface Tension, γ_{lv} (dynes.cm^{-1})
		pH 9.5 ± 0.3			
1	0.10440	0.4709	0.7987	0.6000	72.2
	0.10310	0.4698	0.8021	0.6000	71.2
10	0.10140	0.4663	0.8065	0.5999	70.1
	0.09580	0.4576	0.8220	0.5997	66.2
	0.09700	0.4595	0.8185	0.5998	67.1
25*	0.05162	0.3723	0.5371	0.6405	62.8
	0.05474	0.3797	0.5267	0.6440	66.3
	0.04721	0.3614	0.5534	0.6355	57.4
	0.04612	0.3586	0.5577	0.6344	56.7
40*	0.04430	0.3538	0.5652	0.6329	55.0
	0.04151	0.3462	0.5776	0.6303	51.4
	0.04225	0.3583	0.5742	0.6309	52.2
	0.04218	0.3481	0.5745	0.6309	52.1

*thin-walled tip

CALIBRATION EQUATION

$$\gamma_{lv} = A(H\delta\rho_m + 0.69\, r_1\rho_1)$$

where $\rho_1 = 1.000\ gm.cm^{-3}$

$r_1 = 0.2380 \pm 0.002\ cm$

Determination of $\delta\rho_m$:

$$\delta\rho_m = \rho_w - \rho_o$$

where ρ_w = density of water

ρ_o = density of oil

$\rho_w = 1.000\ gm.cm^{-3}$

ρ_o: determined using a pycnometer

weight s.g. bottle plus oil = w_1

weight s.g. bottle plus water = w_2

weight s.g. bottle = w_3

$$\rho_o = \left(\frac{w_1 - w_2}{w_2 - w_3}\right) \times 1.000\ gm.cm^{-3}$$

Results:

w_1:	37.0052	39.6305	37.0032	36.9923	39.6210*
w_2:	41.5900	44.1915	41.5536	41.5495	44.1738
w_3:	16.5166	19.1500	16.5211	16.5100	19.1440
ρ_o:	0.8171	0.8179	0.8182	0.8180	0.8181

*Oil tested after two weeks contact with conductivity water.

$$\rho_o = 0.8179 \pm 0.0003$$
$$\delta\rho_m = 0.1821 \pm 0.0003$$

Conductivity water at 25° C:

$$\gamma_{lv} = 71.97 \text{ dynes.cm}^{-1} \quad (106)$$

$$\text{Thus } A = \frac{71.97}{(H \times 0.8179 + 0.08210)} \text{ cm}^2.\text{sec}^{-2}$$

Manometer Readings, cm		Height Difference, cm
h_1	h_2	H
5.63	18.52	12.89
5.62	18.47	12.85
5.69	18.52	12.83
5.71	18.56	12.85

Average: 12.85 ± 0.04

Hence $A = 29.6_8 \pm 0.3 \text{ cm}^2.\text{sec}^{-2}$

and $\gamma_{lv} = 29.6_8 (0.1821 \times H + 0.08210) \pm 0.3 \text{ cm}^2.\text{sec}^{-2}$

RESULTS

TABLE 6

SURFACE TENSION vs. DODECYLAMINE ACETATE CONCENTRATION

DDA Conc'n (mg/l)	Manometer Readings h_1 (cm)	Manometer Readings h_2 (cm)	Height Difference, H (cm)	Surface Tension, γ_{lv} (dynes.cm^{-1})
		pH 4.1 ± 0.1		
10	18.56	5.98	12.58	70.5
100	19.00	6.54	12.46	69.9
	18.53	6.28	12.25	68.7
250	17.45	5.52	11.93	67.0
	18.49	6.46	12.03	67.5
475	17.15	5.80	11.35	63.9
	16.98	5.51	11.47	64.5
625	16.40	6.14	10.26	58.0
1000	14.39	5.34	9.05	51.4
	12.56	3.54	9.02	51.3
1875	14.30	6.58	7.72	44.3
2500	12.30	6.03	6.27	36.7
	12.32	5.99	6.33	36.4
3750	11.05	5.86	5.19	30.6
5000	10.96	5.87	5.09	30.0
	11.10	5.89	5.21	30.7
10000	12.55	7.24	5.31	31.2

TABLE 6 (continued)

DDA Conc'n (mg/l)	Manometer Readings h_1 (cm)	h_2 (cm)	Height Difference, H (cm)	Surface Tension, γ_{lv} (dynes.cm^{-1})
		Neutral		
6	18.65	6.00	12.65	70.8
	18.60	5.97	12.63	70.7
12.5	18.80	6.57	12.23	68.6
60	18.50	6.58	11.87	66.7
	18.17	6.59	11.78	66.2
100	18.57	7.01	11.56	65.0
	18.67	7.07	11.60	65.2
200	18.07	7.13	10.94	61.7
	18.13	7.13	11.00	62.0
400	16.25	6.63	9.62	54.5
	17.44	7.61	9.83	55.7
600	14.93	5.88	9.05	51.4
	15.05	6.27	8.78	50.0
750	15.57	7.31	8.26	47.2
1000	15.39	7.99	7.58	43.5
1500	12.85	6.55	6.30	36.6
2500	11.10	6.04	5.06	29.9
3000	11.10	6.28	4.82	28.6
4000	12.27	7.19	5.08	29.7
6000	11.68	6.70	4.98	29.4
	14.40	9.41	4.99	29.5
10000	13.35	8.28	5.07	30.0

TABLE 6 (continued)

DDA Conc'n (mg/l)	Manometer Readings h_1 (cm)	h_2 (cm)	Height Difference, H (cm)	Surface Tension, γ_{lv} (dynes.cm^{-1})
	pH 9.5 ± 0.3 (1 in 10 bubble rate)			
1	19.38	13.19	12.48	70.1
1.6	19.83 - 19.29	13.60	12.46 - 11.38	69.9 - 64.0
3	19.69 - 19.20	13.70	11.98 - 11.00	67.3 - 62.0
5	19.29 - 18.93	13.59	12.40 - 10.68	69.5 - 60.2
8	18.82	13.31	11.02	62.1
10	18.51	13.27	10.48	59.2
15	18.50 19.10	13.49 13.90	10.00 10.30	56.6 58.2
22.5	18.04	13.52	9.05	51.4
25	17.70 18.42	13.32 13.48	8.76 9.88	49.9 55.9
34	16.99	13.51	6.96	40.2
40	17.25 15.72 16.29	13.10 12.90 13.00	8.30 5.64 6.58	47.4 33.0 38.1
50	16.60	12.98	7.24	41.9
75	16.92	13.18	7.42	42.6
85	17.48 16.72	13.70 13.70	7.56 6.04	43.4
100	16.18	13.39	5.58	32.7
200	15.91	13.39	5.00	29.6

TABLE 6 (continued)

DDA Conc'n (mg/l)	Manometer Readings h_1 (cm)	h_2 (cm)	Height Difference, H (cm)	Surface Tension, γ_{lv} (dynes.cm^{-1})
		(1 in 60 bubble rate)		
1	19.58	13.21	12.70	71.4
1.6	19.30	13.60	11.40	64.1
3	19.00	13.55	10.90	61.4
5	18.79	13.55	10.48	59.3
8	17.80	13.43	8.74	49.8
10	17.50	12.90	9.20	52.3
15	17.65	13.39	8.32	47.5
22.5	15.67	12.60	6.14	35.7
25	14.89	12.49	4.80	28.5
34	15.60	13.29	4.62	27.5
40	16.29	13.68	5.22	30.8
50	14.79	12.68	4.22	25.3
75	15.30	12.88	4.84	28.7
85	15.50	13.40	4.20	25.2
100	15.77	13.32	4.90	29.0

TABLE 7

SURFACE AGING IN ALKALINE SOLUTIONS

DDA Conc'n (molar)	Surface Tension, γ_{lv} (dynes.cm^{-1})	
	10 seconds	60 seconds
8×10^{-6}	68	62
1.6×10^{-5}	66	59
2×10^{-5}	65	57.5
4×10^{-5}	61	51
6×10^{-5}	57	43
8×10^{-5}	53	35
1.6×10^{-4}	42.5	27

APPENDIX III

CALCULATION OF DIFFUSION COEFFICIENT

CALCULATION OF DIFFUSION COEFFICIENT AT 10 mg/l (4×10^{-5}M) ALKALINE DODECYLAMINE SOLUTION

Ward and Tordai[54] equation:

$$\gamma_{lv} = 2\left(\frac{D}{\pi}\right)^{\frac{1}{2}} \left\{C_o t^{\frac{1}{2}} - \int_o^{t^{\frac{1}{2}}} \phi(z) d\left[(t - z)^{\frac{1}{2}}\right]\right\}$$

where $C_o = 4 \times 10^{-5}$M

$t = 40$ seconds (from Fig. 18).

Step 1

Calculation of $C_o t^{\frac{1}{2}}$:

$$C_o t^{\frac{1}{2}} = 4 \times 10^{-5} \times (40)^{\frac{1}{2}}$$

$$= 2.5 \times 10^{-4} \text{ moles.sec}^{\frac{1}{2}}\text{cm}^{-3}$$

Step 2

Calculation of $\int_o^{t^{\frac{1}{2}}} \phi(z) d\left[(t - z)^{\frac{1}{2}}\right]$:

z (sec)	$t - z$ (sec)	$(t - z)^{\frac{1}{2}}$ ($sec^{\frac{1}{2}}$)	γ_{lv}* dynes.cm	$\phi(z)$** 10^{-5} moles.cm^{-3}
5	35	5.9	65.0	0.40
10	30	5.5	61.0	1.20
15	25	5.0	57.5	2.00
20	20	4.5	55.5	2.60
25	15	3.9	54.0	3.00
30	10	3.2	52.6	3.50
35	5	2.2	51.6	3.65
37.5	2.5	1.6	51.5	3.70
40	0	0	51.0	3.90

*From Fig. 18

**From Fig. 16

From area under curve of $\phi(z)$ versus $(t - z)^{\frac{1}{2}}$ (Fig. 44):

$$\int_0^{t^{\frac{1}{2}}} \phi(z) d\left[(t - z)^{\frac{1}{2}}\right] = 1.8 \times 10^{-4} \text{ moles.sec}^{\frac{1}{2}}.\text{cm}^{-3}$$

Step 3

Calculation of Γ_{lv} at 4×10^{-5}M:

Gibbs adsorption equation:

$$\Gamma_{lv} = -\frac{1}{2.3RT} \frac{d\,\gamma_{lv}}{d \log c}$$

$$\frac{d\,\gamma_{lv}}{d \log c} = 31.2 \text{ ergs.cm}^{-2} \text{ (From Fig. 16)}$$

$$T = 298^{\circ} \text{ K}$$

$$R = 8.31 \times 10^{-7} \text{ ergs. } {}^{\circ}\text{K}^{-1} \text{ (mole)}^{-1}$$

$$\Gamma_{lv} = 5.5 \times 10^{-10} \text{ moles.cm}^{-2}$$

FIGURE 44

GRAPHICAL DETERMINATION OF INTEGRAL

$$I = \int_0^{t^{\frac{1}{2}}} \phi(z) d\left[(t - z)^{\frac{1}{2}}\right]$$

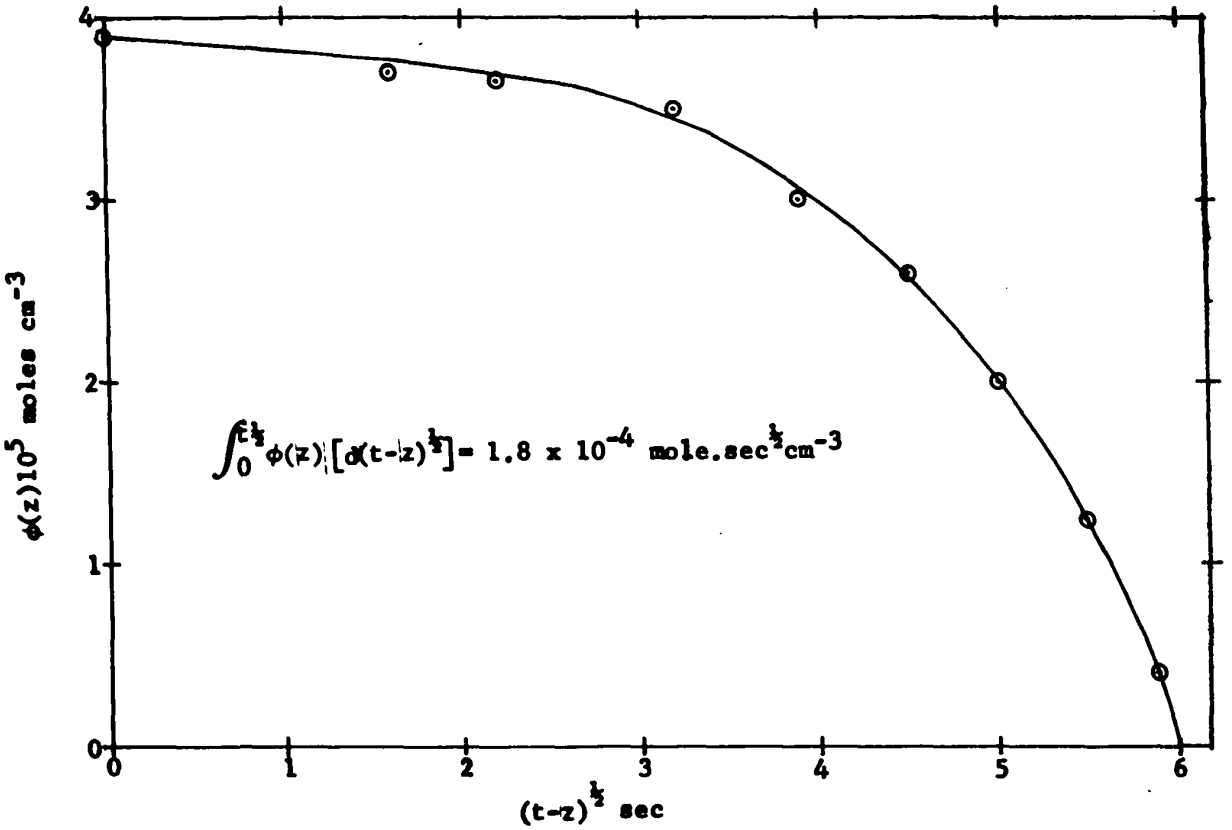
$\phi(z)10^5$ moles cm^{-3}
$\int_0^{t^{\frac{1}{2}}} \phi(z)[d(t-z)^{\frac{1}{2}}] = 1.8 \times 10^{-4}$ mole.$sec^{\frac{1}{2}}cm^{-3}$
$(t-z)^{\frac{1}{2}}$ sec
0
1
2
3
4
5
6

Substituting in Ward and Tordai equation:

$$5.5 \times 10^{-10} = D^{\frac{1}{2}} \frac{2}{\sqrt{\pi}} (2.5 \times 10^{-4} - 1.8 \times 10^{-4})$$

$$D^{\frac{1}{2}} = 7.10^{-4}$$

$$\underline{D \approx 5 \times 10^{-7} \text{ cm}^2.\text{sec}^{-1}}$$

APPENDIX IV

CONTACT ANGLE:

SUCTION POTENTIAL TECHNIQUE

DETERMINATION OF THE INTERNAL RADIUS, r, OF CALIBRATED MEASURING TUBE

Due to the larger bore of tube, relative to those employed in the capillary rise technique, the meniscus correction of Harkins and Brown[97] was used.

	l_1	l_2
Length of mercury column	7.062	3.532
	7.066	3.526
Average	7.064	3.529

	w_1	w_2
Weight of mercury column	13.1317	6.9863

$$r^2 = \frac{w_1 - w_2}{(l_1 - l_2)\rho_{Hg}}$$

$$r^2 = \frac{6.1454}{3.535 \cdot 13.5340}$$

Hence $r = 0.2020$ cm.

CALIBRATION CURVE TO CONVERT '1',
AS DETERMINED IN CALIBRATED MEASURING TUBE,
TO PER CENT SATURATION, 's'

A sample of magnetite was taken from the bed when the length, 1, in the measuring tube was 117 mm.

Weight of sample = 75.4932 gm
Weight of dried sample = 75.3535 gm
Moisture content = 0.1397 gm.

100% saturation corresponds to zero on calibrated measuring tube. Thus moisture content of the bed corresponding to 100% saturation is:

$$M.C. = 0.1397 + 11.7 \times \pi r^2 \text{ gm}$$

where $r = 0.2020$ cm.

Thus, at 117 mm, the % saturation, 's', is:

$$s_{l = 117} = \frac{0.1397}{0.1397 + 11.7 \times \pi(0.2020)^2}$$

$$s_{l = 117} = 8.5\%.$$

FIGURE 45

CALIBRATION CURVE FOR DETERMINING

% SATURATION OF MAGNETITE BED

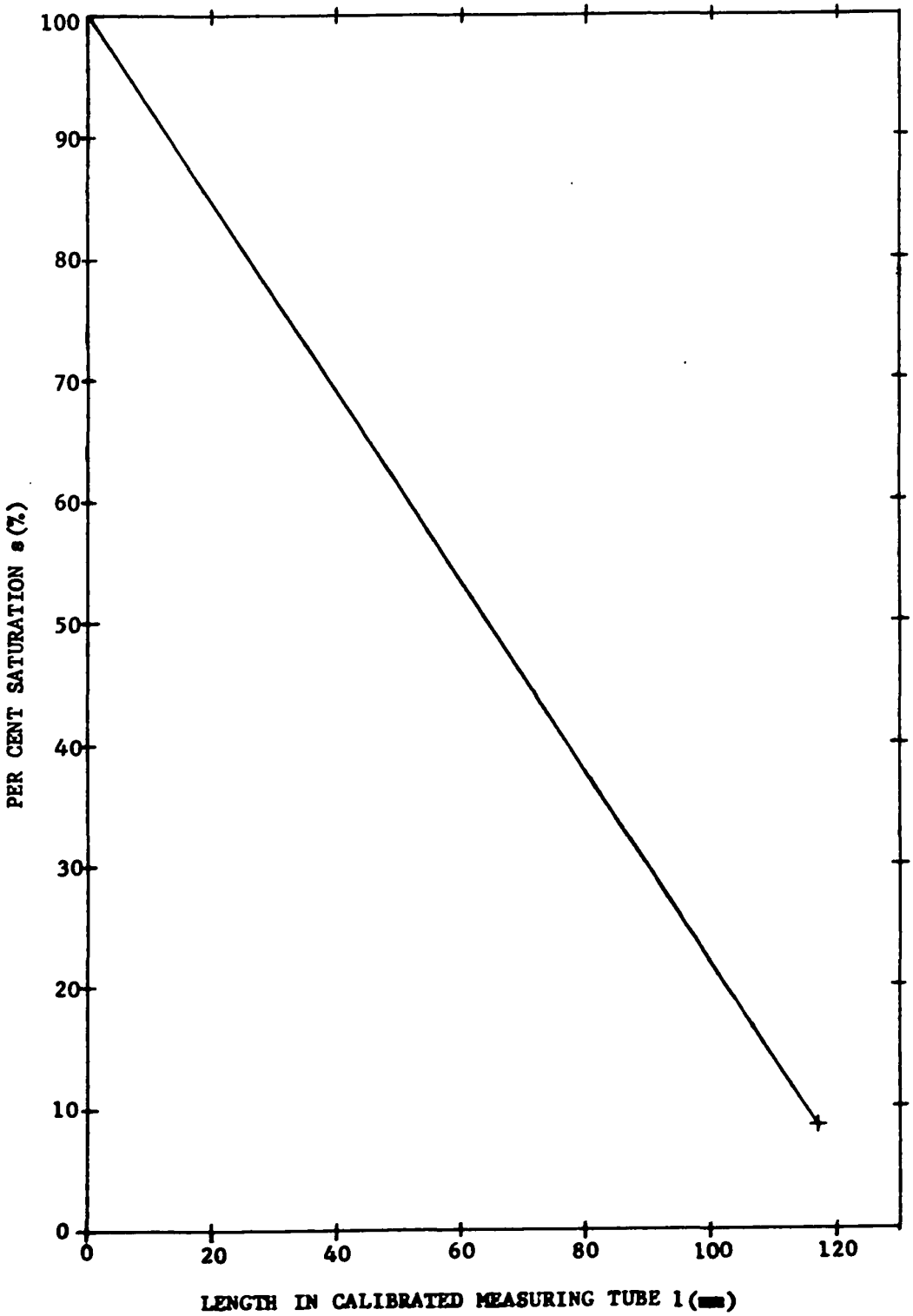
100
90
80
70
60
50
40
30
20
10
0
PER CENT SATURATION s (%)
0
20
40
60
80
100
120
LENGTH IN CALIBRATED MEASURING TUBE l (mm)

TABLE 8

SUCTION POTENTIAL vs. PER CENT SATURATION

	Pressure, ΔP (cm of water)		Length, l				% Saturation, s (%)	
			Observed (mm)		Corrected (mm)			
Test No.	1	2	1	2	1	2	1	2
Curve R_o	12.4		4.8		4.8		96.2	
	13.3		4.8		4.8		96.2	
	18.9		11.0		11.0		91.4	
	18.1		11.0		11.0		91.4	
	24.1		21.0		21.0		84.6	
	24.6		22.2		22.2		82.6	
	24.9		24.0		24.0		81.3	
	25.3		25.0		25.0		80.5	
	25.7		27.0		27.0		79.0	
	27.4		33.0		33.0		74.3	
	30.8		54.0		54.0		58.0	
	33.7		78.0		78.0		39.2	
	35.2		90.0		90.0		29.9	
	40.5		101.0		101.0		21.1	
	47.2		109.0		109.0		15.0	
	55.5		114.0		114.0		11.0	
	64.2		117.0		117.0		8.5	

1: Conductivity water
2: Repeat

TABLE 8 (continued)

	Pressure, ΔP (cm of water)		Length, l Observed (mm)		Length, l Corrected (mm)		% Saturation, s (%)	
Test No.	1	2	1	2	1	2	1	2
Curve								
A	32.7	44.7	107.0	115.0	107.0	124.0	16.5	10.2
	25.8	35.5	98.0	111.9	98.0	120.9	23.5	11.5
	18.4	27.6	73.0	107.0	73.0	116.0	43.0	16.5
	18.0	27.2	70.8	105.5	70.8	114.5	44.8	17.8
	10.5	17.4	36.0	82.0	36.0	91.0	72.0	36.0
	0.0	11.9	16.2	40.0	16.2	49.0	87.5	68.8
		6.4		23.0		32.0		82.0
		0.0		9.0		18.0		93.0
R	18.8	14.2	22.5	4.2	22.5	13.2	82.5	96.5
	25.3	20.7	30.0	12.0	30.0	21.0	76.6	90.7
	29.5	22.3	52.5	20.0	52.5	29.0	59.2	84.5
	32.0	26.7	70.5	43.0	70.5	52.0	45.0	66.5
	34.3	30.0	83.0	56.0	83.0	65.2	35.2	56.5
	36.8	34.8	92.0	83.5	92.0	92.5	28.3	34.8
	43.2	37.7	105.0	94.0	105.0	103.0	18.0	26.5
	50.4	43.7	112.0	107.0	112.0	116.0	12.5	16.5
	62.5	51.9	117.2	114.0	117.2	123.0	8.3	11.0
		66.3		118.0		127.0		7.9

1: Conductivity water
2: Repeat

TABLE 8 (continued)

DDA Conc'n (mg/l)	Pressure, ΔP (cm of water)		Length, l Observed (mm)		Length, l Corrected (mm)		% Saturation, s (%)	
	10.0	15.0	10.0	15.0	10.0	15.0	10.0	15.0
Curve								
R	6.8	13.7	4.0	18.0	12.0	30.0	96.7	86.0
	12.0	15.2	17.1	28.0	25.1	39.7	86.8	78.2
	20.8	19.3	49.1	45.0	57.1	57.0	61.6	65.0
	24.9	24.4	64.0	66.2	72.0	78.2	50.0	48.3
	30.1	26.5	79.0	75.0	87.0	87.0	38.4	41.5
	35.1	31.7	92.0	91.0	100.0	103.0	28.3	29.0
	39.5	39.3	101.0	103.0	109.0	115.5	21.1	19.6
	44.3	49.5	107.5	113.0	115.5	125.0	16.1	11.6
	53.2	62.5	115.0	117.0	123.0	129.0	10.2	8.5
	64.0		117.0		125.0		8.5	
A	40.6	34.0	114.2	113.5	122.2	125.5	10.8	11.3
	31.7	24.7	110.0	109.0	118.0	121.0	14.0	14.9
	25.3	20.3	103.5	104.8	111.5	116.8	19.2	18.2
	20.5	15.9	96.2	96.4	104.2	108.5	25.0	24.8
	17.6	12.3	88.2	87.9	96.2	99.9	31.0	31.5
	13.0	9.3	78.0	72.5	86.0	84.5	39.2	43.4
	6.5	6.0	48.0	54.0	56.0	66.0	62.5	58.0
	3.3	3.0	33.0	37.2	41.0	49.2	74.3	71.0

TABLE 8 (continued)

	Pressure, ΔP (cm of water)		Observed (mm)		Corrected (mm)		% Saturation, s (%)	
Test No.	1	2	1	2	1	2	1	2
Curve								
R	8.7	6.6	7.0	2.0	17.0	9.0	94.5	98.4
	13.0	13.5	21.1	16.5	31.1	23.5	83.5	87.3
	16.9	20.8	37.0	39.0	47.0	46.0	71.0	69.5
	23.2	22.5	64.9	55.0	74.9	62.0	49.3	57.1
	26.0	23.6	80.2	57.0	90.2	64.0	37.4	55.5
	62.5	30.4	117.0	88.3	127.0	95.3	8.5	31.0
		37.0		102.1		109.1		20.2
		61.0		117.2		124.2		8.3
A	30.5	32.5	113.0	116.2	123.0	123.2	11.6	9.2
	24.2	24.5	109.0	114.0	119.0	121.0	14.9	11.0
	16.2	18.3	102.2	107.9	112.2	114.9	20.2	15.6
	10.5	12.5	87.2	93.2	97.2	100.2	32.0	27.3
	6.7	8.6	68.5	83.0	78.5	90.0	47.4	35.2
	2.6		43.5		53.5		66.1	
	0.0		23.0		33.0		82.0	

1: 35.0 mg/l
2: Re-wash

CALCULATION OF θ_A AND θ_R

$$(\cos \theta_y)_R = \left(\frac{h_y}{h_x}\right)_R \frac{(\gamma_{lv})_x}{(\gamma_{lv})_y}$$

$$(\cos \theta_y)_A = \left(\frac{h_y}{h_x}\right)_A \frac{(\gamma_{lv})_x}{(\gamma_{lv})_y}$$

Subscripts x and y refer to base (pure water) condition and test solution condition respectively. The values of h_y, h_x are suction potential measurements in cm of water at s = 50%.

$$\left.\begin{aligned} (h_x)_R &= 31.2 \text{ cm water} \\ (h_x)_A &= 15.8 \text{ cm water} \end{aligned}\right\} \text{(see Fig. 29)}$$

$$(\gamma_{lv})_x = 72.0 \text{ dynes} \cdot \text{cm}^{-1}$$

TABLE 9

RETREATING AND ADVANCING CONTACT ANGLES vs. CONCENTRATION OF DODECYLAMINE ACETATE SOLUTIONS AT pH 9.5

Conc'n (mg/l)	ΔP $(h_y)_R$	$(h_y)_A$	$(\gamma_{lv})_y$	$(\cos \theta_y)_R$	$(\cos \theta_y)_A$	θ_R	θ_A
0.1	31.0	15.8	72.0	1	1	0	0
1.0	30.2	14.3	65.0	1.07	1.01	0	0
10.0	24.6	10.5	51.0	1.12	0.937	0	21
15.0	23.0	7.5	43.5	1.22	0.785	0	38
20.0	22.4	6.6	36.0	1.43	0.835	0	34
25.0	21.6	6.0	30.0	1.66	0.910	0	25
35.0	23.0	6.1	27.0	1.94	1.04	0	0

TABLE 10

ADVANCING AND RETREATING CONTACT ANGLES:

DEPENDENCE ON PER CENT SATURATION OF MAGNETITE BED

DDA Concentration = 0.1 mg/l; $(\gamma_{lv})_y$ = 71.0 dynes.cm^{-1}

s	$(\Delta P_x)_R$	$(\Delta P_y)_R$	$(\cos\theta_y)_R$	θ_R
20	41.0	41.0	1	0
30	36.0	36.0	1	0
40	33.5	33.5	1	0
50	31.2	30.8	1	0
60	29.5	28.2	0.968	14
70	27.5	25.1	0.926	22
80	25.0	21.4	0.867	30
	$(\Delta P_x)_A$	$(\Delta P_y)_A$	$(\cos\theta_y)_A$	θ_A
20	26.5	29.5	1.128	0
30	21.0	21.0	1	0
40	18.0	18.0	1	0
50	15.8	15.8	1	0
60	13.6	13.6	1	0
70	11.2	10.9	0.987	9
80	7.0	6.6	0.966	15

TABLE 10 (continued)

DDA Concentration = 1.0 mg/l; $(\gamma_{lv})_y$ = 65.0 dynes.cm^{-1}

s	$(\Delta P_x)_R$	$(\Delta P_y)_R$	$(\cos \theta_y)_R$	θ_R
20	41.0	41.8	1.130	0
30	35.7	35.7	1.107	0
40	33.0	33.0	1.107	0
50	31.2	30.2	1.072	0
60	29.8	27.4	1.019	0
70	27.7	24.1	0.964	15
80	24.9	20.7	0.921	23
	$(\Delta P_x)_A$	$(\Delta P_y)_A$	$(\cos \theta_y)_A$	θ_A
20	26.5	28.1	1.172	0
30	20.8	20.8	1.107	0
40	128.0	127.2	1.059	0
50	15.8	14.3	1.001	0
60	13.6	12.4	1.010	0
70	11.3	10.3	1.010	0
80	6.7	4.6	0.761	40

TABLE 10 (continued)

DDA Concentration = 10 mg/l; $(\gamma_{lv})_y$ = 50.6 dynes.cm^{-1}

s	$(\underline{\Delta P}_x)_R$	$(\underline{\Delta P}_y)_R$	$(\underline{\cos\theta}_y)_R$	$\underline{\theta}_R$
20	41.2	41.2	1.421	0
30	36.0	33.6	1.326	0
40	33.2	28.5	1.220	0
50	31.2	24.4	1.112	0
60	29.4	21.3	1.030	0
70	27.2	18.5	0.968	14
80	24.6	14.8	0.856	31
	$(\underline{\Delta P}_x)_A$	$(\underline{\Delta P}_y)_A$	$(\underline{\cos\theta}_y)_A$	$\underline{\theta}_A$
20	26.6	24.4	1.304	0
30	21.0	17.9	1.211	0
40	18.0	14.3	1.130	0
50	15.8	10.4	0.937	20
60	13.6	6.7	0.702	45
70	11.3	3.7	0.466	62
80	6.7	0.5	0.106	84

TABLE 10 (continued)

DDA Concentration = 15 mg/l; $(\gamma_{lv})_y$ = 43 dynes.cm^{-1}

s	$(\underline{\Delta P}_x)_R$	$(\underline{\Delta P}_y)_R$	$(\underline{\cos\theta}_y)_R$	$\underline{\theta}_R$
20	41.0	38.0	1.532	0
30	35.6	30.8	1.431	0
40	33.0	26.4	1.323	0
50	31.2	23.0	1.220	0
60	29.6	20.3	1.134	0
70	27.4	17.9	1.081	0
80	24.6	15.2	1.020	0
	$(\underline{\Delta P}_x)_A$	$(\underline{\Delta P}_y)_A$	$(\underline{\cos\theta}_y)_A$	$\underline{\theta}_A$
20	26.5	19.0	1.186	0
30	20.8	12.5	0.995	6
40	18.1	9.5	0.867	30
50	15.8	7.4	0.775	39
60	14.0	5.8	0.685	47
70	11.5	3.3	0.475	62
80	6.7	0.0	0.000	90

TABLE 10 (continued)

DDA Concentration = 20 mg/l; $(\gamma_{lv})_y$ = 36.0 dynes.cm^{-1}

s	$(\Delta P_x)_R$	$(\Delta P_y)_R$	$(\cos\theta_y)_R$	θ_R
20	41.0	36.5	1.780	0
30	35.6	29.4	1.647	0
40	33.0	25.4	1.540	0
50	31.2	22.4	1.435	0
60	29.6	19.6	1.324	0
70	27.4	17.4	1.270	0
80	24.6	14.4	1.170	0

	$(\Delta P_x)_A$	$(\Delta P_y)_A$	$(\cos\theta_y)_A$	θ_A
20	26.5	19.0	1.431	0
30	20.8	12.6	1.210	0
40	18.1	9.5	1.044	0
50	15.8	6.6	0.836	33
60	14.0	4.4	0.627	51
70	11.5	2.8	0.474	62
80	6.7	0.6	0.179	80

TABLE 10 (continued)

DDA Concentration = 25 mg/l; $(\gamma_{lv})_y$ = 30.0 dynes.cm^{-1}

s	$(\Delta P_x)_R$	$(\Delta P_y)_R$	$(\cos\theta_y)_R$	θ_R
20	41.0	38.5	2.250	0
30	35.6	30.5	2.055	0
40	33.0	25.2	1.833	0
50	31.2	21.6	1.659	0
60	29.6	18.7	1.514	0
70	27.4	16.5	1.442	0
80	24.6	14.4	1.404	0

	$(\Delta P_x)_A$	$(\Delta P_y)_A$	$(\cos\theta_y)_A$	θ_A
20	26.5	17.5	1.580	0
30	20.8	11.3	1.303	0
40	18.1	0.5	1.126	0
50	15.8	6.0	0.911	24
60	14.0	4.1	0.702	45
70	11.5	2.1	0.438	64
80	6.7	0.0	0.000	90

TABLE 10 (continued)

DDA Concentration = 35 mg/l; $(\gamma_{lv})_y$ = 27.5 dynes.cm^{-1}

s	$(\Delta P_x)_R$	$(\Delta P_y)_R$	$(\cos\theta_y)_R$	θ_R
20	41.0	40.0	2.549	0
30	35.6	30.5	2.220	0
40	33.0	25.2	2.000	0
50	31.2	22.9	1.922	0
60	29.6	21.0	1.854	0
70	27.4	18.8	1.795	0
80	24.6	15.8	1.615	0
	$(\Delta P_x)_A$	$(\Delta P_y)_A$	$(\cos\theta_y)_A$	θ_A
20	26.5	16.6	1.640	0
30	20.8	11.5	1.445	0
40	18.1	8.6	1.241	0
50	15.8	6.2	1.025	0
60	14.0	4.5	0.840	33
70	11.5	2.1	0.477	61
80	6.7	0.0	0.000	90

APPENDIX V

WORK OF ADHESION

TABLE 11

WORK OF ADHESION vs.

DODECYLAMINE ACETATE CONCENTRATION AT pH 9.5

$$W_A = \gamma_{lv} (1 - \cos\theta)$$

Present Investigation

DDA Conc'n	γ_{lv}	θ_A	$\cos\theta_A$	$1 - \cos\theta_A$	W_A
1.0	65.0	0	1	0	0
10.0	51.0	21	0.937	0.063	3.4
15.0	43.5	38	0.785	0.215	9.4
20.0	36.0	34	0.835	0.165	5.9
25.0	30.0	25	0.910	0.090	2.7
35.0	27.0	0	1	0	0

Kim (117,137)

DDA Conc'n	γ_{lv}*	θ_E	$\cos\theta_E$	$1 - \cos\theta_E$	W_A
3.2	60.5	39	0.777	0.223	13.5
10.0	51.0	50	0.643	0.357	18.2
25.0	30.0	61	0.485	0.515	15.4
40.0	27.0	58	0.530	0.470	12.7
60.0	27.0	41	0.755	0.245	6.6
100.0	27.0	0	1	0.000	0.0

*data from present investigation

APPENDIX VI

FLOTATION

RESULTS

TABLE 12

DDA Conc'n (mg/l)	Zero Conditioning			30 minutes Conditioning		
	Sinks	Floats	% Rec'y	Sinks	Floats	% Rec'y
5	0.76	0.00	0.0	1.07	0.00	0.0
	0.94	0.00	0.0	0.87	0.01	1.3
10	0.95	0.00	0.0	1.00	0.02	1.0*
	1.09	0.15	12.1*	0.97	0.01	1.0
15	0.89	0.03	3.3	0.69	0.05	6.8
	0.73	0.02	2.7	0.90	0.17	15.9
				0.94	0.06	6.0
				1.03	0.07	6.4
20	0.23	0.84	78.5	0.49	0.45	47.9
	0.85	0.17	16.7	0.49	0.57	53.8
	0.45	0.68	60.2			
	0.19	0.87	82.1			
25	0.29	0.68	70.1	0.46	0.57	55.4
	0.60	0.52	46.4	0.25	0.75	75.0
	0.89	0.20	18.3			
	0.80	0.30	27.3			
30	0.43	0.49	53.3	0.16	0.92	85.2
	0.60	0.48	44.4	0.02	0.92	97.9
35	0.81	0.25	23.6	0.00	0.94	100.0
	0.46	0.41	47.1*	0.00	0.81	100.0*
	0.56	0.44	44.0			
50	0.33	0.66	66.7	0.00	1.00	100.0
	0.37	0.60	61.9	0.00	0.99	100.0
100	0.10	0.86	90.0*	0.00	0.99	100.0
	0.00	0.91	100.0	0.00	1.00	100.0
200	0.03	0.87	96.7	0.01	0.88	98.9
	0.02	0.85	97.7	0.01	1.00	99.0

*Results obtained using two month old dodecylamine solutions.

17. Orowan, E.; Proc. Roy. Soc. Ser. A. 316, 473 (1970).

18. Shoemaker, P.D., Paul, G.W., de Chazal, M.L. and L.E. Marc; J. Chem. Phys. 52 (2), 491 (1970).

19. Jhon, M.S. and H. Eyring; Proc. Nat. Acad. Sci. U.S. 64 (2), 415 (1969).

20. Houkwink, R. and G. Salomon (Eds.); Adhesion and Adhesives, vol. 1, Elsevier, Amst., Lon., N.Y., 1965, 29-52.

21. Garrett, H.E.; Aspects of Adhesion, 2, 18 (1965).

22. Yen. T.S.; Ph.D. thesis, McGill (to be published).

23. Gibbs. J.W.; Collected Works of J. Willard Gibbs, Longmans, N.Y., 1931, 300.

24. McBain, J.W. and C.W. Humphrey; J. Phys. Chem. 36, 300, (1932).

25. McBain, J.W. and L.A. Wood; Proc. Roy. Soc. Ser. A, 174, 286, (1940).

26. de Bruyn, P.L., Overbeek, J.Th.G. and R. Schuhman, Jr.; Trans. AIME, 199, 519 (1954).

27. Somasundaran, P.; Trans, AIME, 241, 105 (1968).

28. Smolders, C.A.; Chemistry, Physics and Application of Surface Active Agents, vol. 2, Gordon and Breach, Lon., N.Y., Paris, 1964, 343.

29. Padday, J.F.; ibid., 299.

30. McBain, J.W.; Trans. Farad. Soc., 9, 99 (1913).

31. Reference 2, p. 242.

32. Reference 3, p. 251.

33. Adam, N.K.; J. Phys. Chem. 29, 87 (1925).

34. Harkins, W.D., Mattoon, R.W. and M.L. Corrin; J. Am. Chem. Soc. 68, 220 (1946).

35. Anacker, E.W.; "Micelle Formation in Aqueous Media", Cationic Surfactants, Surfactant Sci. Series No. 4, Marcel Dekker, 1970, 203.

36. Miller, I.R. and D.C. Grahame; J. Am. Chem. Soc. 79 (2), 3006 (1957).

37. Mukerjee, P.; Advan. Colloid Interface Sci. 1, 241, (1967).

38. Shinoda, K. and E. Hutchinson; J. Phys. Chem. 66, 577, (1962).

39. Adamson, A.W.; Physical Chemistry of Surfaces, Interscience, N.Y., Lon., Syd., 1963, 88.

40. Miles, G.D. and L. Shedlovsky; J. Phys, Chem. 48, 57 (1944).

41. Hutchinson, E.; J. Coll. Sci. 3, 413 (1948).

42. Kragh, A.M.; Trans. Farad. Soc. 60 (1), 225 (1964).

43. Wan, L.S.C. and P.K.C. Poon; J. Pharm. Sci. 58 (12), 1562, (1969).

44. Hertzfeld, S.H., Corrin, M.L. and W.D. Harkins; J. Phys. & Coll. Chem. 54, 271 (1950).

45. Debye, P. and E.W. Anacker; Private communication, recorded in reference 34.

46. Elworthy, P.H. and K.J. Mysels; J. Coll. & Int. Sci. 21, 331 (1966).

47. Lange. H.; J. Coll. & Int. Sci. 20, 50 (1965).

48. Owen, D.K.; J. Coll. & Int. Sci. 29, 496 (1969).

49. Okun, D. and J.K. Baers; Chemistry, Physics and Application of Surface Active Substances, vol. 2, Gordon and Breach, Lon., N.Y., Paris, 1964, 1179.

50. Defay, R. and J.R. Hommelen; J. Coll. Sci. 14, 411 (1959).

51. Milner, S.R.; Phil. Mag. (6) 13, 96 (1907).

52. Bond, W.N. and H.O. Puls; Phil. Mag. (7) 24, 864 (1937).

53. Langmuir, I. and V.J. Shaefer; J. Am. Chem. Soc. 59 (2), 2400 (1937).

54. Ward, A.F.H. and L. Tordai; J. Chem. Phys. 14, 453 (1946).

55. Addison, C.C.; J. Chem. Soc. 98 (1945).

56. Sutherland, K.L.; Revs. Pure and Appl. Chem. (Australia) 1, 35 (1951).

57. Kuffner, R.J.; J. Coll. Sci. 16, 497 (1961).

58. Alexander, A.E.; Trans. Farad. Soc. 37, 15 (1941).

59. Brown, D.J.; Unpublished results, Dept. Metallurgy, M.I.T., quoted by de Bruyn, P.L., "Flotation of Quartz by Cationic Collectors". Trans. AIME, 202, 292 (1955).

60. Ruch, R.J. and L.S. Bartell; J. Phys. Chem. 64, 513 (1960).

61. Traube, J.; Ann. Chem. Justus Liebigs 265, 27 (1891).

62. Hoerr, C.W., McCorkle, M.R. and A.W. Ralston; J. Am. Chem. Soc. 65, 328 (1943).

63. Kellogg, H.H. and H. Vasquez-Rosas; Trans. AIME 169, 476 (1946).

64. Smith, R.W.; Trans. AIME 223, 113 (1962).

65. Manser, R.M.; Rep. LR 67 (MST), Warren Spring Lab., Herts., Eng.

66. de Bruyn, P.L.; Ph.D. thesis, M.I.T., 1950.

67. Hoffman, E.J., Boyd, G.E. and A.W. Ralston; J. Am. Chem. Soc. 64 (2), 2067 (1942).

68. Lawrence, A.S.C. and M.P. McDonald; Proc. 2nd. Int. Congr. Surf. Activity 1, 385 (1957).

69. Sandvik, K.L. and M. Digrè; Trans. I.M.M. 77 (739), C61 (1968).

70. Brown, A.S., Robinson, R.U., Sirois, E.H., Thibault, H.G., McNeill, W. and A. Tofias; J. Phys. Chem. 56, 701 (1952).

71. Austin, M., Bright, B.B. and E.A. Simpson; J. Coll. & Int. Sci. 23, 108 (1967).

90. Bendure, R.L.; J. Coll. & Int. Sci. 35 (2), 238 (1971).

91. Feuhrer, C. and J. Ghadially; Pharm. Acta Helv. 43 (10), 653 (1968).

92. Finkelstein, N.P.; N.I.M. (S. Afr.) Res. Rep. No. 437 (Dec. 1968).

93. Saunders, L.; J. Chem. Soc. 00 , 969 (1948).

94. Sugden, S.; Trans. Chem. Soc. 121, 858 (1922).

95. Moelwyn-Hughes, E.A.; Physical Chemistry, Edn. 2, Pergamon, Oxford, Lon., N.Y., Paris, 1964, 921.

96. Harkins, D.W. and F.E. Brown; J. Am. Chem. Soc. 38 (1), 246 (1916).

97. Harkins, D.W. and F.E. Brown; ibid. 41 (1), 499 (1919).

98. Rehfeld, S.J.; J. Phys. Chem. 71, 738 (1967).

99. Shergold, H.L. and O. Mellgren; Trans. I.M.M. 78, C121 (1969).

100. Parreira, H.C.; J. Coll. Sci. 20, 44 (1964).

101. Adam, N.K.; The Physics and Chemistry of Surfaces, Edn. 2, O.U.P., 1938, 402.

102. Gaddum, J.H.; Proc. Roy. Soc. (Lon.) Ser. B 109, 114 (1931).

103. Lord Rayleigh; Scientific Papers, 6, C.U.P. 1920.

104. Sugden, S.; Trans. Chem. Soc. 123, 27 (1924).

105. Brown, R.C.; Phil. Mag. 13, 578 (1932).

106. Weast, R.C., Ed.; Handbook of Chemistry and Physics, Edn. 51, Chem. Rubber Co., Cleveland, 1970, F-31.

107. Tate, T.; Phil. Mag. 27, 176 (1864).

108. Ralston, A.W., Hoerr, C.W. and E.T. Hoffman; J. Am. Chem. Soc. 64 (1), 97 (1942).

109. Gaudin, A.M. and F.W. Bloecher, Jr.; Trans. AIME 187, 499 (1950).

110. Reference 3, p. 48.

111. Oko, M.U. and R.L. Venable; J. Coll. & Int. Sci. 35 (1), 53 (1971).

112. Fuerstenau, D.W., Healy, T.W. and P. Somasundaran; Trans. AIME 229, 321 (1964).

113. Adam, N.K.; Dis. Farad. Soc. 3, 5 (1948).

114. O'Brien, W.J.; Surface Sci. 19 (2), 387 (1970).

115. Bartell, F.E. and H.J. Osterhof; J. Phys. Chem. 32, 1553 (1928).

116. Adam, N.K. and R. Shute; Trans. Farad. Soc. 34, 758 (1938).

117. Iwasaki, I., Cooke, S.R.B. and Y.S. Kim; Trans. AIME 223, 113 (1962).

118. Joy, A.S. and D. Watson; Trans. I.M.M. 73, 323 (1963).

119. Ginn, M.E.; "Adsorption of Cationic Sufractants on Mineral Substrates", Cationic Surfactants, Surfactant Sci. Series No. 4, Marcel Dekker, 1970, 341.

120. Partridge, A.C.; M.Sc. thesis, McGill, 1970.

121. Hendriks, D.W.; M.Sc. thesis, McGill, (to be published).

122. Kuffner, R.J., Bush, M.T. and L.J. Bircher; J. Am. Chem. Soc. 79, 1587 (1957).

123. Smith, R.W. and R.W.M. Lai; Trans. AIME 235, 413 (1966).

124. Kung, H.C. and E.D. Goddard; Chemistry, Physics and Application of Surface Active Agents, vol. 2, Gordon and Breach, Lon., N.Y., Paris, 1964, 751.

125. Ghigi, G. and C. Botre; Trans. I.M.M. 75, C240 (1966).

126. Ghigi, G.; Trans. I.M.M. 77, C212 (1968).

127. Fuerstenau, D.W. and B.J. Yamada; Trans. AIME 223, 50 (1962).

128. Belajee, S.R. and I. Iwasaki; Trans. AIME 244, 407 (1969).

129. Partridge, A.C. and G.W. Smith; Can. Met. Quart. To be published, Sept. 1971.

130. Aplan, F.F. and P.L. de Bruyn; Trans. AIME 226, 235 (1963).

131. Philipoff, W., Cooke, S.R.B. and D.E. Cadwell; Trans. AIME 283 (1952).

132. Wark, I.W. and A.B. Cox; Trans. AIME 112, 189 (1934).

133. Rehbinder, P.; Trans. Farad. Soc. 36, 295 (1940).

134. Fuerstenau, D.W.; Trans. AIME 208, 1365 (1957).

135. Reference 1, pp. 163-171.

136. Reference 2, p. 53.

137. Kim. Y.S.; M.Sc. thesis, U. of Mich., U.S.A., 1959.

138. Iwasaki, I., Cooke. S.R.B. and A.F. Colombo; U.S. Bur. Mines Rep. Invest. 5593 (1960).

139. Lord Rayleigh, Phil. Mag. 30, 397 (1890).

140. Cassie, A.B.D.; Dis. Farad. Soc. 3, 11, (1948).

141. Bikerman, J.J.; Surface Chemistry; Theory and Applications, Edn. 2. Academic Press, N.Y., 1958, 352.

142. Reference 1, p. 169.

143. MacDougall, G. and C. Okrent; Proc. Roy. Soc. Lon. A180, 151 (1942).

144. Harris, C.C., Jowett, A. and N.R. Morrow; Trans. I.M.M. 73, 335 (1964).

145. Gaudin, A.M., Witt, A.F. and T.G. Decker; Trans. AIME 107 (1963).

146. Hertzberg, W.J. and J.E. Marian; J. Coll. & Int. Sci. 33 (1), 161 (1970).

147. Gray, V.R.; Chemistry, Physics and Application of Surface Active Agents, vol. 2, Gordon and Breach, Lon., N.Y., Paris, 1964, 321.

148. Adam, N.K. and G. Jessop; J. Chem. Soc. 127, 1863 (1925).

149. Fowkes, F.M. and W.D. Harkins; J. Am. Chem. Soc. 62, 3377 (1940).

150. Shuttleworth, R. and G.L.J. Bailey; Dis. Farad. Soc. 3, 16 (1948).

151. Wenzel, R.N.; Ind. Eng. Chem. 28, 988 (1936).

152. Reference 3, p. 61.

153. Mitrovanov, S.I.; Min. Dress. J. 3, Nos. 9-10 (1937).

154. Bailey, R. and V.R. Gray; J. Appl. Chem. 8, 197 (1958).

155. Sulman, H.L.; Trans. I.M.M. 29, 44 (1920).

156. Reference 101, p. 193.

157. Wark, I.W.; J. Phys. Chem. 40, 661 (1936).

158. Reference 2, pp. 257-267.

159. Reference 3, p. 261.

160. Rogers, J., Sutherland, K.L., Wark, E.E. and I.W. Wark; Trans. AIME 169, 287 (1946).

161. Reference 1, p. 275.

162. Leja, J.; Discussion, Trans. AIME 238, 189 (1967).

163. Schulman, J.H. and J. Leja; Surface Phenomena in Chemistry and Biology. Pergamon, 1958, 236.

164. Ferguson, A.; Proc. Roy. Soc. (Lon.) 53, 554 (1941).

165. Taggart, A.F., Taylor, A.C. and C.R. Ince; Trans. AIME 87, 285 (1930).

166. Michaels, A.S. and S.W. Dean Jr.; J. Phys. Chem. 66, 1790 (1962).

167. Mack, G.L.; J. Phys. Chem. 40 (2), 159 (1936).

168. Mack, G.L. and D.A. Lee; ibid, 40 (2), 169 (1936).

169. Ehrlich, R.; J. Coll. & Int. Sci. 28, 5 (1968).

170. Ablett, R.; Phil. Mag. (6) 46, 244 (1923).

171. Elliott, G.E.P. and A.C. Riddiford; J. Coll. & Int. Sci. 23, 392 (1967).

193. Harris, C.C.; Ph.D. thesis, U. of Leeds, Eng., 1959.

194. Morrow, N.R.; Chem. Eng. Sci. 25 (11), 1799 (1970).

195. Janis, N.A.; "Investigations of the Interaction of Cationic Reagents with Aluminosilicates", Mechansbr. Inst. Rep. Invest. No. 135, Leningrad, 1965.

196. Ter-Minassian-Seraga, L.; "Chemisorption and Dewetting of Glass and Silica", Advances in Chem. Series No. 43, 1964, 232.

197. Bernett, M.K. and W.A. Zisman; "Prevention of Liquid Spreading or Creeping", Advances in Chem. Series No. 43, 1964, 332.

198. Partridge, A.C. and G.W. Smith; Trans. I.M.M., to be published Sept. 1971.

199. Fuerstenau, D.W., Metzger, P.H. and G.D. Seale; Eng. & Min. J. 158, 93 (1957).

200. Gaudin, A.M. and D.W. Fuerstenau; Trans. AIME 202, 958, (1955).

201. Wada, M. et al.; "Experimental Study on Aerosol Flotation", VIII Int. Miner. Process. Congr. Leningrad, 1968, Preprint D-8, 8pp.

202. Weast, R.C. Ed.; Handbook of Chemistry and Physics, Edn. 50, Chem. Rubber Co., Cleveland, 1970, F-6.